Application of click chemistry for PET

Mirfeizi, Leila

Link to publication in University of Groningen/UMCG research database

APPLICATION OF CLICK CHEMISTRY FOR PET
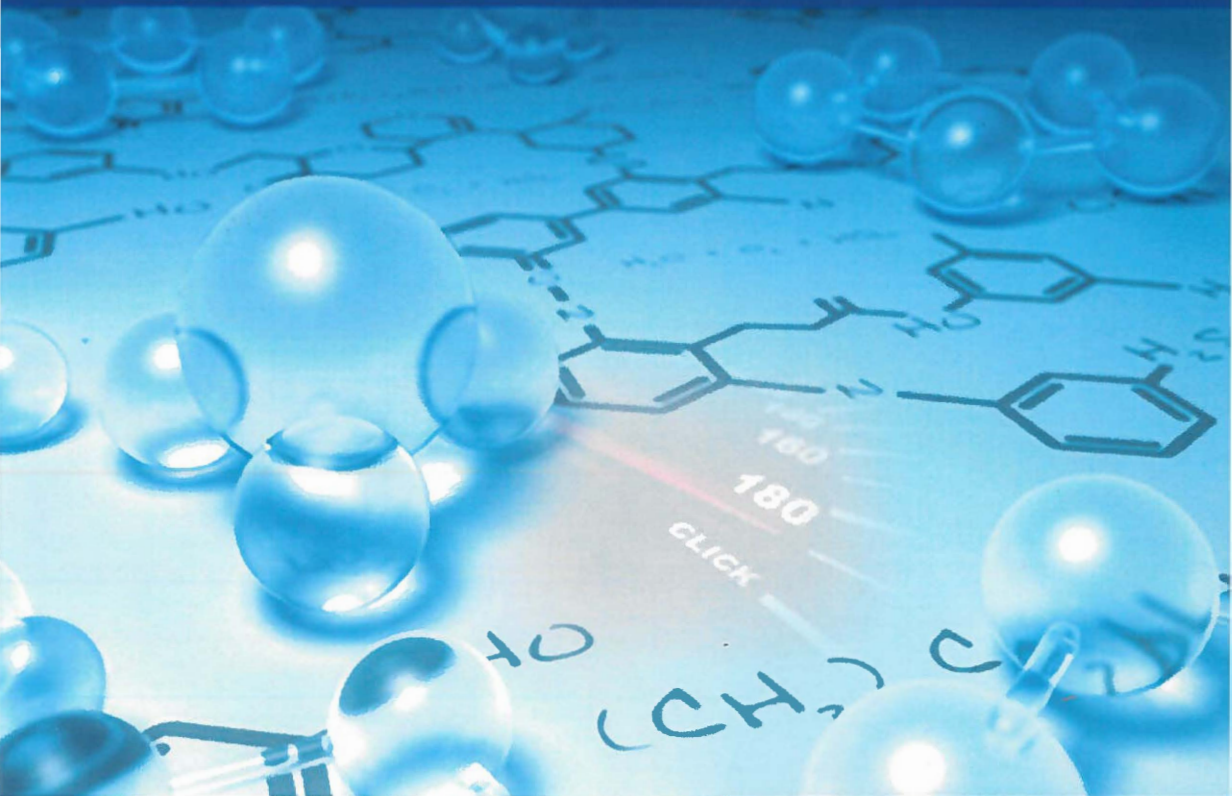
Leila Mirfeizi

Application of
Click Chemistry for PET

Leila Mirfeizi

Stellingen

1. Click chemistry is a new approach for the synthesis of drug-like molecules, which can accelerate the drug discovery process. *Sharpless* .

2. In a field where simplicity and speed of reaction are crucial, it is only natural that 'click' chemistry began to emerge as an excellent radiolabelling technique. *Chapter 2*

3. The use of MonoPhos as ligand results in accelerated click reaction, less precursor consumption and a higher radiochemical yield. *Chapter 3*

4. The synthesis of [^{18}F]Galacto-RGD is very complex and time consuming, therefore a better option is synthesising [^{18}F]-RGD-K5 offering a simplified procedure leading to robust clinical study and a short synthesis time. *Chapter 6*

5. The imaging of integrin expression (using [^{18}F]-RGD-K5) provides valuable information to determine the indication of surgical atherosclerotic plaques removal. *Chapter 7*

6. Catalytic copper which is toxic at high micromolar concentrations is forming complexes with PET-labelled peptide. This is why considerable effort is put into developing Cu-free click chemistry. *Chapter 8*

7. If the strain-promoted azide-alkyne cycloaddition methodology could be extended as pretargeting method to antibodies, the use of radionuclides for imaging such targets will not be limited to the longer-lived metallic radioisotopes, and higher resolution images using [^{18}F] can be achieved.

8. The most fundamental and lasting objective of synthesis is not production of new compounds, but production of properties. *George S. Hammond, Norris Award Lecture, 1968*

9. In the PET-lab there is no excuse for not wearing safety glasses and a radiation badge.

10. Being a good scientist is being a good seller because "In science credit goes to the man who convinces the world, not to the man to whom the idea first occurs". *F. Darwin*

11. To increase the productivity in science, brainstorm as much as you can, and only test the most probable ideas. You may miss the possibility of the rare accidental discovery, but your approach is more logical than being dependent on pure luck.

12. There are sadistic scientists who hurry to hunt down errors instead of establishing the truth. *Marie Curie*

RIJKSUNIVERSITEIT GRONINGEN

Application of
Click Chemistry for PET

Proefschrift

ter verkrijging van het doctoraat in de
medische wetenschappen
aan de Rijksuniversiteit Groningen
op gezag van de
Rector Magnificus, dr. E. Sterken,
in het openbaar te verdedigen op
maandag 12 november 12
om 11:00 uur
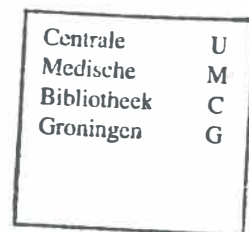
door

Leila Mirfeizi
geboren op 21 maart 1973
te Teheran,Iran

Promotores: Prof. dr. P.H. Elsinga
Prof. dr. B.L. Feringa
Prof. dr. R.A.J.O. Dierckx

Beoordelingscommissie: Prof. dr. H.H. Coenen
Prof. dr. H.J. Haisma
Prof. dr. J.G. Roelfes

Paranimfen: Silvana Berghorst-Kruizinga

                                      Janine Doorduin

Chapter 1
Introduction

Introduction

Positron Emission Tomography

Positron Emission Tomography (PET) is an imaging technology in nuclear medicine that is able to provide 3D functional images of the human body. It is based on radioactive positron emitting atoms that are incorporated in pharmaceuticals [Joliot, 1934]. These radionuclides undergo decay, and when this happens they emit a positron, called β+ decay. After having travelled a short distance in the tissue the emitted positron meets an electron. This combination will result in annihilation of both particles under the emission of two photons. During this reaction, mass is converted into energy following $E=mc^2$. The emitted photons have an energy of 511 keV and move in opposite directions [Phelps, 2000]. During a PET scan a subject is injected with a positron emitting radiopharmaceutical. After radioactive decay the emitted photons are detected and subsequently it can be determined where high concentrations of the radioactive tracer were present in the subject (Figure 1.1).
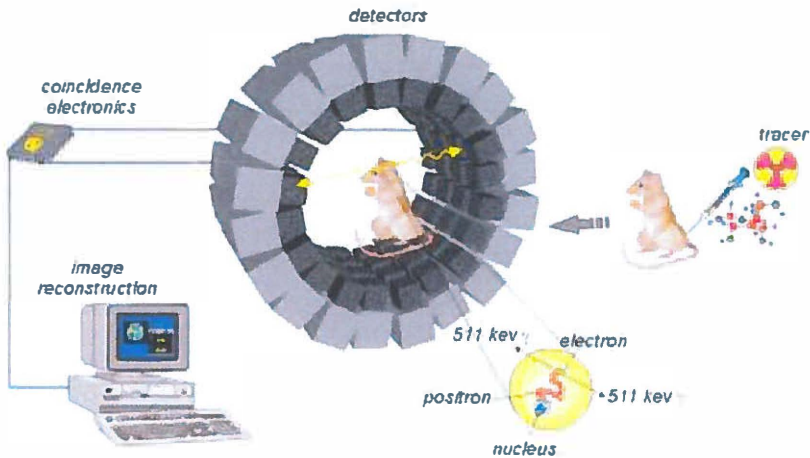
Figure 1.1. Principle of PET, the readily used FDG molecule with ^{18}F emitting two photons, which can be detected by the PET apparatus leading to a 3D image of the subject. From: http://www2.fz-juelich.de/zel/index.php?index=136

There are several radionuclides that can be used for PET. Amongst several others, ^{15}O, ^{13}N, ^{11}C and ^{18}F are positron emitters that are very frequently used. Because of the relatively short half life, the radionuclides are produced on-site using a cyclotron. ^{18}F is most often used because of its half life of 110 min [Schirrmacher, 2007]. A commonly used radiopharmaceutice compound for PET is the glucose analogue 2-[^{18}F]Fluoro-2-Deoxy-D-Glucose (FDG). FDG can, just as glucose, be phosphorylated by hexokinase. The difference with glucose is that the phosphorylated product of FDG, FDG-6-PO_4 is not significantly used in subsequent reactions in the body on the PET timescale. The FDG-6-PO_4 will remain in the cell where it was phosphorylated thereby giving a measure of the extent to which glucose is phosphorylated in that cell [Schirrmacher, 2007].
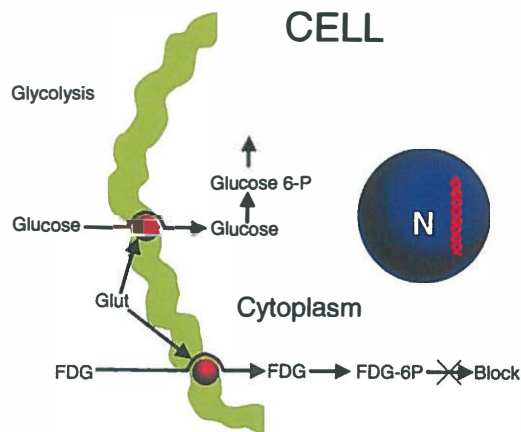
Figure 1.2. Phosphorylation of FDG and resulting PET images.
From: http://radiographics.rsna.org/content/24/2/523/F3.expansion.html

Several diseases are biological processes that often require more energy, as in the form of glucose, than normal processes especially in cases like that of cancer where tumors are fast growing. The injected FDG will be phosphorylated in higher amounts in the cancerous areas than in other areas giving a good high resolution 3D image of the disease (Figure 1.2). Besides FDG many other 18F-radiopharmaceuticals are being developed during the last decades for many different purposes as shown in table 1.1.

Table1.1- Examples of ^{18}F PET Tracers

PET Tracer	General target	Biochemical process
^{18}F-Fluorodeoxyglucose (FDG)	Glucose consumption	Cellular energetics
^{18}Fluoro-L-thymidine (FLT)	Thymidine Kinase-1 (TK-1)	Proliferation
^{18}F-5-fluorouracil (5-FU)	Thymidylate synthase	Proliferation
^{18}F-fluoroethyltyrosine (FET)	Amino acid transport	Amino acid transport
^{18}F-choline analogues	Choline kinase	Phospholipid metabolism
^{18}F-annexine A5	Exposure of phosphatidylserine	Apoptosis/cell death
^{18}F-fluoroestradiol (FES)	Estrogen receptor	Endocrine metabolic activity
^{18}F-L-dihydroxyphenylalanine (DOPA)	Excretion of neyrotransmitters	Endocrine metabolic activity
^{18}F-octreotide analogues	Somatostatin receptor	Endocrine metabolic activity
^{18}F-fluorinated androgen analogues	Androgen receptor	Endocrine metabolic activity
^{18}F-fluoromisonidazole (FMISO)	Intracellular reductases	Hypoxia
^{18}F-florbetaben	Cerebral Amyloid β	ß-Amyloid deposition in Alzheimer's disease
^{18}F-flurpiridaz	Mitochondrial membrane potential	Cardiac perfusion

Click chemistry for PET

There is a great need for versatile radiolabelling methods for the production of ^{18}F-radiopharmaceuticals to increase their availability.

In most cases, ^{18}F-labeling of small molecules to form PET imaging probes involves nucleophilic substitution by [^{18}F]-fluoride of a precursor with the appropriate leaving group in compatible reaction media, such as acetonitrile, DMF or DMSO using temperatures of 80-160 ^{0}C. Under such reaction conditions, the reactivity of [^{18}F]fluoride can be influenced by steric and electronic effects within the target molecule. In addition, protecting groups for a variety of functional groups such as carboxylic acidic protons are required. Although a lot of knowledge exists on protecting groups the proper selection will have to be investigated in each new case. Therefore, this conventional way of ^{18}F-fluorination cannot not be generally applied for the preparation of each ^{18}F-radiopharmaceutical.

Recently, click chemistry has been introduced as a potential method. The preparation of several receptor binding ligands, labeled with a positron emitting radionuclide, via a click reaction is described in this thesis. Sharpless et al. presented, in 2001, a review in which they introduced the concept of "click chemistry" [Kolb, 2001]. One of the most applied click reaction is the Huisgen 1,3 dipolar cycloaddition that is catalyzed by Cu (I). To be a "click reaction" a reaction needs to:
- be modular
- be applicable to a wide range of substrates
- produce high yields
- produce only inoffensive byproducts
- be orthogonal to other functional groups,

  that can be removed by non-chromatographic methods, be stereospecific, although not necessarily enantioselective.

Ideally, the reaction conditions should be simple, involving no or benign solvents and the reaction itself should be insensitive to oxygen and water. To be able to obtain all of these characteristics these reactions need a high thermodynamic driving force. One could thus look at these reactions as being "spring loaded", so that as soon as the functional groups are in place the reaction can proceed easily and rapidly with high yields. The Huisgen 1,3 dipolar cycloaddition involves the reaction between an alkyne and an azide to form a triazole

linkage as is extensively reviewed in chapter 2. The reaction is very suitable for application in ^{18}F-radiochemistry.

Aims of this thesis

The goal of this research consists of two objectives. The first objective is to develop click chemistry for the synthesis of PET tracers with focus on ^{18}F as radionuclide and the second objective part of the project is to apply click chemistry for the synthesis and evaluation of biologically active molecules. Thereby the triazole moiety will be applied as integral part of the molecule or as means to attach a prosthetic group.

In Chapter 3, the results of a study towards optimization ^{18}F click chemistry are presented. Research results obtained from work of Lachlan Campbell-Verduyn [Campbell-Verduyn, 2008] are translated to ^{18}F-radiochemistry. It is of utmost importance to accelerate the reaction to obtain high radiochemical yields with short-lived ^{18}F. Furthermore minimizing the amounts of reagents will simplify purification and workup procedures. Our aim is to achieve rate acceleration and to perform a systematic study of the reaction parameters of the catalytic 1,3-dipolar cycloaddition of azides and alkynes using phosporamidite ligands for the application to PET- imaging precursors.

In chapter 4, we will develop a rapid synthesis method of a ^{18}F-labeled tracer aimed for imaging of cerebral beta adrenergic receptors (β-ARs). Using click chemistry the hydroxyl propylamine moiety (crucial for binding to β-ARs) is partly maintained but ^{18}F was introduced as a novel moiety, possibly not resulting in toxicity of the carazolol derivatives. A tracer based on the β-azidoalcohol motif is designed for targeting cerebral β-adrenergic receptors and its stability and binding affinity for the targeted receptors are investigated.

In chapter 5, a study is presented on the synthesis of a new ^{18}F-labeled bombesin derivative by click chemistry to achieve high tumor uptake and optimal pharmacokinetics for specific targeting of Gastrin-Releasing Peptide (GRP) receptors in human prostate cancer cells. Bombesin is a 14 amino acid peptide sequence which serves as a tumor marker for various cancers. Amino acids 7-14 are considered to be the sequence responsible for binding to the GRP-receptor. We use 1,3-dipolar cycloaddition to label the peptide modified at the lys3-position with a triple bond. Binding affinity for the target receptor is tested *in vitro* and *in vivo*.

In chapter 6, the optimized ^{18}F-click chemistry method as described in Chapter 3 will be applied on the synthesis of the PET-biomarker RGD K5. The optimized synthesis method will be compared with the current method as developed by Siemens and aspects to translate RGD-K5 to the clinic will be elaborated in cooperation with the University Hospital in Leuven, Belgium. The described synthetic methodology can generally be applied for other click reactions using [^{18}F]fluoroalkynes as prosthetic group.

In chapter 7, the potential use of [^{18}F]RGD-K$_5$ for the diagnosis of vulnerable atherosclerotic plaques by $a_v b_3$ integrin expression, such as cancer and inflammation will be investigated. In this study, for the first time we investigated whether it is feasible to detect $a_v \beta_3$ integrin in human carotid endarterectomy (CEA) specimens using an ex vivo imaging method recently developed (Masteling, 2011). This method allows using high resolution microPET system to illustrate heterogeneous tracer uptake within atherosclerotic plaque and correlating tracer uptake with pathologic finding of plaques in different regions.

In chapter 8, we investigate reaction conditions and substrates to apply copper-free click chemistry. Since copper is very toxic, when one can avoid copper the metal does not have to be removed afterwards. Furthermore it opens the possibility for reactions to occur in vivo. To this purpose new strained alkynes will be investigated. The neuropeptide bombesin will be used as model compound for testing the ^{18}F-radiochemistry. Hydrophilicity can be tuned by selection of the proper complementary azide synthon. Furthermore stability of tracer and binding affinity will be tested in in vitro studies.

References

- Campbell-Verduyn L, Elsinga P H, Mirfeizi L, Dierckx R A, Feringa B L Org. Biomol. Chem.,   2008, 6, 3461–3463.
- Joliot F, Curie I, Nature. 1934, 133-201.
- Kolb HC, Finn MG, Sharpless KB, Angew. Chem., Int. Ed. 2001, 40, 2004–2021.
- Phelps ME, Proc. Natl. Acad. Sci. U. S. A. 2000, 97, 9226.
- Masteling MG, Zeebregts CJ, Tio RA, J Nucl Cardiol. 2011, 18, 1066-1075.
- R. Schirrmacher R, Wangler C, Schirrmacher E, Organic Chemistry., 2007, 4, 317.

Chapter 2
Application of click chemistry for PET

Leila Mirfeizi[a], Lachlan Campbell-Verduyn[b], Rudi A. Dierckx[a, c], Ben L. Feringa[b], and Philip H. Elsinga[a,c] *

[a]Department of Nuclear Medicine and Molecular Imaging, University Medical Center Groningen, University of Groningen, Groningen, The Netherlands. E-mail: p.h.elsinga@ngmb.umcg.nl; Fax: +31 50 3696750; Tel: +31 50 3614850

[b]Stratingh Institute for Chemistry, University of Groningen, Groningen, The Netherlands. E-mail: b.l.feringa@rug.nl; Fax: +31 50 363 4278; Tel: +31 05 363 4296

[c]Department of Nuclear Medicine, Ghent University, Ghent, Belgium

Abstract

Sharpless et al. presented, in 2001, a review in which they introduced the concept of "click chemistry". In this review a "new way" of making chemicals, with a particular emphasis on drugs, is presented. Current drugs are often based on natural products that were first extracted from plants or other organisms and then with enormous effort were synthetically reproduced by chemists. Sharpless et al. propose to shift the focus away from the structure, which chemists focus on when they synthesize natural products, towards the function of molecules. Rather than making natural products with known biological activity and using these as templates for small modifications, it is proposed to make large libraries of compounds using (mainly) modular chemistry. After all, when looking for new and better drugs, it is the function that matters rather than the structure. This approach mimics nature in that it involves making a great variety of different compounds starting from a relatively small number of building blocks via a set amount of reactions. These sets of reactions have been termed "click reactions" in which simple molecules with specific functionalities can be "clicked" to each other to form a large variety of compounds with relative ease that can subsequently be tested as potential drug candidates. For these "click reactions" Sharpless also looks to nature for inspiration. Ideally, the reaction conditions should be simple, involving no or benign solvents and the reaction itself should be insensitive to oxygen and water.

It was found that copper not only accelerates the reaction but also controls the regioselectivity since in the presence of copper, only the 1,4-isomer is formed. The reaction proceeds in water, with or without co-solvent at room temperature and is relatively fast. The reaction is 100% atom efficient which means that there are no side products so the work up is usually simple. It can take place in a wide pH range which makes is suitable for biological compounds that require a specific pH. Furthermore the azide and alkyne functionalities are bioorthogonal, so theoretically, other functional groups present in a biological environment will not touch them. Finally the triazole product is biologically stable.

Introduction

Click chemistry is used to describe the copper(I)-catalyzed azide-alkyne cycloaddition that enables chemical building blocks to "click" forming an irreversible linkage (scheme 2.1). The click reaction was introduced in 2001 by Sharpless and co-workers [Sharpless, 2001]. The copper(I)-catalyzed azide-alkyne reaction has shown its value for conjugating small prosthetic groups to various biomolecules in vitro. In contrast, in vivo use of copper(I)-catalyzed click chemistry for biomolecule labeling in living systems is prohibited by the requirement of the cytotoxic copper(I) catalyst. [Sharpless, 2001, 2002, 2003]

Sharpless described the term click chemistry as a group of reactions that "must be modular, show broad scope, give very high yields, generate only inoffensive by-products that can be removed by non-chromatographic methods, and should be "stereospecific". [Sharpless, 2003] Characteristics are simple reaction conditions. In the ideal case the reaction must be not sensitive to oxygen and water, utilizes readily available starting reagents, uses no or an environmentally benign solvent, that can easily be removed, and includes simple product isolation.

Amongst all types of click chemistry, the most studied reaction is the Cu^I catalyzed formation of 1,2,3-triazoles using Huisgen 1,3-dipolar cycloaddition of terminal alkynes with azides. This reaction is highly regioselective leading to 1,4-disubstituted 1,2,3-triazoles (a triazole group is resembling an amide bond in vivo).[Sharpless, 2003] (anti-isomer). (Scheme1)
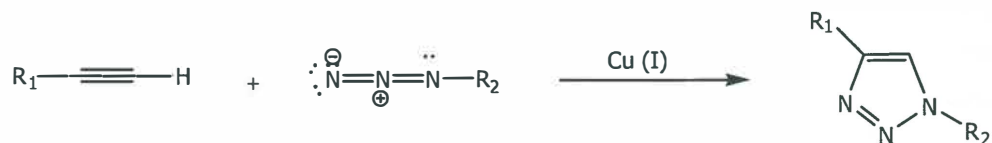
Scheme 2.1. General scheme of the Huisgen "click" chemistry cycloaddition reaction.

Although the Cu(I) catalyzed 1,3-dipolar cycloaddition of terminal alkynes with azides gives the product in high yield and purity the transformation is still relatively slow and requires hours for completion. This is a major drawback especially when the reaction has to be applied in the synthesis of radiopharmaceuticals for Positron Emission Tomography (PET) when using short-lived radionuclides. [Tornoe,2002]

Click chemistry using this Huisgen 1,3-cycloaddition can be highly versatile for application to ^{18}F-radiolabelled pharmaceuticals (possibly also for ^{68}Ga and ^{11}C) in PET. [18]F is attractive for PET because it can be produced in very high yields and has favourable decay characteristics (half-life = 110 min and short positron range). Since the click reaction is orthogonal, no protective groups are required [Burgess,2005]. A potential additional advantage is that reactions can be carried out in water possibly enabling ^{18}F-click reactions in vivo using pretargeting strategies [Burgess,2005]. This article gives an overview of the current status of click chemistry in relation with PET and will discuss directions to future developments.

Cu(I)-CATALYZED HUISGEN 1,3-DIPOLAR CYCLOADDITION OF AZIDES AND TERMINAL ALKYNES

The Cu(I)-catalyzed Huisgen 1,3-dipolar cycloaddition of azides and terminal alkynes to form 1,2,3-triazoles fulfills all the criteria of click chemistry. The reaction is extremely reliable and easy to use. This reaction regiospecifically yields 1,4-substituted triazole products. It typically does not require increased temperatures but if required the reaction can be performed over a wide range of temperatures (0–160°C) and pH values (5<pH<12) and in a variety of solvents (including water).

When Cu(I) is applied as catalyst, the reaction proceeds 10^7 times faster than the uncatalyzed version. Purification essentially consists of product filtration [Maarseveen,2006]. Furthermore, the reaction is hardly affected by steric factors both for the azide and the alkyne. Two additional reasons for the popularity of this cycloaddition are that azides and terminal alkynes are quite easy to prepare and are very stable under standard conditions [Sharpless,2001]. Both starting materials are stable towards oxygen, water, common organic synthesis conditions, tolerate a wide range of functional groups, a large range of solvents and pH's, and the reaction conditions of living systems (reducing environment,

hydrolysis, etc.) [Sharpless,2001, Maarseveen,2006]. Although the decomposition of aliphatic azides is thermodynamically favoured, there is a kinetic barrier that makes them to be stable in click chemistry conditions [Maarseveen,2006]. Therefore azides usually will only react when they meet a dipolarophile, such as an alkyne. [Maarseveen,2006].

Mechanism of Cu^I-Catalyzed Alkyne-Azide coupling

It has been suggested that the first step of the reaction involves n complexation of a Cu(I) dimer to the alkyne **1** (scheme 2.2). [Sharpless,2001] In the second step, deprotonation of the terminal hydrogen occurs resulting in the formation of a Cu-acetylide [Finn,2003]. Several forms of Cu-acetylide complexes are possible, which depend on the reaction conditions; compound **2** represents one of these possibilities [Kolb,2004]. The complexation of Cu(I) lowers the pKa of the terminal alkyne allowing deprotonation in an aqueous solvent without the addition of base [Sharpless,2002]. If a non-aqueous solvent such as acetonitrile was used, then a base, for example 2,6-lutidine or N,N'-diisopropylethylamine (DIPEA), has to be added [Chaiken,2006].
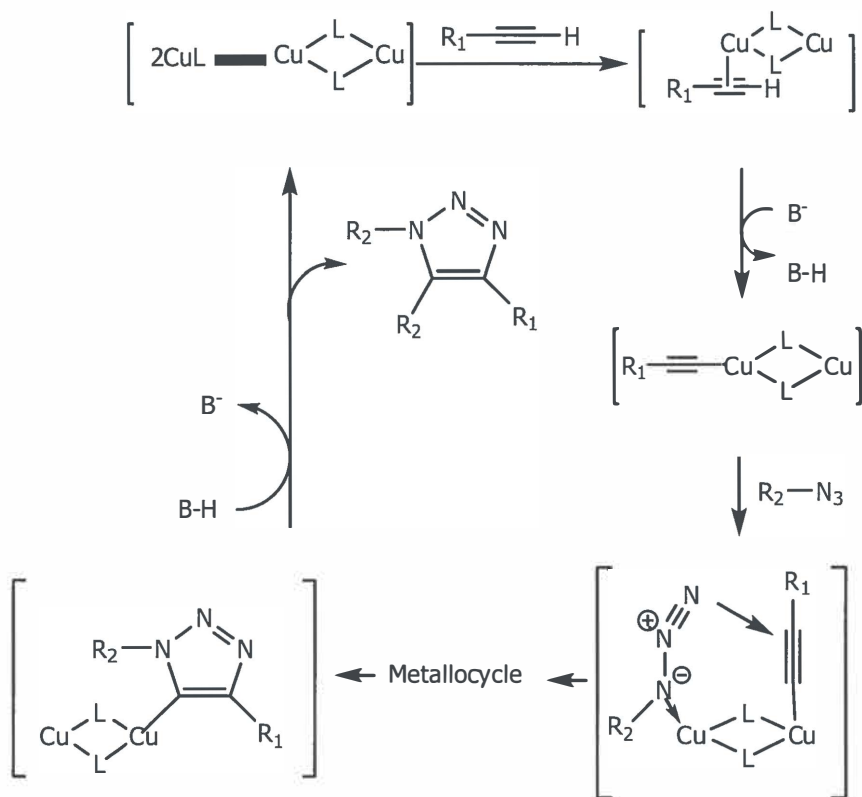
Scheme 2.2. Proposed mechanism of the catalytic cycle in the click reaction.

Application of the radionuclide ^{18}F in PET

PET is a molecular imaging technique that is increasingly used for non-invasive detection of diseases [Sharpless,2001]. PET imaging systems create images based on the distribution of positron-emitting radiopharmaceuticals after intravenous administration to the patient. The injected radiopharmaceuticals contain a positron-emitting isotope, such as ^{18}F,

[11]C, ^{13}N, or ^{15}O, that are covalently attached to a molecule which is then metabolized or trapped in the body or bound to receptor sites within the body. One of the most widely used PET molecular imaging probes is 2-deoxy-2-[^{18}F]fluoro-D-glucose ([^{18}F]FDG). [Sharpless,2001]

In most cases, ^{18}F-labeling of small molecules to form PET imaging probes involves nucleophilic substitution by [^{18}F]-fluoride of a precursor with the appropriate leaving group in compatible reaction media, such as acetonitrile, DMF or DMSO using temperatures of 80-160 °C. Under such reaction conditions, the reactivity of [^{18}F]fluoride can be influenced by steric and electronic effects within the target molecule. In addition, protecting groups for functionalities with acidic protons are required. Although a lot of knowledge exists on protecting groups the proper selection will have to be investigated in each new case. Therefore, this conventional way of ^{18}F-fluorination cannot not be generally applied for the preparation of each ^{18}F-radiopharmaceutical. [Finn,2003, Wong,2003]

Application of Click Chemistry in PET

Radiochemistry development

The use of click chemistry, in particular the Huisgen cycloaddition is receiving increasing interest in the field of radiopharmaceutical chemistry. In addition, there have been several reports recently based on the click-to-chelate approach for radiopharmaceutical applications for ^{99m}Tc-labelling reactions.[Brans,2006] Since non-invasive nuclear-imaging techniques, such as PET with high sensitivity have become available, radiolabeling of biologically active molecules has become an important tool to further develop and extent the clinical applications. Non-metallic positron-emitting isotopes, such as ^{18}F and ^{11}C, possessing short half-lives ($t_{1/2}$=109.8 min and $t_{1/2}$=20.3 min, respectively), have to be produced on-site in a cyclotron or within a short range of a production facility. As described above conventional ^{18}F-fluorination conditions are relatively harsh which are not suitable for the labeling of biomolecules of higher molecular weight since these molecules are generally not stable under these conditions. To overcome this conflict, a bifunctional approach is usually applied, where the ^{18}F is incorporated into a small molecule that is subsequently attached to biomolecules, such as proteins and peptides, under mild conditions.

23

Click chemistry has not been widely applied to the synthesis of ^{11}C-labeled compounds for PET imaging, probably due to the very short half-life of [11]C. The feasibility to apply click chemistry for the preparation of ^{11}C-labeled compounds was investigated by Schirrmacher et al.[Schirrmacher, 2008] They reported a method to prepare a ^{11}C-labeled compound within 5–10 min under nontoxic aqueous conditions with the radiochemical yield of 60% at room temperature.

Cu[I] catalyzed 1,3-dipolar cycloaddition 'click chemistry' for PET has been mainly used to prepare ^{18}F-radiolabeled peptides. Fluorine-18 labeled peptides are becoming more widely used as in vivo imaging agents [Bertozzi,2007]. Although a variety of ^{18}F-labeled prosthetic groups has been developed, only a limited number of chemical reactions have been utilized to incorporate the prosthetic groups into peptides including acylation, alkylation, and oxime formation.

Scheme 2.3. First ^{18}F-Labelling approaches using Click chemistry
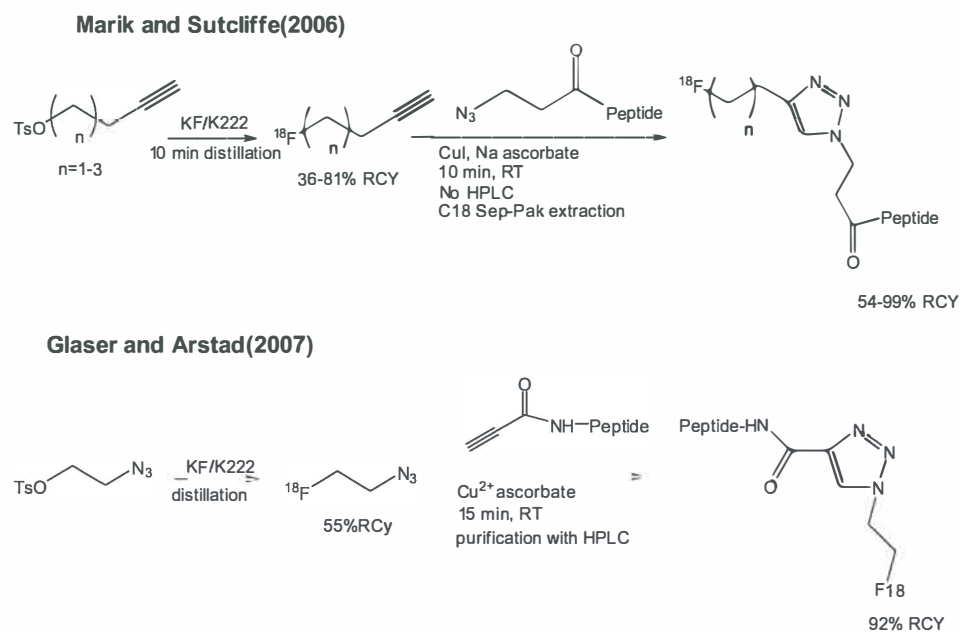
The first report on the use of click-chemistry for ^{18}F-radiolabeling was by Marik and Sutcliffe in 2006, describing a procedure for obtaining ^{18}F-fluoropeptides [Sutcliffe,2006]. ω-[^{18}F]fluoroalkynes (n=1-3) were reacted with peptides containing N-(3-azidopropionyl)-groups (scheme 3). The syntheses of the three different ^{18}F-fluoroalkynes, i.e. [^{18}F]-fluorobutyne, [^{18}F]-fluoropentyne and [^{18}F]-fluorohexyne was performed by reacting the corresponding tosylalkynes with ^{18}F for 10 min, followed by a co-distillation with acetonitrile. The yields varied significantly. The 4-[^{18}F]fluoro-1-butyne was obtained in a moderate RCY of 31%, while 5-[^{18}F]fluoro-1-pentyne and 6-[^{18}F]fluoro-1-hexyne were obtained with a yield of 81% and 61%, respectively. The subsequent reaction of the [^{18}F]fluoroalkynes with the azide-derivatized peptides to provide ^{18}F-labelled peptides proceeded with radiochemical yields of 10% within 30 min. Cu(II)sulfate was added as catalyst in the presence of sodium ascorbate. Cu(II) was reduced to Cu(I) in situ [Sharpless,2002]. Marik and Sutcliffe drastically improved radiochemical yields to nearly 100% after 10 min reaction time by adding a nitrogen base to Cu(I) iodide. Furthermore sodium ascorbate was added to prevent the oxidation of Cu(I) by atmospheric oxygen.

The synthesis of the ω-[^{18}F]fluoroalkyne and the subsequent reaction with the azide containing peptide precursor proceeded rapidly and in good radiochemical yields with final specific activities of >35GBq/µmol of the ^{18}F-labeled peptides.

In several papers the important role of the copper catalysts has been described [Wong,2003]. Cu(I) iodide with triethylamine and diisopropyl ethyl amine (DIPEA) or copper salts without base in organic solvents were investigated [Wong,2003]. It was shown that under water-free conditions, the absence of any base led to very slow reaction rates, probably due to the fact that the copper acetylide is not formed. Also the structure of the base is quite important e.g. the use of triethylamine resulted in no product formation, while the use of DIPEA gave yields of 38%.[Campbell-Verduyn,2008]

Also DIPEA, pyridine and piperidine were tested as base. Although the reaction rate increased using piperidine, several unspecified by-products were formed. The best results were obtained with DIPEA, The nitrogen base was present in 10 fold excess relative to the Cu(I) iodide, or a 400 fold excess relative to the azide derivatized peptide. Glaser and Arstad [Arstad,2007] reported a click-labeling approach with 2-[^{18}F]fluoroethylazide

[Sharpless,2003]. ^{18}F-azides were chosen because alkynes as the "cold" precursors are more readily available and less hazardous than organic azides.

2-Azidoethyl 4-methylbenzenesulfonate [Orlando,1984,Drake,1994,Fedan,1984] was reacted with [18]F$^-$ in acetonitrile (scheme 2.3). After 15 min the ^{18}F-azide was purified by distillation providing a RCY of 54%. Using 2-[^{18}F]fluoroethylazide various 1,4-disubstituted triazoles were prepared.

Different catalysts, including Cu(II)-sulfate with sodium ascorbate and copper powder were used. The best radiochemical yields (15-99%) were obtained by heating the reaction mixture to 80°C. At 80°C, Cu(II)sulfate proved to be the best catalyst for all studied alkynes. This approach also worked for peptide labeling. In this case a model peptide was first derivatized with propargylic acid [Arstad,2007]. The click reaction was subsequently performed at room temperature for 15 min providing excellent yields (92%) (scheme 3).

In the same period Kim and co-workers [Chi,2007] described an alternative synthetic approach for preparation of ^{18}F labeled biomolecules using the 'click reaction' with CuSO$_4$/Na-ascorbate and several model compounds such as small organic molecules, carbohydrates, amino acids, and nucleotides. (Scheme 2.4)

Real -time moleculare imaging of living substance with PET
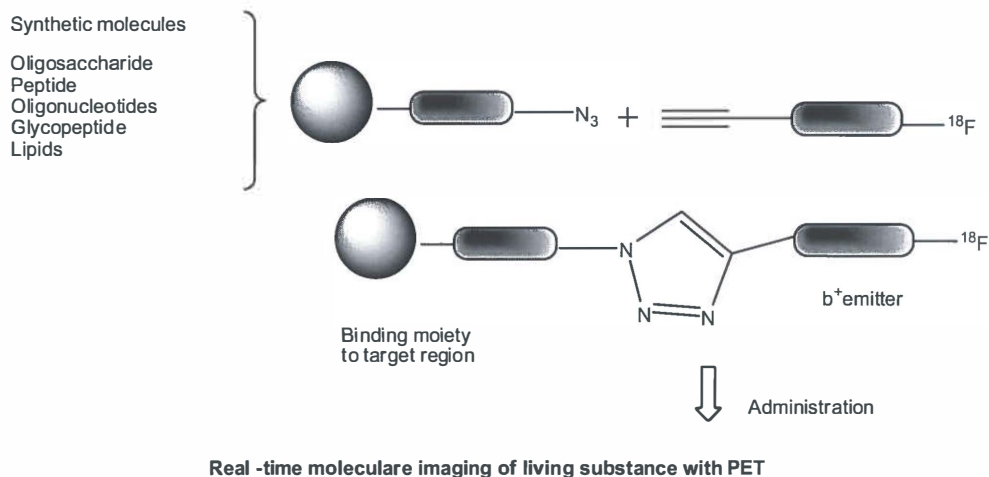
Scheme 2.4. Schematic click conjugation strategy

Several optimization experiments of the 1,3-dipolar cycloaddition for the two-step ^{18}F labeling procedure were performed using two Cu(I) species in water the mixed of organic solvent. organic solvent combinations e.q., acetonitrile, DMF, DMSO, and t-BuOH, The 1,3-dipolar cycloaddition of 4-methoxybenzyl azide and phenyl acetylene was employed as a model reaction. Similar conditions were employed in various 1,2,3-triazole syntheses of ^{18}F-labeled azides or acetylenes and their corresponding azide or acetylene counterparts. [Chi,2007]

Biological application of click chemistry in PET-studies

Prante and co-workers reported studies on a dopamine D_4 selective PET ligand [Tietze,2008]. The dopamine D_4 receptor is an interesting target for the treatment of schizophrenia, Parkinson's disease, depression, and attention deficit hyperactivity disorder (ADHD). Ongoing efforts have been made to develop selective ligands with high D_4 affinity. Employing D_4 selective azaindoles as lead compounds, a library of carbocyclic arene bioisosteres was synthesized employing click chemistry.(scheme 2.5). Radiosynthesis resulted in formation of the [^{18}F]-radioligand which showed a favourable logD of 2.8 and was determined to be highly stable in human serum (Scheme 2.6).

In this way, a promising dopamine D_4 selective radioligand has been developed for PET. [Tietze,2008]
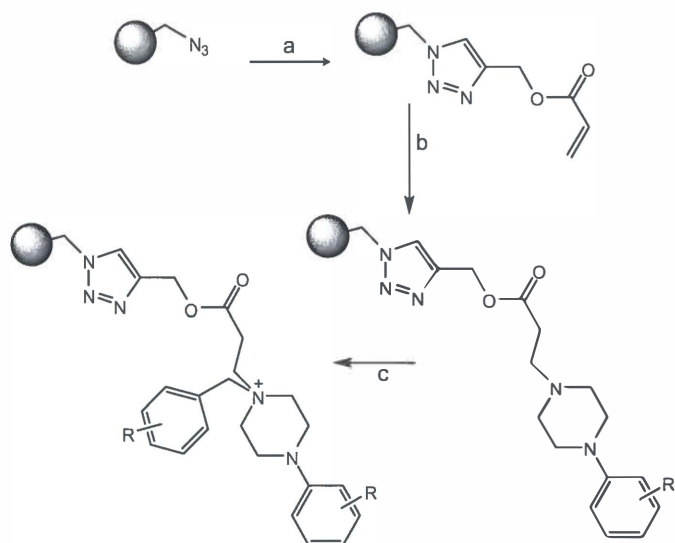
Scheme 2.5. Reagents and conditions: (a) proparagyl acrylate, Cu(I)I, DMF, DIPEA, 35°C, 10 h; (b) NMp,rt, 36h; (c) DMSO, rt, 16h.
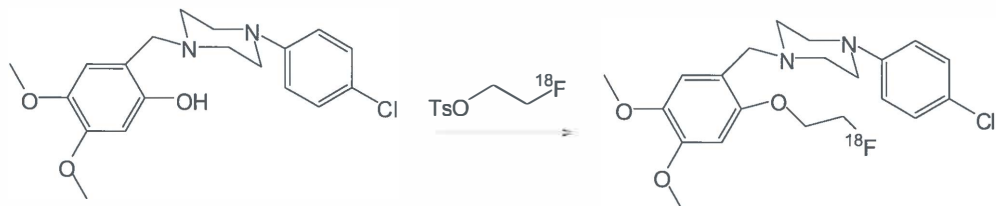
Scheme 2.6. Synthesis of ^{18}F-radioligand for the D$_4$-receptor

Li et al. have applied click chemistry for ^{18}F-labeling of an RGD peptide and performed micro PET imaging of tumour integrin $\alpha_v\beta_3$ expression.[Li,2007]

The cell adhesion molecule integrin plays a important role in tumor angiogenesis and metastasis. A series of ^{18}F-labeled RGD peptides have been developed for PET based on primary amine reactive prosthetic groups. Nucleophilic fluorination of a tosyl-functionalized alkyne provided the corresponding ^{18}F-alkyne in 65% radiochemical yield, which was then reacted with an RGD azide (RCY: 52%). It was demonstrated that the new tracer ^{18}F-FPTA-RGD2 could be synthesized with high specific activity based on click chemistry. This tracer exhibited good tumor-targeting efficacy, relatively good metabolic stability as well as favorable in vivo pharmacokinetics. The new ^{18}F labeling method might also find general application in labeling azido-containing bioactive molecules in high radiochemical yield and high specific activity for successful PET applications.[Li,2007]

To investigate how a triazole moiety compares to more traditionally used prosthetic groups for peptide labelling, Sutcliffe et al. performed the [18]F-"click" reaction as well as solid phase radiolabeling using 4-[^{18}F]fluorobenzoic and 2-[^{18}F]fluoropropionic acids. They present an evaluation of the feasibility of in vivo imaging with a [^{18}F]-labeled "click" probe. A20FMDV2, a peptide that selectively binds to the integrin $\alpha v\beta 6$ was chosen as model peptide. They have shown in a mouse model that [^{18}F]FBA-A20FDMV2 can be used to selectively image $\alpha_v\beta_6$ expressing tumors. All three prosthetic groups were readily introduced at the N-terminus of a tumor targeting model peptide with similar overall radiolabeling yields. The "click" radiolabeling approach was fastest but required a relatively large amount of purified peptide precursor. During in vivo animal studies, they observed that the prosthetic groups had a significant effect on pharmacokinetics, especially on tumor uptake and metabolism which warrants further investigation of these properties in other systems. [Sutcliffe,2006]
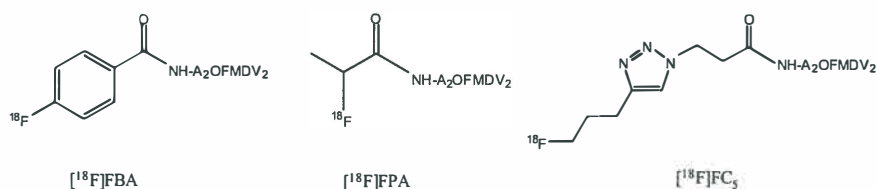
Scheme 2.7. Peptides based on three different ^{18}F-labelling methods

Thonon et al. have worked on new strategy for the preparation of a peptide by reaction with 1-(azidomethyl)-4-[^{18}F]-fluorobenzene. This reaction can be applied to any peptide which is modified beforehand with a p-iodophenylalanine group (Scheme 2.8).1-(Azidomethyl)-4-[^{18}F]-fluorobenzene was produced after 75 min with a 34% radiochemical yield, using azido nitro benzene as a precursor. Favourable results for a four-step procedure have been obtained by solid phase supported reactions and the absence of the solvent evaporation process that allow minimalization of losses in time and radioactivity during reaction workup and purification. Conjugation of [^{18}F]fluoroazide with a model alkyne-neuropeptide produced the desired ^{18}F-radiolabeled peptide in less than 15 min with a yield of 90% and excellent radiochemical purity. [Thonon,2009]
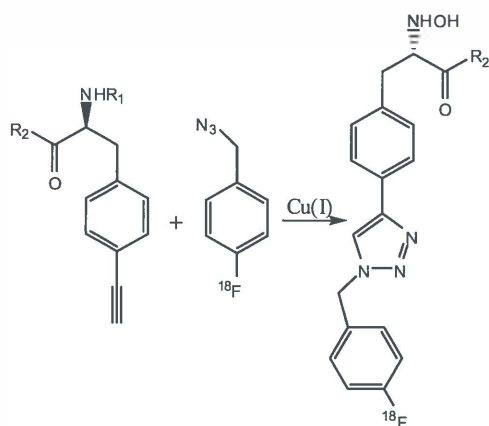
R$_1$= H, R$_2$= OH, Peptide chain

Scheme 2.8. 1,3-dipolar Cycloaddition of 1-(Azidomethyl)-4-[^{18}F]-fluorobenzene with alkyne functionalized peptide

Smith et al. has reported the design, synthesis and biological characterization of a Caspase3/7 selective Isatin by labelling with 2-[^{18}F]fluoroethylazide. They have described the synthesis of the novel bifunctional probe featuring the 3-(trifluoromethyl)-3H diazirin- 3-

yl group as well as an alkynyl side-chain. In a click reaction with the biotinyl azide the triazole was obtained. With the availability of biotinyl azides or fluorescence dyes containing an azide group, applications in chemical biology can be further exploited. Studies along these lines are currently being pursued.[Smith,2008]
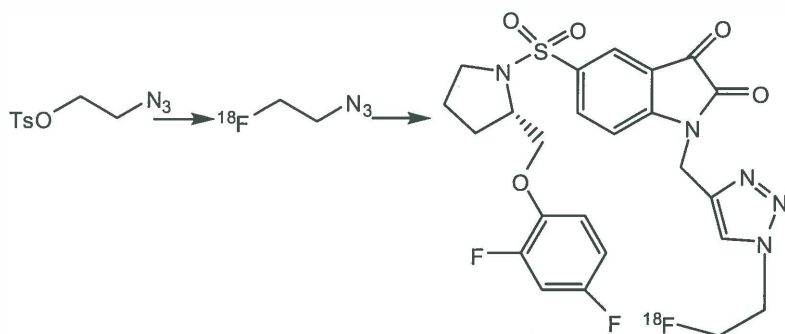
Scheme 2.9. Fluorination of ^{18}F via click reaction

Devaraj et al. have worked on ^{18}F labeled nanoparticles for in vivo PET-CT imaging. They report the synthesis and in vivo characterization of a ^{18}F modified trimodal nanoparticle (^{18}F-CLIO). This particle consists of cross-linked dextran held together in core-shell formation by a super paramagnetic iron oxide core and functionalized with the radionuclide ^{18}F in high yield via "click" chemistry. The particle can be detected with positron emission tomography, fluorescence molecular tomography, and magnetic resonance imaging. The presence of ^{18}F lowers the detection threshold of the nanoparticles, whereas the facile conjugation chemistry provides a simple platform for rapid and efficient nanoparticle labeling. Nanoparticles allow multivalent attachment of small affinity ligands. In combination with optimized pharmacokinetics of parent materials would allow a modular approach to rapidly building and testing such materials.[Devaraj,2009]

Ross et al developed a fluorinated folic acid derivative. ^{19}F-click folate showed nanomolar affinity for the folate receptor on KB tumour cells, which was in a comparable range to that of native folic acid. The click chemistry approach was successfully applied to the radiolabeling of the corresponding ^{18}F-labeled folic acid derivative.
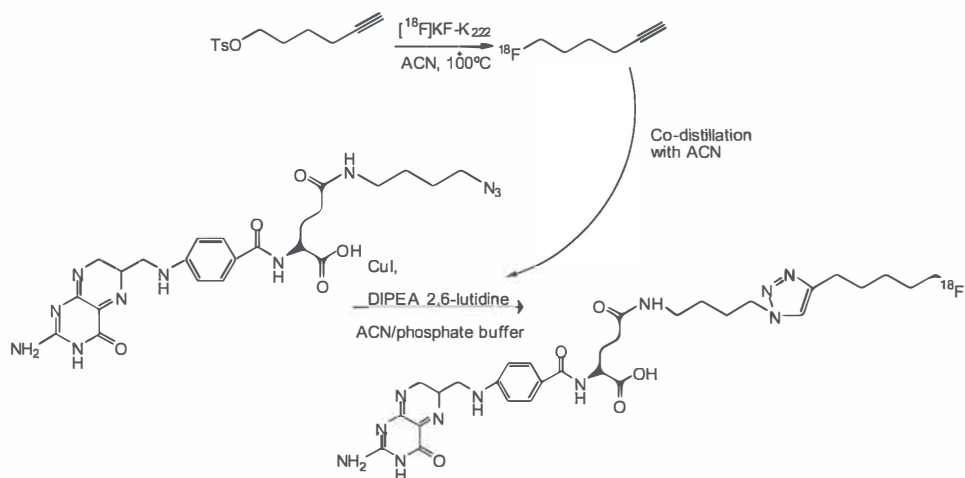
Scheme 2.10. Radiosynthesis of [18F]-Click Folate ([18F]3) via the 1,3-dipolar Cu(I)-catalyzed cycloaddition of no carrier added (n.c.a.) 6-[18F]fluoro-1-hexyne ([18F]5) and γ-(4-azido butyl)-Folic Acid Amide (6)a 4: 5-hexynyl-p-tosylate (precursor for [18F]5).

In biodistribution studies, a high specificity of [18F]-click folate to the (folate receptor) was observed. The high specificity of [18F]-click folate proves the potential of this class of compounds; however, further investigations toward novel [18F]-labeled folates with reduced lipophilicity are required to reduce non-specific uptake. [Ross,2008]

Recently, Hatanaka et al.[Hatanaka,2010] presented a novel technique for labeling siRNA using succinimidyl 4-[18F]fluorobenzoate ([18F]SFB) as a fluorine 18 labeling reagent. The antisense strand must contain a 3'-amino C6 linker for the radioactive labeling of the siRNA duplex, which is obtained with a radiochemical yield of 7.9% (21.1% for the [18F]SFB synthesis and 37.9 % for the coupling with siRNA). Therefore, to avoid the necessity of the presence of this unique phosphorothioate monoester group or a 3'-amino C6 linker, and to increase the radiochemical yield, a radiosynthetic strategy was developed based on a click reaction. Among the click reactions reported to date, the Copper-Catalyzed Azide-Alkyne Cycloaddition (CuAAC) is the most extensively explored reaction. [Sharpless,2003] The applications of the CuAAC for nucleoside, nucleotide, and oligonucleotide modifications,

have been reviewed [Sharpless,2003]. More recently, the Luxen group presented the first direct labeling of siRNA by click chemistry. An original method to functionalize a single-stranded oligonucleotides with alkyne has been described. [Luxen,2009]. After the annealing, the double stranded siRNA is engaged in the Huisgen 1,3-dipolar cycloaddition with the labeled synthon 1-(azidomethyl)-4- [^{18}F]fluorobenzene or the 1-azido-4-(3-fluoropropoxy) benzene to produce the [^{18}F]-labeled siRNA which can be used for in vivo PET imaging studies. (Scheme 2.11)
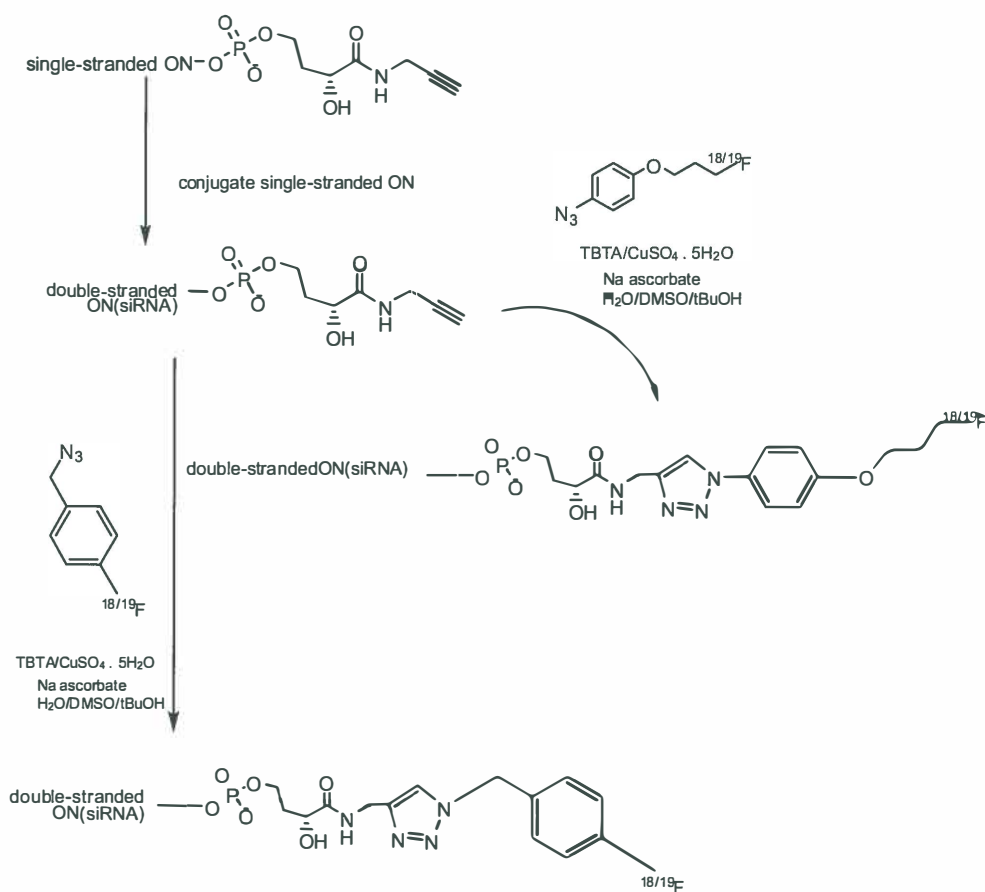
Scheme 2.11. Synthetic strategies for the preparation of ^{18}F-labelled siRNA and ^{19}F.

In the addition, the Pisaneschi group development of a new epidermal growth factor receptor positron emission tomography imaging agent based on the 3-cyanoquinoline core.

The epidermal growth factor receptor (EGFR/c ErbB1/HER1) is overexpressed in many cancers including breast, ovarian, endometrial, and non-small cell lung cancer. An EGFR specific imaging agent could facilitate clinical evaluation of primary tumors and/or metastases. The Pisaneschi group designed and synthesized a small array of fluorine containing compounds based on a 3-cyanoquinoline core. Molecular imaging techniques, such as PET (Positron Emission Tomography) have the potential to provide insights into EGFR biology. Potentially, PET with EGFR probes can determine in a non-invasive manner whether the target protein is overexpressed in a specific primary tumor or metastasis in vivo, the magnitude and duration of receptor occupancy, and target-drug interactions (including possibly the functional consequence of mutations that lead to reduced EGFR-drug interactions). A number of previously reported therapeutic agents have been labeled with radionuclides, including radiometals and radiohalogens, as potential ligands for imaging EGFR. More recent reports by Mishani et al [Mishani, 2008] have described the evaluation of radioligands based on irreversible EGFR inhibitors in which an electrophilic function is incorporated at C-6 of the quinazoline core. These derivatives bind covalently to the Cys 773 located in the tyrosine kinase binding pocket of EGFR thus preventing washout by intracellular ATP and increasing potency [Mishani, 2008].

To enable selection of the most suitable candidate radiotracer the Pisaneschi group [Pisaneschi, 2010] designed a small array of fluorine containing derivatives with the intention of selecting the best candidate on the basis of high affinity to the receptor and ease of labeling. Derivatization of N-Boc-propargylamine and enyne containing quinoline in a manner amenable to the introduction of an ^{18}F radiolabel was envisaged via 'click' cycloaddition with a fluorine containing azide partner. Propargylamine was therefore reacted with 1-fluoro-2-ethyl azide under Cu(I) catalysis and microwave irradiation to give fluorotriazole-containing quinoline as an HCl salt following Boc removal using HCl in 1,4-dioxane. Similarly, enyne reacted with azide to give fluorotriazole-containing quinoline in 32% yield. In both cases, the final yields were compromised by the apparent instability of the Michael acceptor precursors under the reaction conditions (Scheme 2.12).
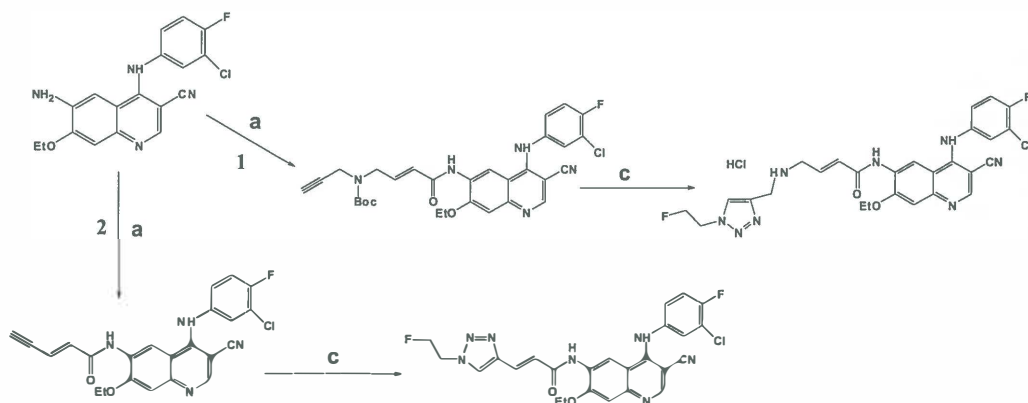
Scheme 2.12. Reagent and condition: (**a**) AlMe$_3$, CH$_2$Cl$_2$, rt., (**1**) Ethyl (E)-4-(tert-butoxycarbonyl-prop-2-ynyl-amino)-but-2-enoate, (**2**) Methyl (E)-pent-2-en-4-ynoate, (**c**) Cu powder, CuSO$_4$, Water, MW 125°C, 15 min

Potential applications for PET of click chemistry currently being employed in biomedical research

Click chemistry is applied in diverse areas such as bioconjugation, drug discovery, materials science, and radiochemistry [Schibli,2007]. Click chemistry has increasingly found applications in many aspects of drug discovery [Schibli,2007], by generating lead compounds through combinatorial methods. Bioconjugation via click chemistry is also employed in proteomics and nucleic research [`Schirrmachar,2008]. In radiochemistry, selective radiolabeling strategies of biomolecules for imaging and therapy have been realized [Schirrmachar,2008]. The following paragraphs describe several applications of click chemistry and their potential for PET is discussed.

Click chemistry in drug discovery, opportunities for PET application

A problem in drug discovery is often the slow, complex synthesis of new compounds. Click chemistry offers the opportunity to simplify and optimize these syntheses, resulting in faster, efficient reactions, especially if combinatorial approaches are being employed. As an example, click chemistry was used to synthesize peroxisome proliferator-activated receptor γ(PPAR-γ) agonists for the treatment of type II diabetes [Devasthale,2009]. Acetylene derivatives of carbohydrates were clicked to the complementary azides for the preparation of a series of multivalent triazole-linked neoglycoconjugates.[Hernandez-Mateo,2000,Morales-Sanfrutos,2003] This approach mimics the preparation of multivalent carbohydrates to increase the interaction between carbohydrates and receptors or enzymes. Another example is the 1,3-dipolar cycloaddition to prepare an AChE (acetylcholinesterase) inhibitor. [Barry,2002]

The click reaction was carried out in the presence of the AChE, so that the association of the triazole click product with AChE would produce an inhibitor. [Radic,1994,Quinn,1987] It was shown that AChE catalyzed the 1,3-dipolar cycloaddition reaction of one of the azide-alkyne combinations. When the active site of the enzyme was blocked, the triazole product was not formed. This triazole product displayed biological activities, such as anti-HIV activity [Alvarez,1994] and antimicrobial activity against Gram-positive bacteria. [Alvarez,1994] prepared a series of 1,2,3-triazole derivatives and evaluated their inhibitory activity against HIV-1 and HIV-2 in MT-4 and CEM cell cultures. No inhibition was observed against HIV-2, but one of the compounds displayed an EC_{50} for HIV-1 in both MT-4 and CEM cells at 3.7 and 3.4 mM, respectively. It was also observed that additional groups at the triazole ring promoted 5–10-fold more inhibition to HIV-1 than the unsubstituted triazole. Genin et al. synthesized a series of 1,2,3- triazole derivatives and found that most compounds had substantial higher antibacterial activity against Gram-positive and Gram-negative bacterial strains than currently used antibiotics.[Anderson,2000] Natarajan et al. reported the synthesis of a divalent single-chain fragment of a monoclonal antibody by using click chemistry to produce the peroxisome proliferator-activated receptor g (PPAR-g) agonists for the treatment of type II diabetes [Natarajan,2007]
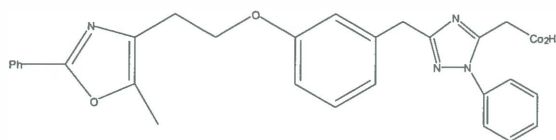
Scheme 2.13. Structure of one of the tested compounds for peroxisome proliferator-activated receptor-Y

Combinatorial approaches as described above using ^{18}F-labelled azides or alkynes could lead to more rapid identification of potent PET-tracers. In addition, such approaches can increase the role of PET in drug development since suitable PET-tracers will become more readily available.

Click chemistry in Bioconjugation

Click chemistry has become an important tool for bioconjugation procedures in the development of bifunctional molecules. Bioconjugation involves the attachment of small labelled synthons to biomolecules, such as fusing two or more proteins together or linking a carbohydrate with a peptide. Although bioconjugation is applicable to the in vivo labeling of biomolecules, only a few reactions are actually useful. [Sharpless, 2001,2003] The use of click chemistry in bioconjugation was first demonstrated by Tornoe et al. for the preparation of peptidotriazoles via solid state synthesis.[Tonon,2009] The goal was the development of efficient synthetic methods to prepare a range of triazole pharmacophores for potential biologic targets. Various novel functional and/or reporter groups were introduced into peptides and proteins, DNA [Bertozzi,2007] and cell surfaces.[Gierlich,2008]

Wang et al. labeled Cowpea mosaic virus (CPMV) with fluorescein in >95% yield.[Wang,2003] The labeling was performed by modifying the surface of the viral protein (either lysine or cysteine residues) with azides or alkynes, followed by reaction with

fluorescein-bearing complementary groups. Similarly, Link and Tirrell reported the modification of Eschericia coli with an azide-bearing outer membrane protein C (OmpC). The modified cell was then biotinylated by reacting with a biotin alkyne derivative using copper catalysis.[Link,2003]

Most bioconjugation reactions, such as isothiocyanateamine, thiol-maleimide, and amine-carboxylic acid couplings, [Kolk,2008,Francis,2006] cannot be used for labeling in vivo because of competing nucleophiles and non-compatible reaction conditions. Also, condensation reactions between ketones or aldehydes and hydrazines or aminoxy derivatives, are not feasible. The reactions are usually carried out at pH of 5–6, under which condition the resulting hydrazone or oxime bond is not very stable. In addition, other ketones or aldehydes are usually present inside the cells.[Kolk,2008] Click chemistry overcomes these obstacles by being bioorthogonal and by proceeding irreversibly in water at neutral pH and biocompatible temperatures (25–37ºC) without any cytotoxic reagents or byproducts, provided that copper-free conditions can be applied. In vivo copper free click reactions would allow pretargeting strategies using first administration of targeted antibodies contained either an alkyne or an azide functionality with slow pharmacokinetics followed by a second administration of a ^{18}F-labelled small molecule with the click counterpart functional group.

A more reactive compound for labeling biomolecules eliminates the need for toxic metal catalyst [Bertozzi,2007]. To be able to eliminate the copper catalysts would make the cycloaddition biologically friendly and thus useful for labeling biomolecules in cells. It was shown that copper-free click chemistry can label cell surface carbohydrates [Sharpless,2002],, which then move inside the cell. This chemistry helped Bertozzi [Bertozzi,2007] to study dynamic biochemical processes that are otherwise difficult to follow in real time. Of particular interest was the study of glycosylation of proteins. This reaction is difficult to follow over time because the sugar molecules, or glycans, are continuously recycled. But azides can be used as a tag for labeling biomolecules. For in vivo, copper-free application a highly reactive difluorinated cyclooctyne (DIFO) reagent was developed which rapidly reacts with azides in living cells without the need for copper catalysis. The crucial property of the substituted cyclooctyne is the high ring strain and electron-withdrawing fluorine substituents that together promote the [3 + 2] dipolar cycloaddition with azides installed metabolically into biomolecules. This Cu-free click reaction showed comparable kinetics to the Cu-catalyzed reaction and proceeded within minutes in vivo with no apparent

toxicity. Laughlin et al. were able to image glycans in developing zebrafish using click chemistry.[Laughlin,2008] Embryonic zebrafish were incubated with an azideperacetylated N-azidoacetylgalactosamine derivative (Ac4- GalNAz), which was then reacted with a difluorinated cyclooctyne attached to a dye (scheme. 2.14).

 The images obtained by flow cytometry showed high contrast and the derivates were not toxic.
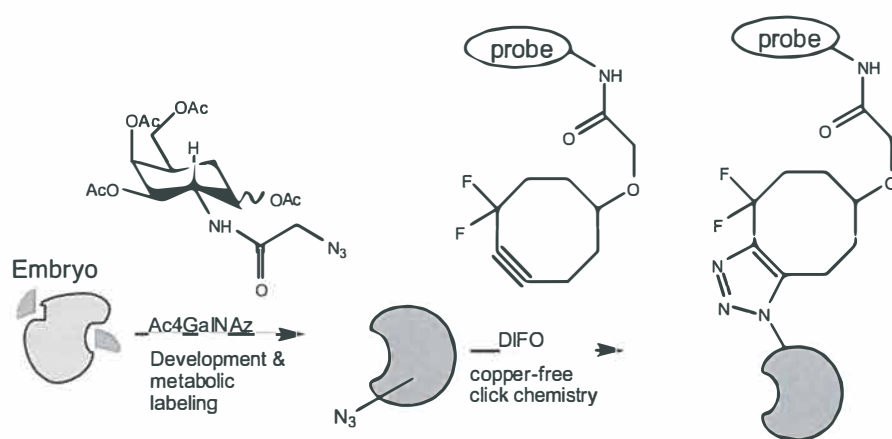
Scheme2.14. Schematic representation of metabolic labelling.

Carbohydrates by click chemistry

Multivalent carbohydrates are attractive synthetic targets as they often bind much stronger to the protein partner than their monovalent equivalents. Multivalency is often used to significantly increase affinity of weakly bound sugars [Kitov, 2000]. Many types of linkages of sugars to biological molecules have been explored and substantial affinity enhancements have been achieved [Fan, 2000- Kitov, 2000]. The copper-catalyzed click reaction has provided an additional tool for the easy construction of multivalent carbohydrates. The click method has already been applied for numerous systems. These

include protected carbohydrates but unprotected carbohydrates have also been used, demonstrating the chemoselective nature of the click reaction.

In carbohydrates an azide group can easily be introduced, either at the anomeric center or via a spacer. Even before copper catalysis was reported, the uncatalyzed click reaction was used by Calvo-Flores group, for conjugating sugars to scaffold molecules aiming at preparing multivalent carbohydrates [Calvo-Flores,2000]. It was needed to perform the reaction for long times (30 h to 6 d) and both the 1,4- and 1,5-linked regioisomeric 1,2,3-triazoles for each linkage were obtained. Prante and co-workers developed ^{18}F-labelling and glycosylation by click chemistry. A new mannosyl azide precursor was reported for the radiosynthesis of a 'clickable' ^{18}F-glycosyl donor as a hydrophilic prosthetic group. With this precursor, a simple and reliable click chemistry-based procedure involving ^{18}F-labeling and glycosylation of alkyne-functionalized molecules in high radiochemical yields has been established. The described procedure for the introduction of an ^{18}F-glucopyranoside label is advantageous due to the stability of the precursor, which is stable for months at -20º C, the hydrophilic nature of the ^{18}F-labeled prosthetic group, its high-yielding and reliable radiochemistry, and its general applicability for ^{18}F-labeling and glycosylation of alkyne-bearing molecules.(Prante,2009) (Scheme 2.15).
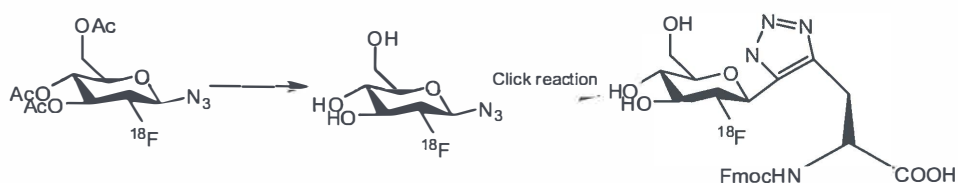
Scheme 2.15. Reagent and condition by click chemistry: $CuSO_4$, sodium ascorbate, tert-butanol, 60ºC, 10 min.

Click chemistry for the in vivo targeting of inorganic nanoparticles

The feasibility of "click" chemistry for the in vivo targeting of inorganic nanoparticles to tumors was investigated by von Maltzahn et al [Maltzahn,2007] Cyclic LyP-1 targeting peptides containing an alkyne group were linked to azido-nanoparticles and their binding to p32-expressing tumor cells in vitro was investigated. "Click" nanoparticles were able to stably circulate for hours in vivo after intravenous injection (>5 h circulation time), extravasate into tumors, and penetrate the tumor interstitium finally to specifically bind p32-expressing cells in tumors. In the future, in vivo use of "click" nanomaterials should move them forward from ligand discovery to in vivo evaluation and develop approaches toward multifunctional nanoparticle development.
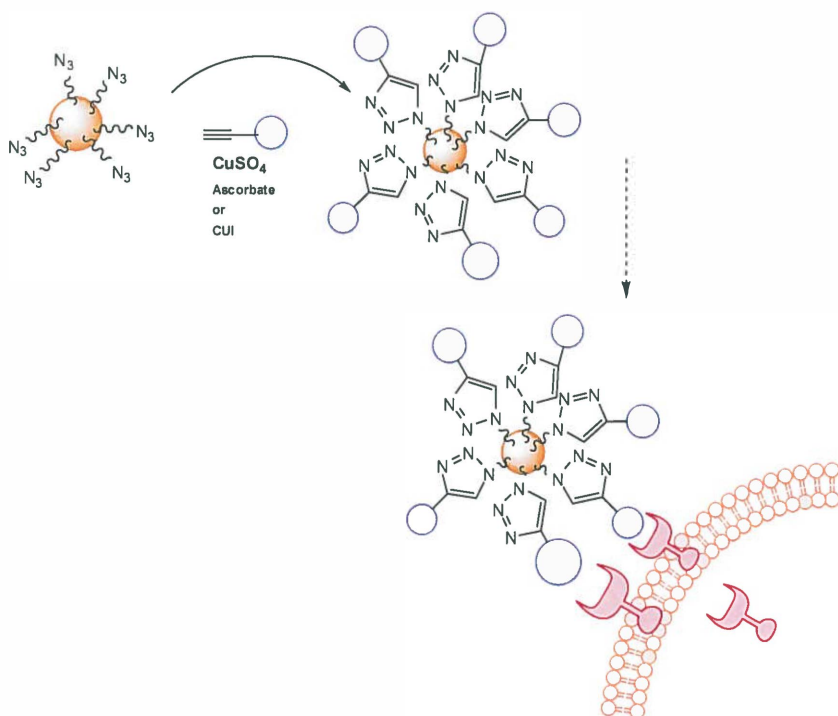
Scheme 2.15. Design of a Clickable Nanoparticle That Target Tumor Cells in Vitro and Vivo

41

Cross-linked, fluorescent, superparamagnetic iron oxide nanoparticles were modified to display azido-PEG group. Conjugation of cyclic targeting peptide bearing pendant alkynes to azido-PEG nanoparticles via the copper(I)-catalyzed Huisgen 1,3-dipolar cycloaddition.

The nanoparticles, functionalized by azido-PEG, were subsequently conjugated by copper catalysis to alkyne modified cyclic targeting peptides.

This strategy opens the way to attach different tags, resulting in nanoparticles suitable for multimodality imaging, including MRI, PET and optical imaging.

Conclusions

Click chemistry is a highly valuable approach for biomedical application. One of the unique, important properties of click chemistry is its bio-orthogonal character. Covalent and rapid linkage of two components under environmentally friendly, nontoxic conditions are properties that are completely complementary to the development of novel agents for the development of both imaging and therapeutic products. Of course, there are areas in click chemistry that require further optimization, such as real time usage in living animals, imaging of living cells, and, ultimately, the substitution of the azide group with other less potentially hazardous species. Although these are significant challenges, taking into account the speed and number of applications that click chemistry facilitates for the development of novel biomolecules for preclinical evaluation, it can be anticipated that these requirements will be met in the near future.

Novel labeling methods in ^{18}F-radiochemistry are highly desired to reduce the scale of effort necessary to obtain ^{18}F-labeled compounds for their application as imaging agents in nuclear medicine and life science. Great progress is currently made by many groups to find novel routes to introduce the ^{18}F-isotope into molecules for in vivo imaging using PET. A special focus is on the labeling of larger biomolecules such as peptides which have not been amenable to simple labeling procedures for a long time. From an economical point of view, to strengthen the role of radiochemistry in medicine and life science, it is necessary to find reliable methods for ^{18}F-labeling which can be applied by technicians on a daily basis to produce PET radiopharmaceuticals for various applications. The refinement and/or combination of the above described methods could be a crucial step into this direction.

Ideally, methodologies which are adaptable to a wide range of target molecules and prosthetic groups can be developed. The advantages gained from the intrinsic simplicity of such protocols would be achieved economically, practically and would benefit the fields of nuclear imaging and medicine. Click chemistry may offer the perfect platform for such advances in labelling due to its exquisite selectivity and tolerance to a wide range of conditions.

The introduction of the Cu(I)-catalyzed 1,3-dipolar cycloaddition click reaction has greatly widened the scope of chemoselective (bio)conjugation reactions of carbohydrates and peptides. Moreover, the 1,3-dipolar cycloaddition has opened possibilities for the synthesis of new biomaterials based on peptides and carbohydrates. The number of dipolar cycloadditions, which can be performed under mild conditions, will rapidly expand as is highlighted in this review.

Applications of Cu-free click chemistry include mammalian disease models where the bioavailability and pharmacokinetic properties of the reagents become important. The cyclooctynes that are currently employed for Cu-free click chemistry are not very soluble in aqueous solutions. The hydrophobicity of these cyclooctyne scaffolds could also promote binding to membranes or nonspecific binding to serum proteins, thereby reducing their bioavailable concentrations and increasing the noise in PET-images.

Finally the suitability of azide labeling and Cu-free click chemistry should enable applications in many areas of glycobiology. For example, direct imaging of glycan trafficking under conditions of cell stimulation or pharmacological intervention has been demonstrated already in cells, tissues, or even whole organisms.

References

- Abourbeh G, Dissoki S, Jacobson O, Litchi A, Daniel R B, Laki D, Levitzki A, Mishani E, Nucl. Med. Biol. 2007, 34, 55.
- Alvarez R, Velazquez S, San-Felix A, Balzarini J, Camarasa MJ. J Med Chem 1994, 37, 4185.
- Ametamey SM, Honer M, Schubiger PA, Chem. Rev. 2008, 108, 1501–1516.
- Angell Y, Burgess K, J. Org. Chem. 2005, 70, 9595–9598.
- Antos JM, Francis MB, Curr Opin Chem Biol 2006, 10, 253.
- Baskin JM, Bertozzi CR. QSAR Comb Sci 2007, 26, 1211.
- Bayley H, Staros JV, Academic Press Orlando FL, 1984, pp 433-490.
- Bertozzi R, PNAS, 2007, 104, 16793-16797.
- Bock VD, Hiemstra H, Maarseveen JHV, Eur. J. Org. Chem. 2006, 51–68.
- -Calvo-Flores FG, Isac-Garcia J, Hernandez-Mateo F, Perez-Balderas F, Calvo-Asin JA, Sanchez-Vaquero E, Santoyo-Gonzalez F, Org. Lett. 2000, 2, 2499 –2502.
- Calvo-Flores FG, Isac-Garcia J, Hernandez-Mateo F, Org Lett, 2000,2, 2499.
- Campbell-Verduyn L, Elsinga P H, Mirfeizi L, Dierckx R A, Feringa B L, Org. Biomol. Chem, 2008, 6, 3461–346.
- Coenen HH, Schubiger PA, Lehmann L, Friebe M, Eds. Springer Berlin Heidelberg, 2007, pp 15–50.
- Devaraj N, Bioconjugate Chem. 2009, 20, 397-410.
- Dissoki S, Aviv Y, Laky D, Abourbeh G, Levitzki A, Mishani E, Appl. Radiat.Isot, 2007, 65, 1140.
- Fan E, Z. Zhang WE, Minke Z, Hou C L, Verlinde M J, Hol WGJ, J. Am. Chem. Soc. 2000, 122, 2663–2664.
- Fazio F, Bryan MC, Blixt O, Paulson J C, Wong C H, J. Am. Chem. Soc., 2002, 124, 14397.
- Fedan J S, Hogaboom G K, O'Donnell J P, Biochem. Pharmacol. 1984, 33, 1167-1180.
- Gauthier MA, Klok HA, Chem Commun, 2008, 2591.
- Genin MJ, Allwine DA, Anderson DJ, J. Med. Chem., 2000, 43, 953.
- Geoffrey von Maltzahnl, Adv. Mater, 2007, 19, 3579–3583.
- Glaser M, Arstad E, Bioconjug. Chem., 2007, 18, 989.

- Gopi HN, Tirupula KC, Baxter , Ajith SChaike I M, Chem. Med. Chem. 1, 2006, pp. 54–57.
- Gramlich PME, Warncke S, Gierlich, J. Angew. Chem. Int., Ed, 2008, 47, 3442.
- Hatanaka K, Asai T, Koide H, Kenjo E, Tsuzuku T, Harada N, Tsukada H, Oku N, 2010, Bioconjugate Chem. 21, 756–763.
- Kitov P I,, Sadowska J M, Mulvey G, Armstrong G D, Ling H, Pannu NS, Read R J, Bundle DR, Nature., 2000, 403, 669–672.
- - Kolb H C, Finn MG, Sharpless KB, Angew. Chem., Int. Ed. 40, 2001, pp. 2004–2021.
- Kolb H C, Sharpless KB, Drug Discovery Today., 2003, pp. 1128–1137.
- Laughlin ST, Baskin JM, Amacher SL, Science 2008, 320, 664.
- Lee M, Mitchell L, Huang S J, Fokin V V, Sharpless K B, Wong C H, J. Am. Chem. Soc. 125, 2003, pp. 9588–9589.
- Lewis W G, Green L G, Grynszpan F, Radic Z, Carlier P R, Taylor P, Finn M G, Barry K, Angew. Chem., Int. Ed. 2002, 41, 1053- 1057.
- Link A J, Tirrell D A, J. Am. Chem. Soc. 125, 2003, 11164–11165.
- Link A J, Tirrell D A, J. Am. Chem. Soc., 2003, 125, 11164.
- Li Z B, Bioconj, Chem. 2007, 18, 1987-1994.
- Marik J, Sutcliffe J L, Tetrahedron Lett. 47, 2006, 6681–6684.
- Massoud T F, Gambhir S S, Genes. Dev. 2003, 17, 545–580.
- Mindt T L, Struthers H, Brans L, J. Am. Chem. Soc. 2006, 128, 15096.
- Mindt, T L, Ross T, Schibli R, J. Label. Compd. Radiopharm., 2007, 50, S34.
- Mishani E, Abourbeh G, Eiblmaier M, Anderson C, J. Curr. Pharm. Des. 2008, 14, 2983.
- Mocharla B, Colasson L, Lee V, Roper S, Sharpless K B, Wong C H, Kolb H C, Angew. Chem., Int. Ed. 44, 2004, 116–120.
- Natarajan A, Du W, Xiong C Y, Chem. Commun., 2007, 695.
- Ortu G, Ben David I, Rozen Y, Freedman N M T, Chisin R, Levitzki A, Mishani E, Int. J. Cancer 2002, 101, 360.
- Perez-Balderas F, Ortega-Munoz M, Morales-Sanfrutos J, Org. Lett., 2003, 5, 1951.
- Perez-Balderas F, Ortega-Munoz M, Morales-Sanfrutos J, Hernandez Mateo F, Calvo-Flores F G, Calvo-Asin, J A, Isac-Garcia J, SantoyoGonzalez F, Org.Lett., 2003, 5, 1951 –1954.

45

- Prante O., Carbohydrate Research, 344, 2009, 753–761.
- Quinn DM. Chem. Rev. 1987, 87, 955.
- Radominska A, Drake R R, Methods Enzymol. 1994, 230, 330-339.
- Ross. T, Bioconjugate Chem. 2008, 19, 2462-2470.
- Rostovtsev V V, Green L G, Fokin, V V, Sharpless K B, Angew. Chem., Int. Ed. 2002, 41, 2596–2599.
- Rostovtsev V V, Green L G, Fokin V V, Sharpless K B, Angew. Chem., Int. Ed. 41, 2002, 2596–2599.
- Schirrmacher R, Lakhrissi Y, Jolly D, Tetrahedron Lett, 2008, 49, 4824.
- Schirrmacher R, Wängler C, Schirrmacher E, Org. Chem. 2007, 4, 317–329.
- Sirion U, Kim H J, Lee B S, OH S J, Chi D Y J, Label. Compd. Radiopharm., 2007, 50, S37.
- Smith G, J. Med. Chem., 2008, 51, 8057-8067.
- Speers G, Adam C, Cravatt B F, J. Am. Chem. Soc. 125, 2003, 4686–4687.
- Struthers H, Mindt T L, Schibli R, 2010, Dalton Trans. 39, 675–696.
- Sutcliffe J L, 2006, Tetrahedron Letters, 47, 6681-6684.
- Taylor P, Radic Z. Ann. Rev. Pharmacol. Toxicol. 1994, 34, 281.
- Thonon D, Bioconjugate Chem. 2009, 20, 817-823.
- Tietze, Bio. Org. and Med. Chem. Lett., 18, 2008, 983-988.
- Tornoe C W, Christensen C, Meldal M, J. Org. Chem. 67, 2002, 3057–3064.
- Wang Q, Chan T R, Hilgraf R, Fokin V V , Sharpless K B, Finn M G, J. Am. Chem. Soc. 125 2003, 3192–3193.
- Wang Q, Chan T R, Hilgraf R, Fokin V V, Sharpless K B, Finn M G, J. Ame. Chemical Society, 2003, 125, 3192-3193.
- - Yun C H, Mengwasser K E, Toms A V, Woo M S, Greulich H, Wong K K, Meyerson, M, Eck M, J. Proc. Natl. Acad. Sci. U.S.A. 2008, 105, 2070.
- Zhang H, Ryono DE, Devasthale P, Bioorg. Med. Chem. Lett 2009, 19, 1451.

Chapter 3

Ligand acceleration and exploration of reaction parameters of ^{18}F-Click chemistry

Leila Mirfeizi[a], Lachlan Campbell-Verduyn[b], Rudi A. Dierckx[a], Ben L. Feringa[b], and Philip H. Elsinga[a]

[a]Department of Nuclear Medicine and Molecular Imaging, University Medical Center Groningen, University of Groningen, Groningen, The Netherlands.
[b]Stratingh Institute for Chemistry, University of Groningen, Groningen, The Netherlands.

Abstract

Objectives The aim is to establish rate acceleration of the copper catalyzed 1,3-dipolar cycloaddition using phosphoramidite ligands and to systematically explore ^{18}F-click chemistry methodology for positron emission tomography imaging tracers. Preliminary studies to find optimal conditions for the 1,3-dipolar cycloaddition of the two-step ^{18}F-labeling procedure were performed in which the cycloaddition of 4-methoxybenzyl azide and phenylacetylene was employed as a model reaction.

In addition, monodentate phosphoramidite ligands are used to accelerate the Huisgen 1,3-dipolar cycloaddition rapidly yielding functionalized 1,4-disubstituted-1,2,3-triazoles.

Methods To test our methodology on the required time scale of radiolabelling, we designed a small azido prosthetic group, [^{18}F]-fluorinated 1-azido-4-fluorobutane and [^{18}F]-fluorinated 1-ethynyl-4-(fluoromethyl)benzene.

After fluorination, the ^{18}F-fluorinated tag was attached to its complementary acetylene or azide in the presence of $CuSO_4 \cdot 5H_2O$, sodium ascorbate and the ligand MonoPhos. Further reaction optimization was performed by varying the amount of acetylene down to 0.01 mg and azide down to 0.05 mg in DMSO/H_2O (1/3).

Results Full conversion to the radiolabeled triazole was detected after 10 min. In the absence of MonoPhos under identical conditions, only minor conversion to the triazole product was observed (<20 %).

One mol % of $CuSO_4$ proved to be a sufficient amount of catalyst, to achieve a short reaction time even using very small amounts of cold precursor.

In conclusion The ligand-accelerated Cu(I)-catalyzed, 1,3-dipolar cycloaddition 'click chemistry' reaction was applied successfully to the synthesis of small, F-18-labeled molecules. [^{18}F]Fluoroalkyne and azide were prepared in yields ranging from 36% to 81%. Conjugation of [^{18}F]fluoroalkynes and azides to varying amounts (> 0.01 mg) of acetylene or azide via the CuI mediated 1,3-dipolar cycloaddition yielded the desired ^{18}F-labeled products in 10 min with yields of 54–99% in triplicate experiments. The total synthesis time was 30 min from the end of bombardment.

Introduction

[18]F-labeled compounds have been developed as the most commonly applied radiotracers for use in PET (positron emission tomography) (Kolb, 2001, 2003). Due to the low reactivity and high basicity of [^{18}F]fluoride, ^{18}F-labeled prosthetic groups are necessary for labeling complex biomolecules such as peptides and molecules with H-acidic functions (Huisgen,1962). Currently, peptide labeling is mostly confined to conjugation of free amino groups, either by direct acylation using ^{18}F-fluorinated activated esters (Huisgen,1962) or indirectly by functionalization, e.g., to an aminooxy group, which subsequently can undergo condensation with ^{18}F-fluorinated aldehydes. The high lipophilicity of the prosthetic groups can hamper application of peptide-based biomarkers. Therefore, new, efficient, and universally applicable synthetic strategies are needed. (Bertozzi, 2005)

The discovery of the Cu(I)-catalyzed version of Huisgen's dipolar [2 + 3] cycloaddition of terminal alkynes and azides by the groups of Sharpless (Sharpless,2003) and Meldal (Agard,2004) had a great impact as demonstrated by the many reports describing its application in different areas of research (P'erez,1992). In general, the formation of 1,4-disubstituted 1,2,3-triazoles by cycloaddition proceeds efficiently and selectively under aqueous reaction conditions and in the presence of various other functional groups (Huisgen,1962). This so-called "click reaction" (Glaser,2007) has also found application in the development of imaging agents (Campbell-Verduyn,2008,2009). The majority of reported applications of the click cycloaddition employ the 1, 2, 3-triazole formed as a stable linker to connect two chemical/biochemical entities. This conjugate design has been successfully applied to the preparation of optical (Candelon, 2008, Arduengo, 1999) and MR imaging agents (Brisford, 1995) and radioactive tracers suitable for SPECT and PET.

Recently, Marik and Sutcliffe adopted this reaction for the preparation of F-18-labeled, short peptide fragments, thereby demonstrating its potential use in PET studies, in which the conjugation reaction of unprotected peptides was also tested to afford good yield and purity based on the reaction tolerance of the click reaction to other functional groups such as amines, alcohols, and acids.(Huisgen,1962) As a Cu(I) catalyst, they used CuI dissolved in acetonitrile, and not in water.(Glaser, 2007) However, considering both various substance dependent reaction conditions and the strong preference of aqueous media for biomolecules, an alternative reaction system is highly warranted. Furthermore, most previous studies were restricted to the use of peptides. Up to now, no systematic studies

49

have been published on optimization of reaction parameters for the ^{18}F-click reaction. Furthermore relatively high amounts of peptide precursor have been used so far which hamper its use, because the peptides are usually quite expensive.

In applying the copper catalyzed cycloaddition to [^{18}F]-radiolabelling, additional studies towards acceleration this reaction, in particular by the use of ligands, are urgently needed. The more general ligand free 'click' reactions are too slow for ^{18}F-labeling in the absence of high copper concentrations. Monodentate phosphoramidite ligands are used to accelerate the Cu(I)-catalyzed 1,3-dipolar cycloaddition of azides and alkynes rapidly yielding a wide variety of functionalized 1,4- disubstituted-1,2,3-triazoles. Cu(I) and Cu(II) salts both function as the copper source and aqueous solutions can be used to provide excellent yields.(Campbell-Verduyn,2008)

We report herein the first example of dramatic rate acceleration and a systematic study of the reaction parameters of the catalytic 1,3-dipolar cycloaddition of azides and alkynes using phosporamidite ligands for the application to PET- tracers.

Experimental procedures

General All reactions were carried out in oven dried glassware. Reagents and solvents were purchased from Sigma-Aldrich Co. Ltd. (Gillingham, United Kingdom) and used without further purification. The radio HPLC system was a Waters System Gold instrument equipped with a gamma detector (Bioscan Flow-count). A semipreparative column (Phenomenex prodigy 5µ C18, 250 x10 mm, with a flow rate of 4 mL/min) was used as the final purification of tracers. MeCN/H_2O 60-40% was used as an analytical and preparative HPLC solvent. ^{1}H- ^{13}C- and ^{19}F-NMR were recorded on a Varian AMX400 (400 and 100.59 MHz, respectively) using $CDCl_3$ as solvent. All reactions were monitored by thin layer chromotography on Merck F-254 silica gel plates or reversed phase HPLC. Mass spectra were recorded on an AEI-MS-902 mass spectrometer by EI (70 eV) measurements. Melting points are uncorrected.

Safety Working with azides should always be done with great care. Organic azides, particularly those of low molecular weight, or with high nitrogen content, are potentially explosive. Heat, light and pressure can cause decomposition of the azides. Furthermore, the azide ion is toxic, and sodium azide should always be handled with gloves. Heavy metal

azides are particularly unstable, and may explode if heated or shaken. Any experiment in which azides are to be heated in the presence of copper should involve the use of a blast shield.

Methods

Bromo azido butane (1) and fluoro azido butane (2)

To a stirred solution of the corresponding bromo chloro butane or fluoro bromo butane (1.0 eq) in a 50 mL water/acetone mixture (1:4), NaN_3 (1.5 eq) was added. The resulting suspension was stirred at room temperature for 24 h. Dichloromethane was added to the mixture and the organic layer was separated. The aqueous layer was extracted with 3 x 10 mL aliquots of dichloromethane and the combined organic layers were dried over $MgSO_4$. Solvent was removed under reduced pressure, and the azide was sufficiently pure to be used without further work up. **(1)**.^{1}H NMR (400 MHz, $CDCl_3$): δ 7.44 (d, J= 6.8 Hz, 4H), 6.89 (d, J= 8.8 Hz, 4H); ^{13}C NMR (100.59 MHz, $CDCl_3$): δ 139.1, 132.7, 120.5, 117.7.

Ethynyl toluenesulfonate methyl benzene (3)

Ethynylbenzyl alcohol (10 mmol) was dissolved in 30 ml dichloromethane and 7 ml Et_3N. After cooling to 0 °C, TsCl (12 mmol; 2.2 g) in dichloromethane was added dropwise. The reaction mixture was stirred for 2 h at room temperature. Aqueous saturated bicarbonate was added and the mixture was extracted with 50 ml dichloromethane. The organic layers were washed with dichloromethane and the combined organic fractions were dried on $MgSO_4$. Solvents were evaporated under reduced pressure. The product was analyzed by TLC (4:1 hexane/ethyl acetate). Product **3** was purified by column chromatography on silica using hexane/dichloromethane 1:1. ^{1}H NMR (400 MHz, $CDCl_3$): δ 6.96 (d, J= 8.8 Hz, 4H), 6.89 (d, J= 8.4 Hz, 4H), 3.79 (s, 6H); ^{13}C NMR (100.59 MHz, $CDCl_3$): δ 156.9, 132.2, 119.9, 115.0, 55.4.

Ethynyl fluoro methyl benzene (4)

To a cooled solution of 350 mg ethynyl benzyl alchohol in dichloromethane (7 ml), DAST 0.24 ml was added dropwise at -10ºC over a period of 30 min, and the mixture was stirred overnight at room temperature. An aqueous solution of 5% $NaHCO_3$ (30 ml) was added to the reaction mixture at 0ºC with vigorous stirring for 30 min. After extraction with chloroform, the organic phase was washed with water and dried over Na_2SO_4. Product **4** was purified by column chromatography on silica using hexane/ether 8:1. ^{1}H NMR (400 MHz, $CDCl_3$): δ 7.27-7.39 (m, 3H), 7.00- 7.11 (m, 2H), 4.30 (s, 2H); ^{13}C NMR (100.59 MHz, $CDCl_3$): δ 162.5 (d, J= 328.7 Hz), 131.4, 129.9 (d, J= 11.4 Hz), 115.7 (d, J= 27.6 Hz), 54.0; ^{19}F NMR (200 MHz, $CDCl_3$): δ -112.3.

Procedure for the Synthesis of 1,4-disubstituted Triazoles (5,6)

$CuSO_4 \cdot 5H_2O$ 7.69 mmol (1.92 mg) of and 7.69 mmol (3.05 mg) sodium ascorbate were dissolved in 1.2 mL distilled water. To this mixture was added 62 μmol of MonoPhos (Campbell-Verduyn, 2008) in 0.4 mL DMSO. The resulting solution was vigorously stirred for 15 min. 1.8 mL of the solution was then added to a 25 mL flask containing 0.854 mmol (100 mg) of azide and 0.769 mmol (78.5 mg) of alkyne in 3 mL of a $DMSO:H_2O$ mixture (1:3). The roundbottom flask was sealed and the reaction mixture was vigorously stirred. Upon completion of the reaction, 10 mL of H_2O was added to the reaction mixture. For solid products, the reaction mixture was placed in an ice bath and the precipitated solid product was filtered and washed with 3 x 5 mL of cold water. For oil products, the resulting reaction mixture was extracted with 3 x 15 mL of dichloromethane. The organic layers were combined and dried over $MgSO_4$ and the solvent was removed by evaporation under vacuum. Crude oils were purified using silica gel chromatography (pentane:ether). The phosphoramidite ligands were also recovered from the mixture by column chromatography.

1-(4-fluorobutyl)-4-phenyl-1H-1,2,3-triazole (5)

White solid: mp 54-55 °C. 90 % yield. ^{1}H NMR (400 MHz, CDCl$_3$): δ 7.82 (d, J= 10.0 Hz, 2H), 7.76 (s, 1H), 7.42 (t, J= 10.0 Hz, 2H), 7.30-7.35 (m, 1H), 4.56 (t, J= 7.2 Hz, 1H), 4.38-4.47 (m, 3H), 2.05-2.15 (m, 2H), 1.65-1.82 (m, 2H); ^{13}C NMR (100.59 MHz, CDCl$_3$): δ 148.1, 130.8, 129.1, 128.4, 125.9, 119.7, 83.5 (d, J= 330.1 Hz), 50.1, 27.3 (d, J= 91.3 Hz), 27.2. HRMS (EI) calcd for C$_{12}$H$_{14}$N$_3$F 219.1172, found 219.1169.

1-benzyl-4-(4-fluoromethyl)phenyl)-1H-1,2,3-triazole (6)

White solid: mp 127-130 °C. 93 % yield. ^{1}H NMR (400 MHz, CDCl$_3$): δ 7.82 (d, J= 7.6 Hz, 2H), 7.67 (s, 1H), 7.31-7.42 (m, 7H), 5.58 (s, 2H), 5.38 (d, J= 48.0 Hz, 2H); ^{13}C NMR (100.59 MHz, CDCl$_3$): δ 148.0, 136.3 (d, J= 16.8 Hz), 134.9, 131.3 (d, J= 3.1 Hz), 129.5, 129.1, 128.3, 128.2 (d, J= 5.3 Hz), 126.1, 120.0, 84.6 (d, J= 166.4 Hz), 54.5. HRMS (EI) calcd for C$_{16}$H$_{14}$N$_3$F 268.1245, found 268.1243.

Radiochemistry [18F]2, [18F]4

Non-carrier added [18F] fluoride was obtained by proton bombardment of an [18O] enriched water target via the ^{18}O(p,n)^{18}F reaction. The radioactivity was trapped by passing the target water through a preactivated Sep-Pak light QMA cartridge (Waters). 1 mL solution of K$_2$CO$_3$ (4.5 mg) and Kryptofix 222 (20 mg) in water was used to elute the [18F]fluoride from the cartridge into a conical glass vial. This eluate was evaporated to dryness by three consecutive azeotropic distillations with acetonitrile (3 × 500 μL) under a gentle stream of nitrogen gas (130 °C). The dried [18F]-fluoride was then added to 3.0 mg of precursor 1 (17 μmol) or 3 (11 μmol) in 0.5 mL dry DMSO, and the mixture was heated at 140 °C for 10 min. The labeled product was absorbed on a C18-light Sep-Pak cartridge followed by washing with 10 mL H$_2$O and eluted with 5 mL pure methanol. The Sep-Pak eluate containing [18F]2 or [18F]4 was then purified and separated from its precursor with semi-preparative HPLC on a semi-preparative C18-reversed phase column (mobile phase 60/40 MeCN/H$_2$O, retention time=12 min). In addition, conversion of the reaction was monitored

by radio-TLC (silica gel, Hexane/EtAc (4:1)) (R_f values: **[^{18}F]2**=0.4; **[^{18}F]4**= 0.36) and HPLC analysis: t_R **[^{18}F]2** 10 min :**[^{18}F]4**: t_R= 12 min.

Preparation of [^{18}F]5, [^{18}F]6

[^{18}F]**2** or [^{18}F]**4** in MeCN / H_2O was added to a solution of sodium ascorbate (0.278 mg, 5 mol), CuSO$_4$ (0.07 mg, 1 mol), and phenylacetylene or benzylazide the amounts as mentioned in figure 2 and 3. Monophos ligand 0.111 mg (0.26 µmol) was added in a solvent mixture of DMF/H_2O 1mL with a ratio of 1:4. The resulting light yellow solution was stirred vigorously at room temperature for 10 min. The reaction mixture was diluted with water (10 mL) and preactivated with a C-18 light Sep-Pak cartridge. The product was trapped on the cartridge, washed with water (5 mL) and eluted with 5 mL methanol. The products were analyzed using analytical RP-HPLC, and conversion of the reaction was monitored by radio-TLC (silica gel, Hexane/EtAc (4:1)) (R_f values: **[^{18}F]5**=0.75; **[^{18}F]6**= 0.75) and HPLC analysis: t_R **[^{18}F]5** 14 min :**[^{18}F]6**: t_R= 16 min. (Scheme 3.1 and 3.2).
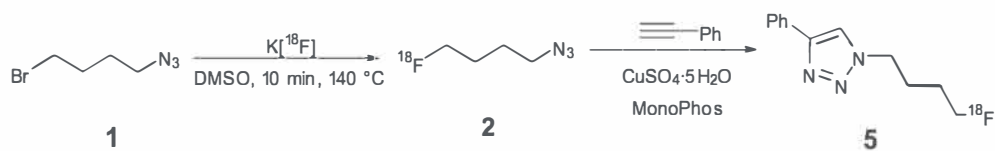
Scheme 3.1. Synthesis of [^{18}F]-labelled triazole **5** using [^{18}F]alkyl azide
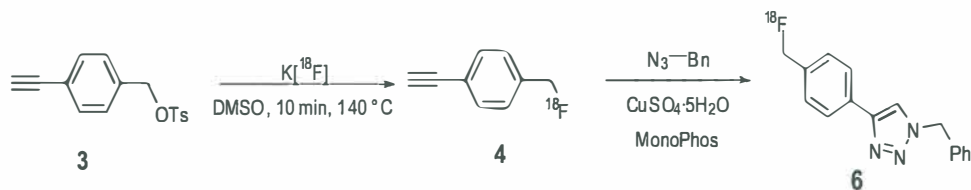
Scheme 3.2. Synthesis of [^{18}F]-labelled triazole **6** using [^{18}F]acetylene

Modified lys3-bombesin for [^{18}F]-labelling in the presence of monphos as a Ligand

Later we used monophos ligand as a acceleration of reaction to synthesis of Lysine amino acide via click reaction to test applicability to ^{18}F-peptide. The synthesis of an alkyne containing lysine analogue was initially started with the synthesis of activated ester.The product was attained by reacting propiolic acid with N-hydroxysuccinimide in the presence of the coupling reagent N,N' dicyclohexylcarbodiimide (DCC). Preparation of methyl ester analogue **7** has been done by Lachlan Campbell-Verduyn in Zernike laboratory.

Methyl-(S)-2-((tert-butoxycarbonyl)amino)-6-(pent-4 ynamido)hexanoate (7).

TMSCHN$_2$ (0.08 mL, 0.153 mmol) was dissolved in 4 mL of a toluene/methanol mixture (5:1 v/v) under an inert atmosphere of N$_2$. To this solution was added (S)-2-(tert-butoxycarbonylamino)-6-pent-4-ynamidohexanoic acid (50.0 mg, 0.153 mmol). The reaction was stirred at room temperature for 1.5 h after which it was diluted with diethyl ether (5 mL) and then with 10% AcOH (5 mL). The organic layers were collected, and the aqueous layer was extracted with diethyl ether (2 x 10 mL) and combined with the other organic layers. These were dried over MgSO$_4$ and the solvent was evaporated. The reaction must be purified immediately, storing the crude reaction mixture leads to degradation of the product. The crude mixture was purified by column chromatography (50:1 DCM:MeOH) to yield the product as a clear oil. R$_f$=0.40 (50:1 DCM:MeOH). Yield=99%. ^{1}H NMR (400 MHz, CDCl$_3$): δ

6.53 (t, J=8.0 Hz, 1H), 5.28 (d, J=8.0 Hz, 1H), 4.08-4.09 (m, 1H), 3.59 (s, 3H), 3.11 (t, J=8.0 Hz, 2H), 2.35-2.38 (m, 2H), 2.27 (t, J=4.0 Hz, 2H), 2.03-2.04 (m, 1H), 1.24-1.67 (m, 15H); ^{13}C NMR (100.59 MHz, CDCl$_3$): δ 173.2, 171.0, 155.5, 83.0, 79.9, 69.3, 53.1, 52.3, 39.0, 35.2, 32.3, 28.8, 28.3, 22.5, 14.9.   HRMS (EI) calcd for C$_{17}$H$_{28}$O$_5$N$_2$Na [M+Na$^+$] 363.1890, found 363.1883.

Compound **7** was reacted with azides **2** and **4** to yield the corresponding triazoles **8** and **9** (Scheme 3.3). The reactions proceeded relatively quickly to full conversion with 1 mol % of catalyst. In this manner, faster reaction times were achieved.
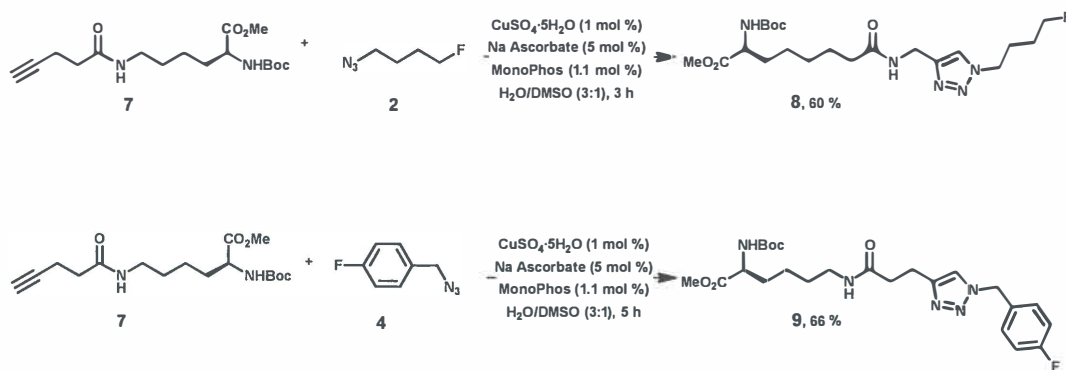
Scheme 3.3. CuAAC with lysine analogue **7**

(S)-Methyl   2-((tert-butoxycarbonyl)amino)-8-(((1-(4-fluorobutyl)-1H-1,2,3-triazol-4-yl)methyl)amino)-8-oxooctanoate (8)

(S)-methyl 2-((tert-butoxycarbonyl)amino)-6-(pent-4-ynamido)hexanoate **7** (67.5 mg, 0.20 mmol) and fluoroazidobutane **2** (28.0 mg, 0.24 mmol) were dissolved in 10 mL of an H$_2$O/DMSO (3:1) mixture. In a separate vial, CuSO$_4$·5H$_2$O (0.50 mg, 2.08 x 10^{-3} mmol) was dissolved in 0.1 mL of water, and sodium ascorbate (1.97 mg, 9.95 x 10^{-3} mmol) was added to this solution. MonoPhos (0.79 mg, 2.20 x 10^{-3} mmol) was added along with 0.1 mL of DMSO. The reagents were stirred together for 10 min and added to the solution of azide

and alkyne. The reaction mixture was allowed to stir at room temperature, and the progress was monitored by ^{1}H NMR. Upon completion of the reaction mixture was diluted with water (10 mL) and extracted with DCM. The organic layers were combined and dried over $MgSO_4$ and purified by column chromatography (1:1 DCM:MeOH) to give the product as a white solid. R_f=0.20 (100% MeOH). ^{1}H NMR (400 MHz, CDCl$_3$): δ 7.39 (br s, 1H), 6.14 (br s, 1H), 5.23 (br d, J=8.0 Hz, 1H), 4.50 (t, J=5.6 Hz, 1H), 4.34-4.37 (m, 3H), 4.21-4.22 (m, 1H), 3.70 (s, 3H), 3.14-3.18 (m, 2H), 3.01 (t, J=8.0 Hz, 2H), 1.97-2.04 (m, 2H), 1.23-1.72 (m, 17H); ^{13}C NMR (100.59 MHz, CDCl$_3$): δ 173.2, 172.1, 157.0, 123.9, 118.4, 84.2, 79.8, 53.2, 52.1, 49.6, 40.9, 38.8, 35.6, 31.9, 29.6, 28.9, 28.2, 26.4, 22.3; ^{19}F NMR (200 MHz, CDCl$_3$): 46.1-46.5 (m). HRMS (EI) calcd for $C_{21}H_{37}O_5N_5F$ [M+H$^+$] 458.2773, found 458.2768.

Methyl-(S)-2-((tert-butoxycarbonyl)amino)-6-(3-(1-(4-fluorobenzyl)-1H-1,2,3-triazol-4-yl)propanamido)hexanoate (9)

(S)-methyl 2-((tert-butoxycarbonyl)amino)-6-(pent-4-ynamido)hexanoate **7** (20.0 mg, 0.054 mmol) and 4-fluorobenzyl azide **4** (8.10 mg, 0.054 mmol) were dissolved in 3 mL of an H_2O/DMSO (3:1 v/v) mixture. In a separate vial, CuSO$_4$·5H$_2$O (0.13 mg, 5.40 x 10^{-4} mmol) was dissolved in 0.1 mL of water, and to this vial was added sodium ascorbate (0.53 mg, 2.67 x 10^{-3} mmol). MonoPhos (0.61 mg, 5.83 x 10^{-4} mmol) was added along with 0.1 mL of DMSO. The reagents were stirred together for 10 min and added to the solution of azide and alkyne. The reaction mixture was allowed to stir at room temperature, and the progress was monitored by thin layer chromatography (100% DCM). Upon completion of the reactionthe mixture was diluted with water (10 mL) and extracted with DCM. The organic layers were combined, dried over $MgSO_4$ and purified by column chromatography (1:1 DCM:MeOH) to give the product as a white solid. R_f=0.20 (100% MeOH). Yield=66%. ^{1}H NMR (400 MHz, CDCl$_3$): δ 7.31 (s, 1H), 7.23-7.26 (m, 2H), 7.04 (t, J=8.0 Hz, 2H), 5.94 (br s, 1H), 5.45 (s, 2H), 5.22 (br d, J=8.0 Hz, 1H), 4.21-4.27 (m, 1H), 3.72 (s, 3H), 3.14-3.17 (m, 2H), 3.01 (t, J=8.0 Hz, 2H), 2.52 (m, 2H), 1.32-1.83 (m, 15H); ^{13}C NMR (100.59 MHz, CDCl$_3$): δ 173.2, 172.0, 164.4, 161.1, 147.1, 130.7, 129.8 (d, J=11.3 Hz), 121.4, 116.0 (d, J=29.4 Hz), 79.9, 53.2, 53.1, 52.2, 38.8, 35.6, 32.1, 29.7, 28.3, 22.7, 21.4; ^{19}F NMR (200 MHz, CDCl$_3$): -113.4 (m). HRMS (EI) calcd for $C_{24}H_{35}O_5N_4F$ [M+H$^+$] 478.2586, found 478.2554.

Preparation of [^{18}F]8, [^{18}F]9

[^{18}F]**2** or [^{18}F]**4** in MeCN / H$_2$O was added to a solution of sodium ascorbate (0.278 mg, 5 mol), CuSO$_4$ (0.07 mg, 1 mol), and Methyl-(S)-2-((tert-butoxycarbonyl)amino)-6-(pent-4 ynamido)hexanoate **7**, and Monophos ligand 0.111 mg (0.26 µmol) was added in a solvent mixture of DMF/H$_2$O 1mL with a ratio of 1:4. The resulting light yellow solution was stirred vigorously at room temperature for 15 min. The reaction mixture was diluted with water (10 mL) and preactivated with a C-18 light Sep-Pak cartridge. The product was trapped on the cartridge, washed with water (5 mL) and eluted with 5 mL methanol. The products were analyzed using analytical RP-HPLC, and conversion of the reaction was monitored by radio-TLC (silica gel, Hexane/EtAc (4:1)) (R$_f$ values: **[^{18}F]8**=0.75; **[^{18}F]9=** 0.75) and HPLC analysis: t$_R$ **[^{18}F]8** 14 min :**[^{18}F]9**: t$_R$= 16 min. (Scheme 4 and 5).

Results and Discussion

For exploring both options of the click reaction either an alkyne or azide have been radiolabelled with fluorine-18. Nucleophilic fluorination of **1** with anhydrous non-carrier added Kryptofix 222 K$^+$[^{18}F]F$^-$ (acetonitrile, 130 °C, 15 min) provided the azide [^{18}F]**2** in 65% radiochemical yield. The same conditions were used to provide ethynyl[^{18}F] methyl benzene **4** in 85% radiochemical yield.

The phenyl acetylene or benzyl azide and catalyst were used in a large excess to [^{18}F] **2** and [^{18}F]**4**. In the experiments with CuSO$_4$ catalyst (1 mol %) was generated in situ using sodium ascorbate (5%) which was required to prevent oxidation of Cu(I) to Cu(II). This catalytic system provided [^{18}F]**5** and [^{18}F]**6** in high radiochemical yields at room temperature in 10 min in presence of Cu(I) and monophos as a ligand (figure 3.1).
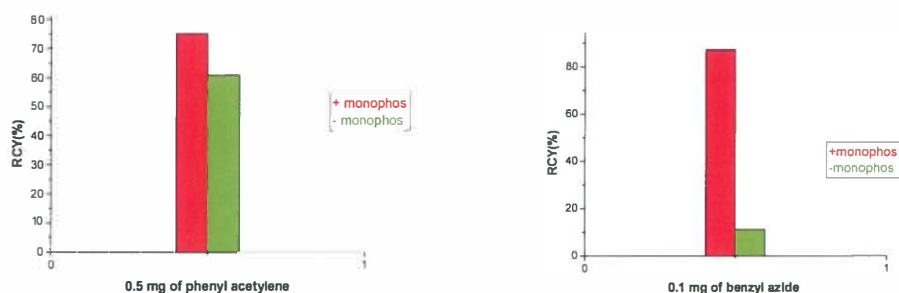
Figure 3.1. Comparison RCY % of click reaction with and without monophos as a ligand for A: [^{18}F]**5** and B: [^{18}F]**6**

The radiolabeled compounds were isolated from the reaction mixture using a C18 Sep-Pak by extraction with methanol. The radiochemical purity of the products was determined by RP-HPLC analysis providing RCP of >99% and specific activities of 95 GBq/μmol. The phosphoramidite ligand Monophos providing to be an excellent ligand for the catalytic click reaction giving high yields, but in absence of ligand only minor conversion to the triazole product [^{18}F]**6** was observed. (Figure 1)

For the synthesis of triazole [^{18}F]**5** this ligand acceleration effect was much less pronounced since the radiochemical yield was already 60 % without the use of Monophos as a ligand for copper. (Figure 1)

Further reaction optimization was performed by varying the amount of acetylene from 0.01 mg to 0.5 mg. (Scheme 1), (Fig. 2). Reactions with only 0.01 mg acetylene yielded the ^{18}F-triazole [^{18}F]**5** in more than 50% radiochemical yield with a total synthesis time of 55 min.
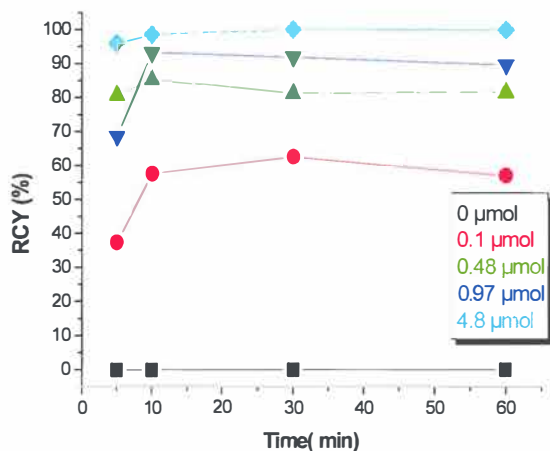
Figure 3.2. Result of optimization of reaction by varying the amount of phenyl acetylene in [^{18}F]**5**

Also the complementary click reaction to **[^{18}F]6** was investigated by varying the amount of azide from 0.01 mg to 0.05 mg (scheme 3.2; figure 3.3). Again, 1 mol % of CuSO$_4$ in the presence of 1.1 mol % monophos showed a sufficient catalysis effect within 10 min.

Figure 3.3. Result of optimization of reaction by varying the amount of benzyl azide in [^{18}F]**6**

The optimized conditions utilizing Cu(I) and Monophos as a potent catalyst provide an important tool to use reduced amounts of peptide precursor, that are expensive in many cases. In literature reports usually amounts of >1 mg peptide have been used and no additional catalyst besides Cu(I) was employed. Assuming an average MW of 2000 for peptides, 1 mg is 0.5 umol, whereas under the conditions described in this paper 10-fold lower amounts of cold precursor have been used. The click reaction is completed in 10 min, whereas in comparable system described in the literature reaction times of 15-30 min are required.

The modified lysine alkyne and catalyst were used in a large excess to [^{18}F] **4** and [^{18}F]**2**. In the experiments with CuSO$_4$ catalyst (1 mol %) was generated in situ using sodium ascorbate (5%) which was required to prevent oxidation of Cu(I) to Cu(II). This catalytic system provided [^{18}F]**8** and [^{18}F]**9** Scheme 3.4 and 3.5. in high radiochemical yields at room temperature in 15 min in presence of Cu(I) and monophos as a ligand .

The radiolabeled compounds were isolated from the reaction mixture using a C18 Sep-Pak by extraction with methanol. The radiochemical purity of the products was determined by RP-HPLC analysis providing RCP of >99% and specific activities of 95 GBq/μmol.
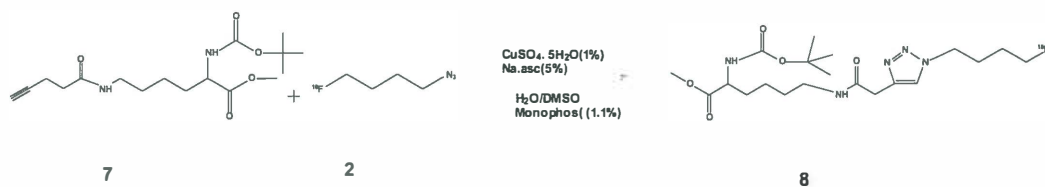
Scheme 3.4. CuAAC with lysine analogue **8**
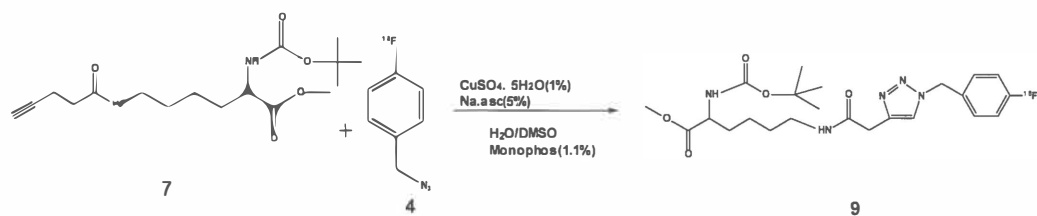
Scheme 3.5. CuAAC with lysine analogue **9**

Further reaction optimization was performed by varying the amount of modified lysine with alkyne from 1 mg to 12 mg. (Fig. 3.4) Reactions with only 1 mg lysine yielded the ^{18}F-triazole [^{18}F]**8** in more than 40% radiochemical yield purity with a total synthesis time of 55 min.
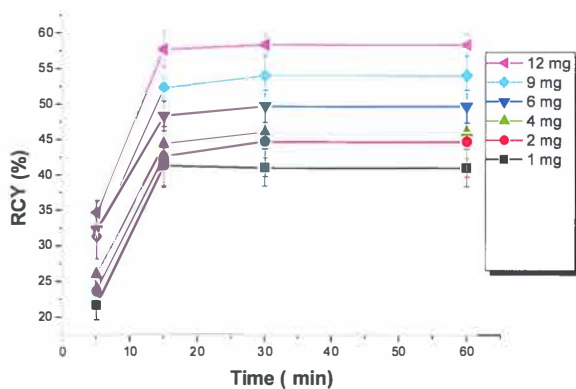
Figure 3.4. Result of optimization of reaction by varying the amount of lysine in [^{18}F]**8**

Also the complementary click reaction to **[^{18}F]9** was investigated by varying the amount of azide from 1 mg to 12 mg (figure 3.5). Again, 1 mol % of CuSO$_4$ in the presence of 1.1 mol % monophos showed a sufficient catalysis effect within 10 min. ^{18}F-triazole [^{18}**F]9** in more than 90% radiochemical yield purty with a total synthesis time of 55 min.
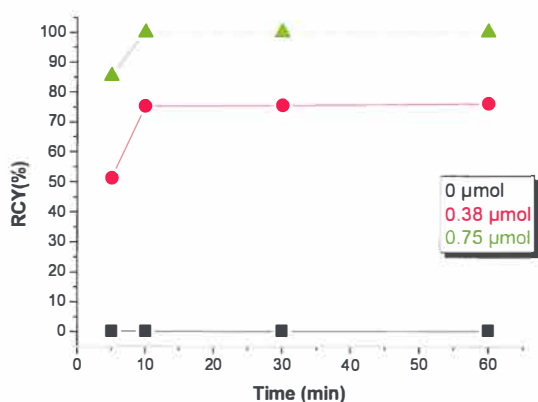

Figure 3.5. Result of optimization of reaction by varying the amount of lysine in [^{18}F]**9**

Conclusion

The ligand accelerated Cu(I)-catalyzed, 1,3-dipolar cycloaddition 'click chemistry' reaction was applied successfully to the synthesis of small, F-18-labeled molecules, and an optimal condition was developed for a one-pot, two-step reaction. After purification by semipreparative HPLC fluoroalkynes were obtained in yields ranging from 65% to 85%. Conjugation [^{18}F]fluoroalkynes to various amount (> 0.01 mg) of acetylenes or azide with via CuI mediated 1,3-dipolar cycloaddition yielded the desired ^{18}F-labeled products in 10 min with yields of 54–99% and excellent radiochemical purity (81–99%). The total synthesis time was 30 min from the end of bombardment.

In conclusion, a highly versatile fast ligand-accelerated copper catalyzed click reaction for the introduction of ^{18}F-radiolabel was developed.

References

- Agard N J, Prescher J A, Bertozzi C R, J. Am. Chem. Soc., 2004, 126, 15046.
- Arduengo A J, Krafczyk R, Schmutzler R, Craig H A, Goerlich J R, Marshall W J, Unverzagt M, Tetrahedron, 1999, 55, 14523.
- Berrisford D J, Bolm C, Sharpless K B, Angew. Chem. Int. Ed., 1995, 1059.
- Campbell-Verduyn L, Elsinga P H, Mirfeizi L, Dierckx R A, Feringa B L Org. Biomol. Chem., 2008, 6, 3461–3463.
- Campbell-Verduyn L, Mirfeizi L, Elsinga P H, Dierckx R A, Feringa B L Chem. Commun., 2009, 2139–2141.
- Candelon N D, Lastécouères A K, Diallo J R, Aranzaes D, Vincent J, Chem. Comm., 2008, 741-743.
- Feringa B L, Acc. Chem. Res., 2000, 33, 346.
- Glaser M, Bioconjugate Chem., 2007, 18,989.
- Huisgen R, Knorr R, Naturwissenschaften, 1962, 48, 716.
- Kolb H C, Sharpless K B, Drug Discovery Today, 2003, 8, 1128.
- Kolb H C, Finn M G, Sharpless K B, Angew. Chem., Int. Ed., 2001, 40, 2004.
- Li Z T, Seo S, Ju J, Tetrahedron Lett., 2004, 45, 3143.
- P´erez D, Guiti´ E, Castedo L, J. Org. Chem., 1992, 57, 5911.
- Prescher J A, Bertozzi C R, Nat. Chem. Biol., 2005, 1, 13.

Chapter 4

[18]F-(fluoromethoxy)ethoxy)methyl)-1H-1,2,3-triazol-1-yl)propan-2-ol (^{18}F-FPTC), a novel PET-ligand for cerebral beta-adrenoceptors

L. Mirfeizi[a], A. A. Rybczynska[a], A. van Waarde[a], L. Campbell-Verduyn[b], B.L. Feringa[b], R.A.J.O Dierckx[a], P.H. Elsinga[a]

a. Dept. of Nuclear Medicine and Molecular Imaging, University Medical Center Groningen, University of Groningen, Groningen, the Netherlands

b. Stratingh Institute for Chemistry, University of Groningen, Groningen, the Netherlands

Abstract

Cerebral β-adrenergic receptors (β-ARs) play important roles in normal brain and changes of ß-AR expression are associated with several neuropsychiatric illnesses. Given the high density of β-AR in several brain regions, quantification of β-AR levels using PET is feasible. However, there is a lack of radiotracers with suitable biological properties and meeting safety requirements for use in humans. We developed a PET tracer for β-AR by ^{18}F-fluorination of (R)-1-((9H-carbazol-4-yl)oxy)-3-4(4-((2-(2-(fluoromethoxy)-ethoxy)methyl)-1H-1,2,3-triazol-1-yl)propan-2-ol (^{18}F-FPTC).

Methods ^{18}F-FPTC was synthesized by Cu(I)-catalyzed alkyne-azide cycloaddition. First, ^{18}F-PEGylated alkyne was prepared by ^{18}F-fluorination of the corresponding tosylate. Next ^{18}F-PEGylated alkyne was reacted with an azidoalcohol derivative of 4-hydroxycarbazol in the presence of the phosphoramidite Monophos as a ligand and Cu(I) as a catalyst. After purification with radio-HPLC, the binding properties of ^{18}F-FPTC were tested in β-AR-expressing C6-glioma cells in vitro, and in Wistar rats in vivo, using microPET.

Results The radiochemical yield of ^{18}F-PEGylated alkyne was 74-89%. The click reaction to prepare ^{18}F-FPTC proceeded in 10 min with a conversion efficiency of 96%. The total synthesis time was 55 min from the end of bombardment. Specific activities were >120 GBq/μmol. Propranolol strongly and dose-dependently inhibited the binding of both ^{125}I-ICYP and ^{18}F-FPTC to C6 glioma cells, with IC50 values in the 50-60 nM range. However, although both FPTC and propranolol inhibited cellular ^{125}I-ICYP binding, FPTC decreased ^{125}I-ICYP uptake by only 25%, whereas propranolol reduced it by 83%. [18]FPTC has the appropriate lipophilicity to penetrate the blood brain barrier (logP +2.48). The brain uptake reached a maximum within 2 min after injection of 20-25 MBq [18]FPTC. SUV values ranged from 0.4 to 0.6 and were not reduced by propranolol. Cerebral distribution volume of the tracer (calculated from a Logan plot) was increased rather than decreased after propranolol treatment.

Conclusion 'Click chemistry' was successfully applied to the synthesis of ^{18}F-FPTC resulting in high radiochemical yields. ^{18}F-FPTC showed specific binding in vitro, but not in

vivo. Based on the logP value and its ability to block ^{125}I-ICYP binding to C6 cells, FPTC may be a lead to suitable cerebral β-AR ligands.

Ch. 4

Introduction

β-Adrenoceptors (β-ARs) belong to the family of guanine nucleotide binding regulatory protein-coupled receptors (G-protein coupled receptors) (Kobilka 2011).

Based on ligand binding studies, β-ARs have been classified into three subtypes: β_1, β_2 and β_3 (Kobilka 2011). β_1-ARs are located mainly in heart and kidney, whereas β_2-ARs are localized mostly in smooth muscles (bronchial muscle, ciliary muscle of eye and detrusor muscle of the bladder), skeletal muscles (Kim 1991), liver and GI tract (Arner 1990, Sano 1993, Krief 1993). β_3-ARs are found in adipose tissue (Krief 1993).

β_1- and β_2-ARs are present in several brain regions, such as frontal cortex, caudate, and putamen (Rainbow 1984). β_1-ARs are highly expressed in neurons and β_2-ARs in glia. The receptors are involved in astrogliosis and microglial proliferation. Cerebral β-AR levels were shown to be altered in several neurological disorders (e.g. Parkinson's, Alzheimer's and Huntington's disease), and in mood disorders (e.g. major depressive disorder and schizophrenia) (van Waarde 2004, Russo-Neustadt 1997, McEwen 1999).

Several radioligands for β-AR (e.g. S-^{11}C-carazolol, S-^{11}C-CGP12388 and S-^{11}C-CGP12177) have been validated for imaging of myocardial receptors using positron emission tomography (PET) (Law 1993, Berridge 1994, van Waarde 1995, 2004, Elsinga2004, van Waarde 2005). Nevertheless, there is a lack of clinically applicable radioligands capable of penetrating the blood-brain barrier (BBB) and monitoring changes in cerebral β-AR expression in various stages of the disease, or receptor occupancy during treatment (e.g. with norepinephrine, serotonin reuptake inhibitors and tricyclic antidepressants).

Two tracers that have shown good BBB penetration, high affinity and specificity towards β-ARs, S-1'-^{18}F-fluorocarazolol and S-1'-^{18}F-fluoroethylcarazolol, displayed mutagenic properties and are therefore unsuitable for human use (Doze 2000, 2002). Radiolabeled analogs of pindolol (e.g. ^{125}I-ICYP) also display high affinity and specificity towards β-ARs. However, their use for imaging of cerebral β-ARs is limited because of low brain uptake and low signal-to-noise ratios (Doze 2002). Therefore, to date the development of tracers for β-ARs in the human brain has been unsuccessful.

In this study, we report a rapid synthesis method of a ^{18}F-labeled tracer aimed at imaging of cerebral β-ARs, using Huisgen's 1,3-dipolar cycloaddition of an alkyne with an azide, a reaction known as 'click chemistry'.

The 'click reaction' catalyzed by Cu(I) is a well established method for rapid and highly efficient synthesis of 1,4-disubstituted-triazoles from a wide variety of substrates (Campbell-Verduyn 2010). Using this method the hydroxyl propylamine moiety (crucial for binding to β-ARs) was partially maintained but ^{18}F was introduced as a novel moiety, hopefully not causing mutagenicity of the carazolol derivatives. The resulting ^{18}F-fluorinated analog of carazolol, carbazol fluoroethoxy methyl triazolyl propanol ([18]FPTC, **7**), was produced by a click reaction between a PEGylated ^{18}F-alkyne and a (R)-azidoalcohol derivative of 4-hydroxycarbazol. We have evaluated this new β-AR tracer both in vitro and in vivo.

Materials and Methods.

General

Chemicals and solvents were obtained from commercial sources and were of analytical grade. ^{125}I-ICYP was obtained from Perkin Elmer (Waltham, MA, USA) and R-(±)propranolol hydrochloride was purchased from Sigma-Aldrich (St. Louis, MO, USA). For the semi-preparative HPLC-purification of ^{18}F-FPTC, a Phenomenex Prodigy C_{18} (250 mm * 10 mm, 5 µm) HPLC column was used. NMR spectra were acquired on a GE 7 T (400 MHz) spectrometer. Chemical shifts are given in ppm relative to the internal TMS signal, coupling constants J in Hz. Unless otherwise indicated, all NMR data were collected at room temperature in $CDCl_3$. MS were measured under ESI, MALDI or APCI conditions. Analytical thin-layer chromatography (TLC) was carried out on commercial Merck silica gel 60 plates (0.25 µm thickness) with fluorescent indicator (F-254). Column chromatography was performed with 40-63 µm silica gel. Tetrahydrofuran (THF) was freshly distilled from sodium/benzophenone; other solvents were used as received. Unless otherwise specified, all reactions were carried out under an atmosphere of dry nitrogen in oven-dried (at least 6 h at 140 ºC) glassware.
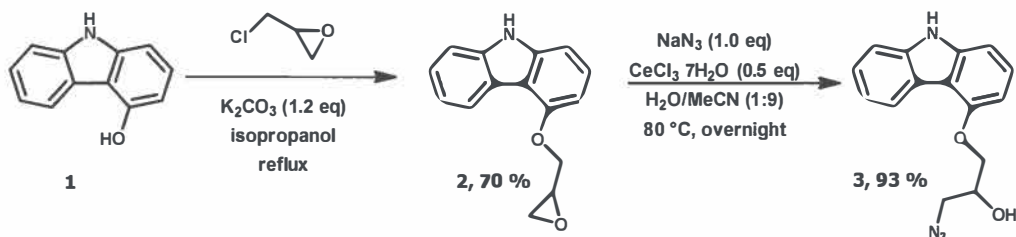
Scheme 4.1. Synthesis of racemic carbazol epoxide **2** and azidoalcohol **3**

(R,S)-4-(oxiran-2-ylmethoxy)-9H-carbazole (2)

9H-Carbazol-4-ol **1** (100.0 mg, 0.55 mmol) was dissolved in 20 mL of isopropanol, supplemented with (R,S)-epichlorohydrin (75.9 mg, 0.82 mmol) and potassium carbonate (90.5 mg, 0.65 mmol), and reacted overnight (at 80 °C). After subsequent cooling, NH_4Cl (15 mL) was added to the solution. The resulting mixture was extracted with dichloromethane (3 x 15 mL). The organic layers were separated, washed with brine, dried over $MgSO_4$ and the solvent was removed by Rotavapor. The product **2** (Scheme 4.1) was isolated by column chromatography (EtOAc:pentane, 3:1); R_f = 0.75 (EtOAc:pentane, 3:1). Yellow solid; yield: 91 mg (70%). ^1H NMR (400 MHz, $CDCl_3$): δ 8.36 (d, J = 8.0 Hz, 1 H), 8.04 (s, 1 H), 7.25-7.42 (m, 4 H), 7.01 (d, J = 8.0 Hz, 1 H), 6.64 (d, J = 12 Hz, 1 H), 4.44 (d, J = 16.0 Hz, 1 H), 4.22 (m, 1 H), 3.54 (m, 1 H), 2.98 (m, 1 H), 2.88 (m, 1 H). ^{13}C NMR (100.59 MHz, $CDCl_3$): 155.1, 141.2, 139.0, 126.8, 125.3, 123.4, 122.6, 119.9, 112.9, 110.3, 104.3, 101.5, 69.0, 50.6, 45.1. The spectroscopic data is in accordance with the literature (S.L. Heald 1983).

1-((9H-carbazol-4-yl)oxy)-3-azidopropan-2-ol (3)

NaN_3 (12.1 mg, 0.19 mmol) was added to a mixture of 4-(oxiran-2-ylmethoxy)-9H-carbazole **2** (40.5 mg, 0.17 mmol) and $CeCl_3·7H_2O$ (22.2 mg, 0.09 mmol) in 4.0 mL of acetonitrile/water (9:1). The resulting solution was stirred at reflux overnight. The reaction

mixture was diluted with dichloromethane and washed with water (5 mL) and brine (2 x 5 mL). The organic layer was separated dried over $MgSO_4$ and the solvent was removed under reduced pressure. The product **3** (Scheme 4.1) was purified by column chromatography (EtOAc:pentane, 2:1); R_f = 0.8. White solid; yield: 41.35 mg (93 %). ^{1}H NMR (400 MHz, $CDCl_3$): δ 8.21 (d, J = 8.0 Hz, 1 H), 8.07 (s, 1 H), 7.26-7.44 (m, 4 H), 7.02 (d, J = 8.0 Hz, 1 H), 6.61 (d, J = 8.0 Hz, 1 H), 4.33 (m, 1 H), 4.20 (d, J = 8.0 Hz, 2 H), 3.60 (m, 2 H), 2.78 (br s, 1 H). ^{13}C NMR (100.59 MHz, $CDCl_3$): 154.4, 140.8, 138.6, 126.4, 124.9, 122.5, 121.9, 119.4, 112.2, 110.1, 104.1, 100.8, 69.4, 69.0, 53.6. The spectroscopic data is in accordance with the literature (G. Madhusudhan 2010).

2-{2-[2-(Prop-2-ynyloxy)ethoxy]ethoxy}ethanol (4)

Sodium hydride (2.60 g, 65 mmol, 60%) was slowly added to a solution of triethylene glycol (15.02 g, 100 mmol) in distilled THF (75 mL) and the mixture stirred for 30 min (all carried out at 0 ºC under nitrogen atmosphere). Propargyl bromide (5.40 mL, 7.44 g, 50 mmol) was slowly injected to the reaction flask, thereafter stirred at 0 ºC for 2 h and at 25 °C for 20 h. The mixture was poured into water, extracted with CH_2Cl_2 and the organic phase dried over Na_2SO_4. The crude product was purified by flash chromatography using EtOAc:hexane (3:2) as the eluent, to afford compound **4** (Scheme 4.2).

Clear yellow oil; yield: 7.1 g (75%). ^{1}H NMR (400 MHz, $CDCl_3$): δ 4.21 (d, 2 H, J = 2.2 Hz, $CHCCH_2O$), 3.74-3.66 (m, 11 H, OCH_2 and OH) 3.61 (t, 2 H, J = 4.6 Hz, CH2OH), 2.43 (t, 1 H, J = 2.4 Hz, $CHCCH_2$). ^{13}C NMR (125 MHz, $CDCl_3$): δ 79.68, 74.72, 72.60, 70.76, 70.51, 70.47, 69.20, 61.89, 58.54.

2-{2-[2-(Prop-2-ynyloxy)ethoxy]ethoxy}ethyl-methylbenzenesulfonate (5)

p-Toluenesulfonyl chloride (20.82 g, 109.24 mmol) was slowly added to a solution of: **4** (10.28 g, 54.62 mmol), triethylamine (19.0 mL, 136.5 mmol) and trimethylamine hydrochloride (0.522 g, 5.46 mmol) in acetonitrile (140 mL) (at 0 °C under nitrogen atmosphere). This mixture was stirred at 0 °C for 50 min and at room temperature for 30 min under nitrogen atmosphere, subsequently poured into water, extracted with EtOAc and

the organic solution dried over MgSO$_4$. The crude product was purified by flash chromatography using EtOAc:hexane (1:3) as eluent to afford compound **5** (Scheme 4.2). Clear yellow oil; yield: 16.19 g (87%). ^{1}H NMR (400 MHz, CDCl$_3$): δ 7.80 (d, 2 H, J = 8.2 Hz, ArH), 7.34 (d, 2 H, J = 8.2 Hz, ArH), 4.19 (d, 2 H, 2.2 Hz, CHCCH$_2$O), 4.16 (t, 2 H, J = 4.7 Hz, CH$_2$OTs), 3.70-3.67 (m, 4 H, OCH$_2$), 3.65-3.63 (m, 2 H, OCH$_2$), 3.59 (s, 4 H, OCH$_2$), 2.45 (s, 3 H, ArCH$_3$), 2.43 (t, 1 H, J = 2.3 Hz, CHCCH$_2$). ^{13}C NMR (125 MHz, CDCl$_3$): δ 144.93, 133.18, 129.97, 128.14, 79.77, 74.68, 70.90, 70.72, 70.59, 69.37, 69.24, 68.85, 58.55, 21.79.

1-((9H-carbazol-4-yl)oxy)-3-(4-((2-(2-(fluoromethoxy)ethoxy)ethoxy)methyl)-1H-1,2,3-triazol-1-yl)propan-2-ol (7)

Compound **3** (6.0 mg, 0.021 mmol) and 3-(2-(2-(fluoromethoxy)ethoxy)ethoxy)prop-1-yne (7.8 mg, 0.043 mmol) were dissolved in 3.0 mL of water:DMSO (4:1). To this solution were added: 5 mol % CuSO$_4$·5H$_2$O (1.0 x 10^{-3} mmol), 25 mol % sodium ascorbate (5.25 x 10^{-3} mmol) and 5.5 mol % MonoPhos (1.12 x 10^{-3} mmol). The reaction mixture was allowed to stir at room temperature and progress of the reaction was monitored by thin layer chromatography. Upon complete consumption of the azidoalcohol, the reaction mixture was diluted with water and extracted with DCM. The organic layer was dried over MgSO$_4$ the solvent evaporated and the product **7** FPTC (Scheme 4.2) was purified by column chromatography (EtOAc:pentane, 2:1); R$_f$ = 0.15 (EtOAc:pentane, 1:1).
White solid; yield: 25.0 mg (88 %). ^{1}H NMR (400 MHz, CDCl$_3$): δ 8.23 (d, J = 8.0 Hz, 1 H), 8.20 (s, 1 H), 7.70 (s, 1 H), 7.41-7.45 (m, 2 H), 7.24-7.27 (m, 2 H), 7.09 (d, J = 8.0 Hz, 1 H), 6.62 (d, J = 8.0 Hz, 1 H), 4.77-4.80 (m, 1 H), 4.64-4.67 (m, 4 H), 4.58 (t, J = 4.0 Hz, 1 H), 4.46 (t, J = 4.0 Hz, 1 H), 4.22 (d, J = 4.0 Hz, 2 H), 3.73 (t, J = 8.0 Hz, 1 H), 3.63-3.67 (m, 8 H), 3.30 (br s, 1 H). ^{13}C NMR (100.59 MHz, CDCl$_3$): 154.3, 147.2, 141.0, 138.7, 136.1,135.9, 126.7, 125.2, 122.6,122.1, 119.8, 112.5, 110.4, 104.4, 101.2, 70.7, 70.5, 70.4, 69.6, 69.1, 68.8, 64.5, 53.4. ^{19}F NMR (200 MHz, CDCl$_3$): 42.6 (m).

Radiolabeling (7)

Aqueous ^{18}F-fluoride was produced by irradiation of ^{18}O water with a Scanditronix MC-17 cyclotron via the ^{18}O(p,n)^{18}F nuclear reaction. The ^{18}F-fluoride solution was passed through a Sep-Pak Light Accell plus QMA anion exchange cartridge (Waters) to recover the ^{18}O-enriched water. ^{18}F-fluoride was eluted from the cartridge with 1 mL of K_2CO_3 (4.5 mg/mL) and collected in a vial with 20 mg Kryptofix 2.2.2. To this solution, 1 mL acetonitrile was added and the solvents were evaporated at 130 °C. The ^{18}F-KF/ Kryptofix complex was dried 3 times by the addition of 0.5 mL acetonitrile, followed by evaporation of the solvent. ^{18}F-PEGylated alkyne **4** was prepared by ^{18}F-fluorination of the corresponding tosylate **5** (1-2 mg) in DMSO at 140°C during 15 min. Thereafter, the product was diluted with 20 mL of water and passed through a tC18 cartridge (activated with 5 mL EtOH and 10 mL H_2O). The product **4** (scheme 4.2) was eluted from the cartridge with 4 mL of water and purified by HPLC (10% EtOH in NaH_2PO_4, 0.025 M, (pH 7); 4 mL/min; retention time of 16 min). ^{18}F-FPTC **7** was synthesized by click reaction (reaction time 10 min) of **4** with **3** in the presence of the phosphoramidite Monophos (1,1 mol %) as a ligand,(1.1mol %) and $CuSO_4 \cdot 5H_2O$ (1 mol%), Na-ascorbate (5 mol %) in mixture of DMF:H_2O (3:1) as catalyst, followed by purification with radio-HPLC, The retention time was 16 min. (Scheme 4.2)
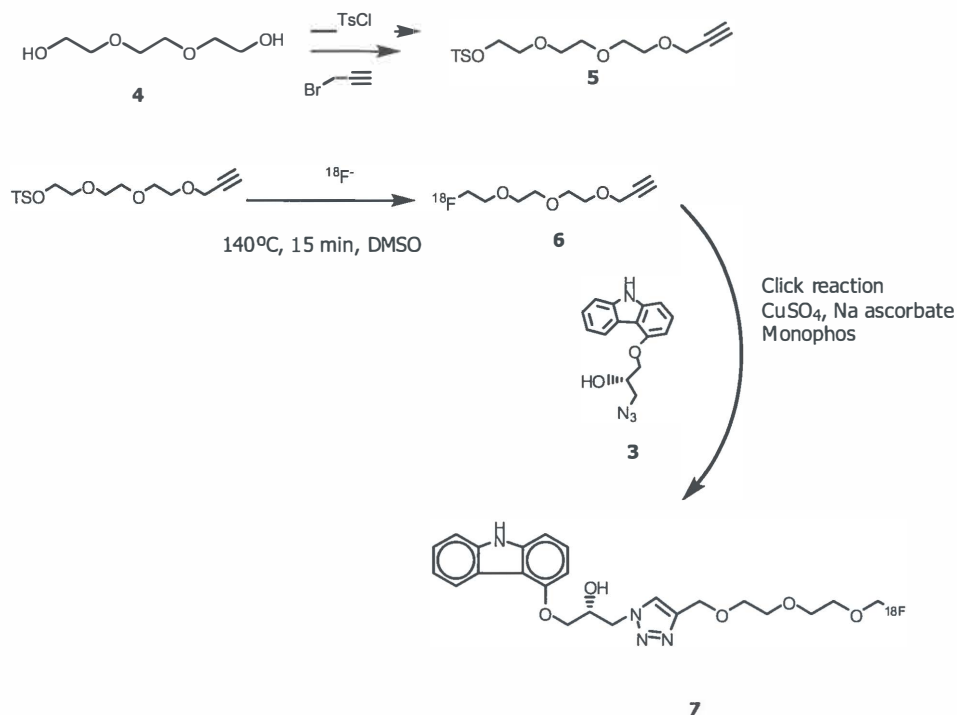
Scheme 4.2. Synthesis of ^{18}F-FPTC

Stability of ^{18}F-FPTC

Samples of ^{18}F-FPTC were dissolved in Phosphate buffered saline (PBS) (1 mL) or rat plasma (1 mL) and incubated at 37 °C. After 1 h and 3 h of incubation, respectively, the stability of the radiolabeled ^{18}F-FPTC was determined by Radio-TLC (R_f FPTC 0.4; eluent: MeOH:CH$_2$Cl$_2$ (2:8) + 0.1% Et$_3$N). After elution, the TLC plates were analyzed by phosphor storage imaging using a Cyclone Phosphor Storage System (PerkinElmer). The conversion rate of ^{18}F-FPTC was calculated by ROI analysis using Opti-Quant software (PerkinElmer) and expressed as a percentage of the parent compound lost over the incubation time.

Distribution Coefficient (logP)

To determine the logP of ^{18}F-FPTC, an aliquot of 1 mL of HPLC purified ^{18}F-FPTC solution was added to a mixture of n-octanol/PBS (1:1, v/v) at pH 7.4. The tubes were vortexed at room temperature for 1 min, followed by 30 min of shaking in a water bath at 37 °C. Aliquots of 25 and 1000 µL were drawn from the n-octanol and aqueous phase, respectively, and the radioactivity was counted using an automated gamma counter (Compugamma 1282 CS, LKB-Wallac, Turku, Finland). The experiments were performed in triplicate.

Cell Culture

C6 (rat glioma) cell line was purchased from the American Type Culture Collection (ATCC) and has been previously shown to express β_1- and β_2-ARs (Terasaki 1979, Neve et al 1986, Zhong 1996). C6 cells were maintained in 5 mL Dulbecco's Modified Eagle Medium (DMEM, Invitrogen, Merelbeke, Belgium) supplemented with 4.5 g/ml glucose and 7.5% fetal calf serum (FCS, Bodnico, Alkmaar, The Netherlands) in 25 cm^3 cell culture flasks. Cells were grown in a humidified atmosphere containing 5% CO_2 in air and were passaged every 3-4 days.

Cellular Uptake of ^{18}F-FPTC in C6 Glioma Cells

In vitro β_1-/β_2-AR ligand binding affinities and specificities of FPTC were assessed via a competitive displacement assay with ^{125}I-ICYP as the β_1-/β_2-AR ligand. For comparison, propranolol was used as another competitive inhibitor. Similar binding studies were performed with ^{18}F-FPTC as the radioligand.

Binding studies were performed 48 h after seeding the C6 cells in 12-well plates (when confluency had reached 80–90%). One hour before addition of the radiotracer, various concentrations of an unlabelled competitor (propranolol or FPTC) were dispensed to the culture medium in the wells. Then, 2 MBq of ^{125}I-ICYP or 4 MBq of ^{18}F-FPTC in <30 µl of ethanol:saline mixture (1:3) were added to each well containing 1 ml of medium. After 1 h incubation, the medium was quickly removed and the monolayer of cells was washed 3

times with cold PBS. Cells were then treated with 0.2 ml of trypsin (Invitrogen, Merelbeke, Belgium). When the monolayer had detached from the bottom of the well, 1 ml of medium containing 7.5% FCS was added to stop the proteolytic action. Cell aggregates were resolved by repeated (at least tenfold) pipetting. Radioactivity in the cell suspension (1.2 ml) was assessed using a gamma counter and corrected for the number of viable cells. A sample of the suspension was mixed with trypan blue solution (1:1, v/v) and was used for cell counting. Cell numbers were determined manually, using a phase contrast microscope (Olympus, Tokyo, Japan), a Bürker bright-line chamber (depth 0.1 mm; 0.0025 mm^2 squares) and a hand tally counter. All experiments were performed as a quadruplicate study at two different occasions. The 50% inhibitory concentration (IC_{50}) values were calculated from a nonlinear fit, using GraphPad Prism 5.0 (GraphPad Software, San Diego, California, USA). IC_{50} values are reported as mean ± SD. Experiments were repeated thrice, each with triplicate samples.

Animal Model

The animal experiments were performed by licensed investigators in compliance with the Law on Animal Experiments of the Netherlands. The protocol was approved by the Committee on Animal Ethics of the University of Groningen. Male Wistar rats (Hsd/Cpb:WU; Harlan/CPB, Zeist, the Netherlands) were maintained at a 12 h light/12 h dark regime and were fed standard laboratory chow ad libitum.

MicroPET Scanning

Each rat was placed in an induction chamber and subjected to isoflurane anesthesia (5% for induction, 2-3% maintenance). Subsequently, body weight of the rat was determined and a cannula was placed into one of its femoral arteries. This cannula was later used for blood sampling. In blocking studies, rats were pretreated with propranolol (2.5 mg/kg of body weight), 1 min prior to injection of the radioligand. Two rats were scanned simultaneously, using a Siemens/Concorde microPET camera (Focus 220). Each animal was carefully positioned in the microPET scanner (brain, heart and lungs in the field of view) and injected via the penile vein with ^{18}F-FPTC (25 ±MBq). Data acquisition (a list mode protocol; 90 min) was started at the moment of tracer injection into the first rat, the second animal was injected 16 min later. During the scan, 15 arterial blood samples (volume 0.1-0.15 mL)

were drawn, using a standard protocol (at 15, 30, 45, 60, 75, and 90 s, and 2, 3, 5, 7.5, 10, 15, 30, 60 and 90 min after injection, respectively). Plasma was separated from these samples by short centrifugation (5 min at 13,000 rpm). Radioactivity in plasma samples (25 µL) was measured using a calibrated gamma counter.

MicroPET Data Analysis

List mode data were reframed into a dynamic sequence of 4 * 60 s, 3 *120 s, 4 * 300 s, 3 * 600 s frames after tracer injection. The data were reconstructed per time frame employing an interactive reconstruction algorithm (OSEM2D with Fourier rebinning, 4 iterations and 16 subsets). The final data sets consisted of 95 slices with a slice thickness of 0.8 mm and an in plane image matrix of 128 * 128 pixels. Voxel size was 0.5 mm * 0.5 mm * 0.8 mm. The linear resolution at the center of the field-of-view was about 1.5 mm. Data sets were fully corrected for decay, random coincidences, scatter, and attenuation. A separate transmission scan was acquired for attenuation correction. This scan was performed right before the emission scan.

Three-dimensional regions of interest (3-D ROIs) were manually drawn around the brain, as described previously. Time-activity curves (TACs) for the ROIs were calculated, using Inveon Research Workplace software (Siemens, USA). TACs were expressed in mean standardized uptake values (SUVs), normalized for body weight and injected dose. The parameter SUV is defined as: [tissue activity concentration (MBq/g) x body weight (g) / injected dose (MBq)].

Dynamic PET data were analyzed using plasma radioactivity from arterial blood samples as an input function and a graphical method according to Logan (2000). Software routines for MatLab 7 (The MathWorks), written by Dr. Antoon T.M. Willemsen (University Medical Center Groningen), were used for curve fitting. The Logan fit was started at 15 min. The cerebral distribution volume (V_T) of the tracer was estimated from the Logan plot. Cerebral blood volume was fixed to 3.5%.

Biodistribution Studies

After the scanning period, the anesthetized animals were terminated by extirpation of the heart. Blood was collected, and plasma and a cell fraction were obtained from the blood sample (5 mL) by centrifugation (5 min at 1000g). Several brain regions and peripheral tissues were excised (see Tables 1 and 2). All tissue samples were weighed and counted for radioactivity using a gamma counter. The results were expressed as SUV values.

Results and discussion

The structure of β-hydroxytriazoles may be an interesting scaffold for designing β-AR ligands. Therefore, we investigated whether ^{18}F-FPTC, a β-hydroxytriazole derivative, has affinity for β-ARs. Two reaction steps were performed to prepare the azidoalcohol. First, the racemic epoxide **2** was synthesized from hydroxycarbazole **1** and epichlorohydrin in the presence of potassium carbonate. Second, the epoxide **2** underwent azidolysis promoted by $CeCl_3 \cdot 7H_2O$ to give the desired 1,2-azidoalcohol **3**, (Scheme 4.1).

[18F]-PEG-alkyne served as a ^{18}F-buidling block and was prepared in radiochemical yields ranging from 74 to 89%. Specifically, a PEG-ylated alkyne was chosen to maintain an acceptable logP. Conjugation of ^{18}F-PEG-alkyne to (S)-azidoalcohol via Cu(I)-mediated 1,3-dipolar cycloaddition resulted in rapid reaction (10 min) and high conversion (96%) to the final product, ^{18}F-FPTC.

The radiolabeled compound **7,** Scheme 4.2 was obtained from ^{18}F-fluoride in 55 min, in 35% overall (decay-corrected) radiochemical yield. At the end of synthesis (EOS), the specific activity was >120 GBq/μmol and the radiochemical purity was >96%.

^{18}F-FPTC has an appropriate lipophilicity to penetrate the blood brain barrier (logP ±2.48).
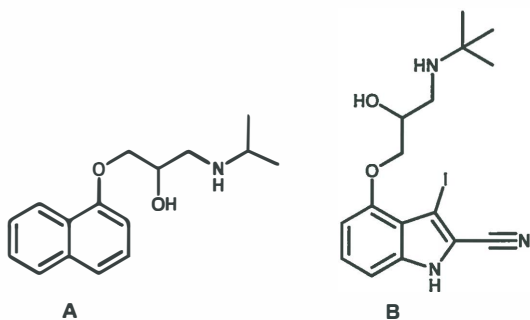
Scheme 4.3. Propranolol and iodocyanopindolol

In Vitro Competitive Receptor-Binding Assay.

FPTC dose-dependently inhibited ^{125}I-ICYP and ^{18}F-FPTC binding to C6 glioma cells. With the highest concentration, propranolol reduced the cellular binding of ^{125}I-ICYP by >80% (Fig 4.1). Propranolol blocked ^{125}I-ICYP and ^{18}F-FPTC binding with IC_{50} values of 49 and 59 nM respectively, indicating that the hydroxytriazole moiety indeed maintains binding affinity of the ligand towards β-ARs.
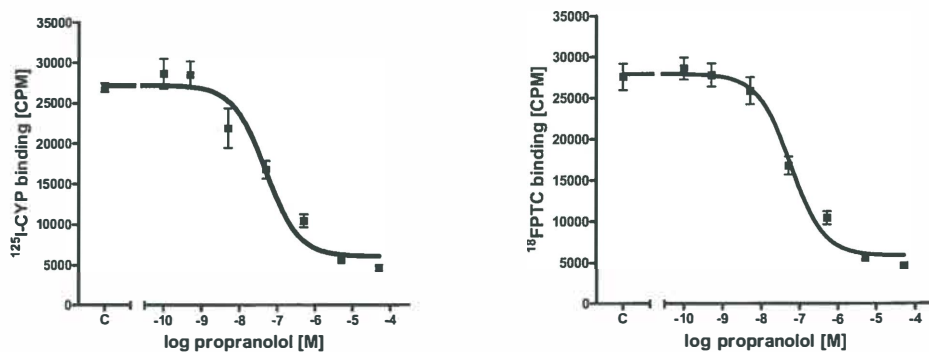

Figure4.1. Competitive Receptor-Binding Assay: Dose-response plot of propranolol competition with ^{125}I-ICYP and ^{18}F-FPTC binding to C6 cells. Error bars indicate SEM. Specific binding was calculated by subtracting nonspecific binding.

Tissue distribution.

^{18}F-FPTC accumulated in the brain with SUV values of approximately 0.4-0.6. The logP value was therefore sufficient for BBB penetration. Radioactivity uptake throughout the brain proved to be homogeneous. Pretreatment of animals with propranolol did not significantly reduce the uptake of ^{18}F in any brain region compared to controls (Table 4.1). In addition, propranolol pretreatment also did not diminish the uptake of ^{18}F in peripheral organs like heart, lung, red blood cells, and spleen although these are β-AR rich organs (Table 4.2).

Thus, ^{18}F-FPTC showed a similar in vivo behavior as was reported for ^{11}C-toliprolol and ^{18}F-derivatives of bupranolol and penbutolol (Doze 2002a). Since the regional uptake of

radioactivity in the brain was homogeneous and propranolol treatment did not reduced tracer uptake in target organs, specific in vivo binding of ^{18}F-FPTC was not observed.

Tissue	SUV-Control		SUV-Block	
Amygdala/Piriform cortex	0.37±	0.29	0.61±	0.36
Bulbus olfactorius	0.53±	0.40	0.58±	0.38
Cerebellum	0.55±	0.44	0.66±	0.40
Cingulate/Frontopolar cortex	0.56±	0.37	0.72±	0.44
Entorhinal cortex	0.54±	0.44	0.61±	0.38
Frontal cortex	0.61±	0.40	0.39±	0.21
Hippocamppus	0.47±	0.31	0.56±	0.38
Medulla	0.51±	0.39	0.46±	0.24
Par./Temp./Occ. Cortex	0.51±	0.43	0.58±	0.37
Pons	0.53±	0.39	0.66±	0.35
Striatum	0.46±	0.30	0.62±	0.36
Rest brain	0.46±	0.34	0.58±	0.35

Table 4.1. Biodistribution of ^{18}F-FPTC in various brain regions derived from control rats (n=6) and propranolol pretreated (n=6) rats. Data are expressed as mean ± SD.

Tissue	SUV-Control		SUV-Block	
Lung	0.62	±0.41	0.64	±0.34
Bone	0.98	±1.25	0.49	±0.18
Colon	0.47	±0.38	0.77	±0.44
Duodenum	0.67	±0.33	0.63	±0.25
Heart	0.48	±0.34	0.74	±0.33
Illeum	0.73	±0.31	0.78	±0.26
Kidney	1.23	±0.85	1.65	±1.035
Liver	1.01	±0.35	0.91	±0.21
Lung	0.62	±0.41	0.60	±0.35
Muscle	0.44	±0.32	0.66	±0.34
Pancreas	1.06	±0.40	1.34	±0.81
Urine	1.26	±0.78	0.23	±0.16
Testicles	0.49	±0.38	0.60	±0.30
Spleen	0.53	±0.26	0.67	±0.23
Submandubilar gland	0.62	±0.28	0.72	±0.15
Thymus	0.98	±0.32	0.74	±0.15
Plasma	0.77	±0.53	0.86	±0.61
RBC	0.71	±0.30	0.89	±0.28
Lung	0.62	±0.41	0.64	±0.34

Table 4.2. Biodistribution of ^{18}F-FPTC in rat tissues (expressed as Standard Uptake Values). Data are expressed as mean ± SD.

Kinetics of Radioactivity in Brain.

Cerebral kinetics of radioactivity after injection of ^{18}F-FPTC is presented in Figure 4.2. Maximal uptake was already observed in the first few frames (i.e., < 5 min after tracer injection) and was followed by an exponential washout. After pretreatment of animals with propranolol (20 mg/kg), the brain uptake of ^{18}F-FPTC appeared to be increased, although the difference with control animals was not statistically significant.
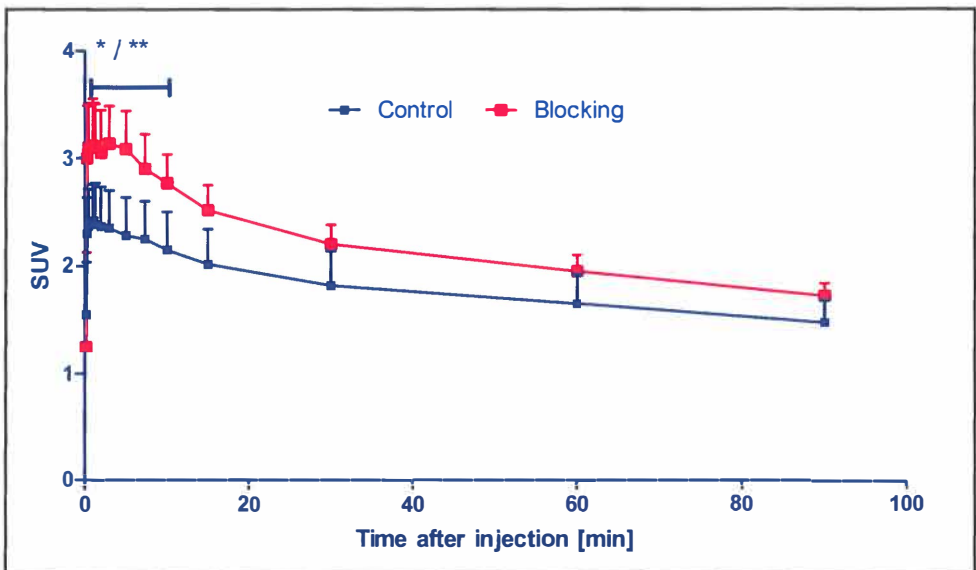

Figure 4.2. Cerebral kinetics of ^{18}F-FPTC with control animals and blocking animals treated with propranolol with saline, data are SUV-PET values for the entire brain, expressed as mean ± SEM.

Kinetics of Radioactivity in Plasma

Plasma kinetics of radioactivity after injection of ^{18}F-FPTC is presented in Figure 4.3. Drug treatment did not significantly affect the clearance of ^{18}F-FPTC from rat plasma, although plasma levels of radioactivity appeared to be lower in animals pretreated with propranolol.
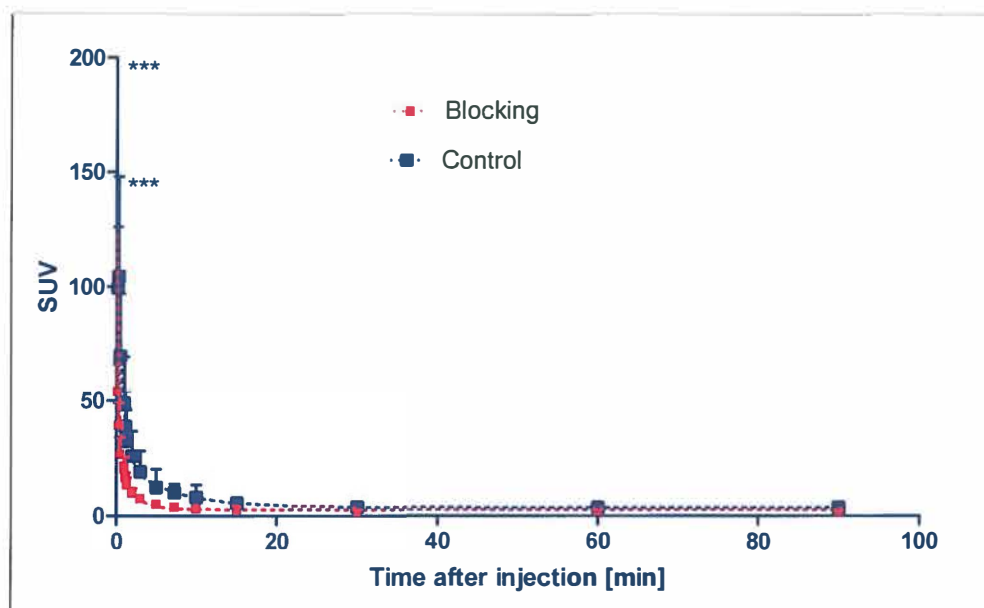
Figure 4.3. Clearance of radioactivity from blood plasma of control animal (n=6) after injection of ^{18}F-FPTC tracers and animals pretreated with propranolol (n=6). Data are SUV values, expressed as mean ± SEM.

Cerebral Distribition Volumes

The cerebral distribution volume of the tracer (V_T), calculated from Logan plots, was significantly increased after treatment of animals with propranolol (from 0.420 ± 0.070 to 0.974 ± 0.077, p < 0.0001, see Figure 4.4). Two possible mechanisms may be underlying

this phenomenon. First, propranolol may be metabolized by the same hepatic enzyme system as ^{18}F-FPTC and, therefore, propranolol treatment may increase the fraction of radioactivity in plasma representing parent compound. Second, both FPTC and propranolol may be weak substrates for ABC transporters in the blood-brain barrier, such as P-glycoprotein. Many ß-blockers are substrates for P-glycoprotein (Neuhoff et al. 2000). The administration of an excess of propranolol may saturate this efflux system, resulting in greater entry of the tracer ^{18}F-FPTC into the brain. Since the brain uptake of ^{18}F was homogeneous and tracer uptake in peripheral target organs with high beta-adrenoceptor density (lungs, heart, spleen) was not affected by propranolol, indicating lack of specific in vivo binding, we have not examined whether the change of V_T is due to mechanism 1 or 2, or both.
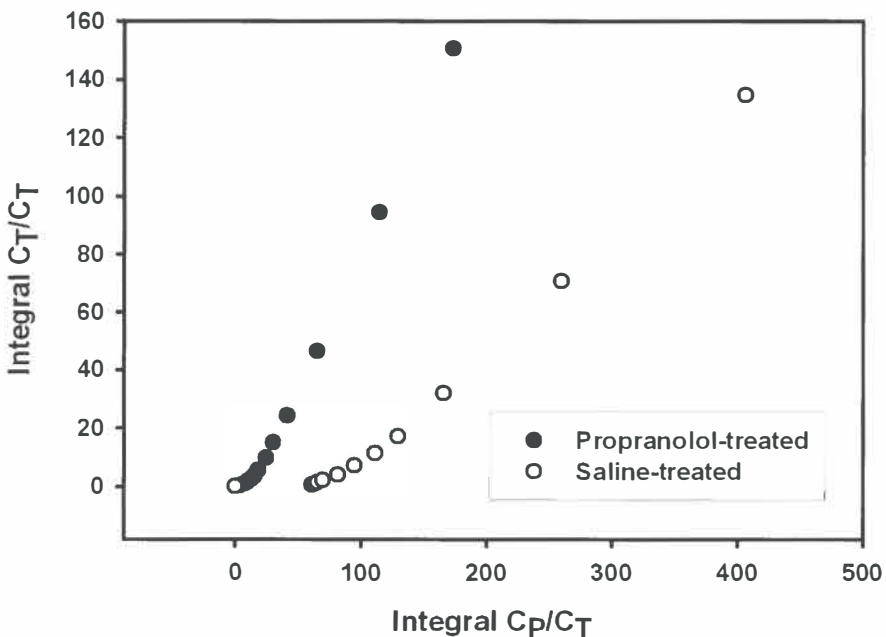
Figure 4.4. Logan plots of ^{18}F-FPTC in a control and propranolol-treated animal.

Conclusions

We have demonstrated that it is possible to prepare ^{18}F-FPTC in good radiochemical yield. Based on its appropriate logP value and its specific in vitro binding to C6 cells, ^{18}F-FPTC could have been suitable for PET imaging of cerebral β-ARs. However biodistribution and microPET data indicated that these criteria were insufficient to ensure visualization of β-ARs in rodent brain, heart or lungs.

References

- Arner P, Engfeldt P, Hellström L, J, Clin. Endocrinol. Metab., 1990, 71, 1119–1126.

- Berridge M S, Nelson A D, Zheng L, Leisure G P, Miraldi F, J. Nucl. Med., 1994, 35, 1665-1678.

- Campbell-Verduyn L S, Szymański W, Postema C P, Dierckx R A, Elsinga P H, Janssen -D B, Feringa B L, Chem. Commun., 2010, 46, 898-900.

- Doze P, Elsinga P H, de Vries E F, van Waarde A, Vaalburg W, Nucl. Med. Biol. 2000, 27, 315-319.

- Doze P, Elsinga P H, Maas B, van Waarde A, Wegman T, Vaalburg W, NeuroChem. Int. 2002, 40,145-155.

- Doze P, van Waarde A., Tewson T J, Vaalburg W, Elsinga P H, Neurochem. Int. 2002, 41, 17-27.

- Elsinga P H, Hendrikse N H, Bart J, Vaalburg W, van Waarde A, Curr. Pharm. Des., 2004, 10,1493-503.

- Heald S L, Lavin T N L, Nambi P, Lefkowitz R J, Caron M G, J. Med. Chem., 1983, 26, 832-8.

- Kim Y S, Sainz R D, Molenaar P, Summers R J, Biochem. Pharmacol, 1991, 42, 1783-9.

- Krief S, Lönnqvist F, Raimbault S, J. Clin. Invest., 1993, 91, 344–349.

- Law M P, J. Pharmacol., 1993, 109, 1101-1109.

- Logan J, Nucl. Med. Biol., 2000, 27, 661–670.

- Madhusudhan G, Kumar B A, Chintamani U S, Rao M N, Udaykiran N, Suresh T, Kumar V K, Mukkanti K, Indian J. Chem. B. Org., 2010, 49, 606-610.

- McEwen B S, Tanapat P, Weiland, N G, Endocrionology, 1999, 140, 1044-1047.

- Neuhoff S, Langguth P, Dressler C, Andersson T B, Regardh C G, Spahn-Langguth H, Int. J. Clin. Pharmacol. Ther., 2000, 38, 168-179.

- Neve K A, Molinoff P B, Mol. Pharmacol., 1986, 30, 104-11.

- Rasmussen S G, DeVree B T, Zou, Y, Kruse A C, Chung K Y, Kobilka T S, Thian F S, Chae, P S, Pardon E, Calinski D, Mathiesen J M, Shah S T, Lyons, J A, Caffrey M, Gellman S H, Steyaert J, Skiniotis G, Weis W I, Sunahara R K, Kobilka B K, Nature., 2011, 19, 477, , 549-55.

- Rainbow T C, Parsons B, Wolfe B, Proc. Natl. Acad .Sci., 1984, 1585–1589.
- Russo-Neustadt a, Cotman C W, J. Neuroscience., 1997, 17,5573-5580.
- Sano M, Yoshimasa T, Yagura T, Yamamoto I, Life Sci., 1993, 52, 1063–1070.
- Terasaki W L, Linden J, Brooker G, Proc. Natl. Acad. Sci. U S A., 1979, 76, 6401-5.
- Van Waarde A, Elsinga P H, Brodde O E, Visser G M, Vaalburg W, Eur. J. Pharmacol., 1995, 272, 159-168.
- Van Waarde A, Vaalburg W, Doze P, Bosker F J, Elsinga P H, Curr. Pharm. Des., 2004, 10, 1519–1536.
- Zhong H, Guerrero S W, Esbenshade T A., Minneman K P, Mol. Pharmacol., 1996, 50, 175-84.

Ch. A

Chapter 4

Chapter 5

Synthesis and evaluation of a ^{18}F-bombesin derivative prepared by click chemistry

L. Mirfeizi[a], Z. Yu[a], G. Carlucci[c], L. Campbell-Verduyn[b], B.L. Feringa[b], R.A.J.O. Dierckx[a]. I.J. de Jong[c] , W. Helfrich[d], P.H. Elsinga[a]

a. University Medical Center Groningen, University of Groningen, Dept. of Nuclear Medicine and Molecular Imaging, Groningen, Netherlands b. University of Groningen, Stratingh Institute for Chemistry, Groningen, Netherlands c. Department of Urology, University Medical Center Groningen, Groningen, The Netherlands d. Surgical Research Laboratory, University Medical Center Groningen, Groningen, The Netherlands

Abstract

The goal of our study was the synthesis of a new ^{18}F-labeled bombesin derivative by click chemistry for specific targeting of Gastrin-Releasing Peptide (GRP) receptors in human prostate cancer cells. Bombesin is a 14 amino acid peptide sequence which serves as a tumor marker for various cancers. Amino acids 7-14 are considered to be the sequence responsible for binding to the GRP-receptor. Click chemistry, in particular the copper-mediated 1,3-dipolar [3+2] cycloaddition between azides and alkynes, has entered the field of radiopharmaceutical sciences. We used a 1,3-dipolar cycloaddition to label bombesin modified at the Lys3-position with a triple bond.

The [Lys3]-Bombesin (BN3) analogue [^{18}F]-Bombesin ([^{18}F]-TBN3) was designed and synthesized for the targeting of gastrin-releasing peptide receptors in prostate cancer cells. It incorporates a terminal alkyne at the Lys[3] residue of the 14 amino acid peptide sequence, where [^{18}F] can be readily introduced. The *in vitro* binding affinity to GRPR, cell uptake, internalization and efflux kinetics of the radiolabeled bombesin analogue were investigated in the GRPR-expressing human prostate cancer cell line PC-3. The tracer proved to have good *in vitro* properties. Biodistribution and the GRPR-targeting potential were evaluated in PC-3 tumor-bearing athymic nude mice. Tumor uptake and *in vivo* pharmacokinetics in PC-3 tumor-bearing mice were not in agreement with the *in vitro* results. The GRPR targeting ability of the [^{18}F]- BN3 was proven *in vitro* but not *in vivo*.

Introduction

The gastrin-releasing peptide receptor (GRP-r) is a seven trans membrane G-protein coupled receptor that is overexpressed in primary breast, prostate, colon cancer and lymph node metastases (Reubi 2003). Bombesin (BN) is a peptide that binds with high affinity to GRP-r. Several bombesine derivatives have been reported as a radiopeptide with high stability in human serum, specific cell receptor binding and rapid internalization (Ananias 2008, Baidoo 1998, Ferro-Flores 2006). Bio-distribution data in mice showed rapid blood clearance, with predominant renal excretion and specific binding towards GRP receptor-positive tissues such as pancreas and prostate tumors (Ferro-Flores 2006, Santos-Cuevas 2009). Most of the bombesin derivatives are SPECT radioligands.

The goal of our study was the synthesis of PET-based bombesin derivatives that can be easily prepared by click chemistry with high tumor uptake and optimal pharmacokinetics for specific targeting of Gastrin-Releasing Peptide (GRP) receptors in human prostate cancer cells. Bombesin is a 14 amino acid peptide sequence which serves as a tumor marker for various cancers. Amino acids 7-14 are considered to be the sequence responsible for binding to the GRP-receptor. There are synthetic challenges associated with the introduction of [18F] when compared with the ease of chelation techniques used for metallic radionuclides. The synthetic time frame of [18F] ($t_{1/2}$~110 min) is also much reduced as compared to metallic radionuclides such as [64Cu] ($t_{1/2}$~12 h). A further drawback to the use of [18F] is the necessity for multi-step synthetic procedures to synthesize current prosthetic groups such as succinimidyl-[18F]-4-fluorobenzoate ([18F]SFB) or [18F]-4-fluorobenzaldehyde which are commonly used to label bombesin. (Chang 2005)

An ideal prosthetic group is one that can be easily synthesized, in which the radionuclide is introduced in the last step of the synthesis, and which requires only the mildest of conditions to attach it to the biomolecule of interest.

Many groups have begun to exploit the bioorthogonality of the copper-catalyzed azide-alkyne cycloaddition (CuAAC) to allow for straightforward labeling of sugar, protein and peptide targets with [18F] and other radionuclides by introducing a 'click' handle into the target molecules. An advantage of introducing a 'click' handle such as an alkyne into bombesin is the ability to easily tune the properties of the analogue by designing various azides of different sizes, linker lengths or hydrophobicities. Since the 'click' reaction is known to be very robust and to withstand a very wide substrate scope, changing the azide

prosthetic group to achieve new tracers should not require much optimization of the conditions for the labeling protocol.

We use 1,3-dipolar cycloaddition to label the peptide modified at the lys3-position derivatized with a triple bond providing a functional group to perform click chemistry. The "click chemistry" method has been useful in coupling two molecules, in particular azide and alkyne to get a 1,2,3-triazole via a so called the Huisgen's reaction which occurs through 1,3-dipolar cycloaddition.

Materials and Methods

All reagents and solvents were obtained from Fluka and Sigma/Aldrich and used without further purification.

Bromo azido butane

The synthesis of bromoazidobutane was carried out by adding NaN$_3$ (1.5eg) to a stirred solution of the corresponding bromochlorobutane (1.0 eq) in a 50 mL water/acetone mixture (1:4). The resulting suspension was stirred at room temperature for 24 hours. Dichloromethane was added to the mixture and the organic layer was separated. The aqueous layer was extracted with 3 x 10 mL aliquots of dichloromethane and the combined organic layers were dried over MgSO$_4$. The solvent was removed under reduced pressure, and the azide was sufficiently pure to use without further work up (Scheme 5.1).

Schem 5.1. Bromo Azido Butane

Production and workup of [^{18}F]fluoride

[^{18}F]fluoride was obtained by proton (17 MeV) bombardment of an [^{18}O]enriched water target via the ^{18}O(p,n)^{18}F reaction. The radioactive material was trapped by passing the target water through a preactivated Sep-Pak light QMA cartridge (Waters). 1 mL H$_2$O solution of the K$_2$CO$_3$ (4.5 mg) and Kryptofix 2.2.2. (20 mg) was used to elute the [^{18}F]fluoride from the cartridge into a conical glass vial. This eluate was evaporated to dryness by three consecutive azeotropic distillations after addition of acetonitrile (3 × 500 μL) under a gentle stream of nitrogen gas (130 °C).


Scheme 5.2. Synthesis of [^{18}F]Fluoroazidobutane

[^{18}F]-Fluoroazidobutane. The dried [^{18}F]-fluoride was then added to 3.0 mg of bromoazidobutane (17 μmol) in 0.5 mL dry DMSO, and the mixture was heated at 140 °C for 10 min (Scheme 5.2). The labeled product was absorbed on a C18-light Sep-Pak cartridge followed by washing with 10 mL H$_2$O and eluted with 5 mL pure methanol. The Sep-Pak eluate containing [^{18}F]-fluoroazidobutane was then purified and separated from its precursor using semi-preparative HPLC on a semi-preparative C18-reversed phase column (mobile phase 60/40 MeCN/H$_2$O, retention time=10 min). In addition, conversion of the reaction was monitored by radio-TLC (silica gel, hexane/EtOAc (4:1)) (R$_f$ of product=0.40), (R$_f$ of F$^-$=0.0), and HPLC analysis: retention time= 10 min).

Propargyl-[Lys3]-bombesin (Lys3-BN3) An alkyne-containing lysine amino acid was synthesized by reaction of lysine with the activated succinimide ester of propionic acid and incorporated via standard solid phase peptide synthesis into bombesin.

Peptide synthesis was performed on a 0.1 mmol scale. The Fmoc solid phase method was performed on a Rink amide resin (bead size 100-200 mesh, loading 0.7 mmol/g). After completion of the synthesis, the resin was filtered off, and washed first with DCM (1 x 10 mL) and then diethyl ether (3 x 10 mL). The resin was transferred to a sample vial, and to this vial was added a cleaving solution, a mixture of trifluoroacetic acid (TFA)/triisopropyl silane (TIS)/1,3-ethanedithiol (EDT)/thioanisole /H_2O (85/1/4/5/5). The peptide was cleaved from the resin, and all of the remaining side chain protecting groups were cleaved off by gently stirring the resin in this solution at room temperature for 5 h. The solution containing the peptide was filtered and concentrated. The peptide was precipitated using cold diethyl ether and centrifuged. The supernatant was decanted and the solid was washed with cold diethyl ether (20 mL), centrifuged, and the supernatant decanted. This was repeated a further two times. The solid was allowed to dry and then dissolved in water (with 1% formic acid) and lyophilized. Purification of the peptide was achieved by RP-HPLC (Gradient A). Retention time=32 min. HRMS (EI) calcd for $C_{26}H_{29}O_5N_2$ [M+H$^+$]1671.9194, found 1671.9900. (Scheme 5.3)
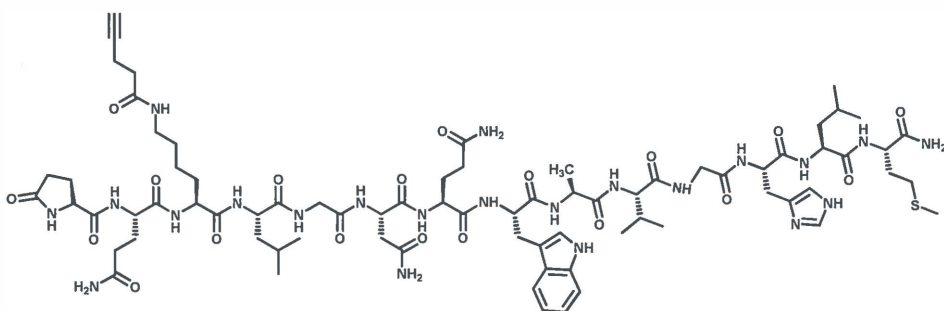
Scheme 5.3. [Lys3]-bombesin

Fluoro triazolyl lysine 3bombesin (FTBN3) Propargyl-[Lys3]-bombesin (1.00 mg, 5.98 x 10^{-4} mmol) and 4-fluorobutaneazide (0.14 mg, 9.2 x 10^{-4} mmol) were dissolved in a H$_2$O/DMSO mixture (3:1, 0.8 mL). In a separate vial, CuSO$_4$·5H$_2$O (1.5 µg, 5.98 x 10^{-6} mmol) was dissolved in 0.1 mL of water, to this was added sodium ascorbate (5.9 µg, 3.00 x 10^{-5} mmol). MonoPhos (2.51 µg, 6.98 x 10^{-6} mmol) was added along with 0.1 mL of DMSO. The reagents were stirred together for 10 min and added to the solution of azide and peptide. The reaction was monitored by RP-HPLC. Upon completion, the reaction mixture was lyophilized. The crude product was purified by RP-HPLC (Gradient A). HRMS (EI) calcd for C$_{83}$H$_{121}$O$_{19}$N$_{25}$FS [M+H$^+$] calc 1821.8901, found 1821.8932. Retention time=36.0 min. (Scheme 5.4)
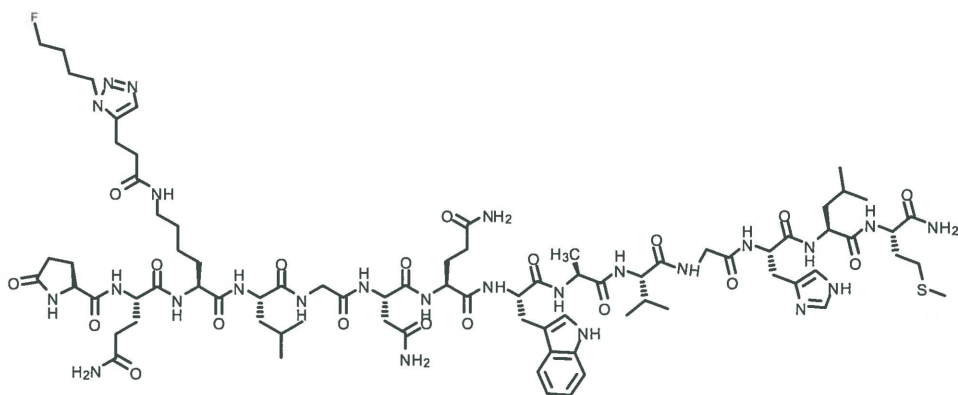
Schem 5.4. Fluoro Triazolyl Lysine 3 Bombesin   (FTBN3)

[^{18}F]-TBN3. [^{18}F]-fluoroazidobutane in MeCN/H$_2$O and propargyl-BN3 were dissolved in a mixture of water and DMF (3:1 v/v). In a separate vial, CuSO$_4$·5H$_2$O (5 mol %) was dissolved in 0.1 mL of water, and to this was added sodium ascorbate (25 mol %). MonoPhos (6 mol %) was added along with 0.1 mL of DMF. The reagents were stirred together for 10 min and added to the solution of azide and peptide. The reaction was monitored by HPLC and radio-TLC until full conversion was reached. [^{18}F]-TBN3 was purified

by RP-HPLC. Retention time=18 min, and analyses was with radio-TLC (silica gel, hexane/EtOAc (4:1)) (R_f=0.20). Radiochemical yield=59%. Specific activity of final product was around 90 GBq/µmol.

Analytical as well as semipreparative reversed-phase high-performance liquid chromatography (RP-HPLC) was performed. Isolation of radiolabeled peptides was performed using a RP-C18 column (4.6 mm × 250 mm, 10 µm). The flow was set at 2.5 mL/min using a gradient system starting from 90% solvent A (0.01 M phosphate buffer, pH=6.0) and 10% solvent B (acetonitrile) (0-2 min) and ramped to 45% solvent A and 55% solvent B at 35 min. The analytical HPLC was performed using the same gradient system but with a reversed-phase Grace Smart RP-C18 column (4.6 mm × 250 mm, 5 µm) and a flow of 1 mL/min. (Scheme 5.5)

Scheme 5.5. [^{18}F]-Fluoro Triazol Lysine 3 Bombesin ([^{18}F]-TBN3)

Octanol/Water Partition Coefficient Study

Water/ Octanol partition coefficients were determined at pH=7.4. Aliquots of 5 µL containing 500 kBq of the radiolabeled compound in PBS were added to a vial containing 1.2 mL 1-octanol and PBS (1:1). After vortexing for 1 min, the vial was centrifuged for 5 min at 10 000 rpm to ensure complete separation of layers. Then, 40 µL of each layer was taken in

a preweighed vial and measured in the γ-counter. Counts per unit weight of sample were calculated. The experiments were performed in triplicate.

Cell culture

The GRPR-positive PC-3 human prostate cancer cell line (ATCC, Manassas, Virginia, USA) was cultured at 37°C in a humidified 5% CO_2 atmosphere. The cells were cultured in RPMI 1640 (Lonza, Verviers, France) supplemented with 10% fetal calf serum (Thermo Fisher Scientific Inc., Logan, Utah, USA). They were subcultured twice a week after detaching with trypsin-EDTA.

In Vitro Stability

The tracer was dissolved in 1 mL saline (1 mg/mL). The resulted solutions were incubated at room temperature and samples were analyzed by RP-HPLC with radiometric detection. Metabolic stability was investigated in human serum. Human serum from healthy donors were incubated at 37°C with [^{18}F]-TBN3 for different time periods. After incubation, 250 μL sample was precipitated with 750 μL acetonitrile/ethanol ($V_{acetonitrile}/V_{ethanol} = 1:1$) and then centrifuged (3 min, 3000 rpm), the supernatants passed through a filter followed by analysis by RP-HPLC.

In Vitro Competitive Receptor-Binding Assay

In vitro GRPR binding affinities and specificities ^{125}I-Tyr^4-BN(1-14) (Perkin Elmer, Oosterhout, The Netherlands) and [^{18}F]TBN3 were assessed via a competitive displacement assay with BN(1-14). Experiments were performed at 37 °C with PC-3 human prostate cancer cells (Chen 2004). The 50% inhibitory concentration bombesin (1-14) ($IC_{50}= 3.5 \pm 0.2$ nM) (n=3, mean ± SD), values were calculated by fitting the data with nonlinear regression using GraphPad Prism 5.0 (GraphPad Software, San Diego, California, USA). Experiments were performed with triplicate samples. IC_{50} values are reported as an average of these samples plus the standard deviation (SD).

Internalization studies and stability of tracer

The tracer was dissolved in 1 mL saline. The resulted solutions were incubated at room temperature and reaction was followed by RP-HPLC with radiometric detection.

The internalization studies were performed according to the method described in the literature (Chen 2004), although slightly modified. In short, PC-3 cells cultured in 6-well plates were incubated in triplicate with $[^{18}F]$-TBN (0.0037 MBq/well) for 2 h at 4°C, afterwards washed twice with ice-cold PBS to remove unbound radioactivity and then incubated in the pre-warmed culture medium at 37°C for 0, 5, 15, 30, 45, 60, 90 and 120 min to allow for internalization. To remove cell-surface bound radiotracer, the cells were washed twice for 3 min with acid (50 mM glycine–HCl/100 mM NaCl, pH 2.8). Next, the cells were lysed by incubation with 1 M aq. NaOH at 37 °C, and the resulting lysate in each well was aspirated to determine the internalized radioactivity in a γ-counter (Compugamma CS1282, LKB-Wallac, Turku, Finland). Results were expressed as the percentage of the total radioactivity (internalized activity/(surface-bound activity plus internalized activity)).

Efflux studies

The efflux studies were also performed according to the method described in literature (Chen et al., 2004), although the procedure was slightly modified. In short, PC-3 cells cultured in 6-well plates were incubated with $[^{18}F]$TBN (0.0037 MBq/well) for 1 h at 37°C to allow for maximal internalization, subsequently washed twice with ice-cold PBS to remove unbound radioactivity and then incubated in the pre-warmed culture medium at 37°C for 0, 15, 30, 45, 60, 90, 120 min in triplicate. To remove cell-surface bound radiotracer, the cells were washed twice for 3 min with acid (50 mM glycine–HCl/100 mM NaCl, pH 2.8). Next, the cells were lysed by incubation with 1 M aq. NaOH at 37°C, and the resulting lysate in each well was aspirated to determine the remaining radioactivity in a γ-counter (Compugamma CS1282, LKB-Wallac, Turku, Finland). Results are expressed as the percentage of maximal intracellular radioactivity (remaining activity at specific time-point divided by activity at time-point 0).

Animal model

The PC-3 tumor model was generated by subcutaneous injection of 2×10^6 PC-3 cells suspended in 0.1 ml of saline into the right front flank of male athymic nude mice (Harlan, Zeist, The Netherlands). The mice were used for biodistribution experiments and microPET imaging when the tumor volume reached a mean diameter of ~0.8-1.0 cm. (3-4 weeks after inoculation). All animal experiments were performed in accordance with the regulations of Dutch law on animal welfare, and the institutional ethics committee for animal procedures approved the protocol.

Biodistribution experiments

Twelve PC-3 tumor-bearing mice were randomly divided into two groups, each of which had three animals. Isoflurane inhalation was used as method of anaesthesia. [18F]TBN (10±2 MBq/mouse) dissolved in 0.1 ml of saline was injected intravenously via the penis vein. A 0-60 min dynamic scan followed by biodistribution and a 120 min static scan followed by biodistribution were carried out. A blocking group followed the same protocol. The mice were anaesthetized and sacrificed by cervical dislocation. Immediately after sacrificing the animals, blood was withdrawn from the eye through a capillary tube and organs of interest (heart, liver, spleen, lung, kidney, small intestine, large intestine, stomach, bone, muscle, tumour) were collected and weighed. Radioactivity was determined in a γ-counter (Compugamma CS1282, LKB-Wallac, Turku, Finland).

To determine specificity of the *in vivo* uptake, another group of mice received an intravenous injection of 250 µg of unlabeled ε-aminocaproic, Aca-BN(7-14) at 30 minutes prior to injection of [18F]TBN (10±2 MBq /mouse). Mice were sacrificed 1 h after injection of the radiotracer and processed as described above.

Organ uptake was calculated as a percentage of the injected dose per gram of tissue mass (%ID/g). Biodistribution data was reported as an average plus the standard deviation based on the results from four animals at each time point. Significant blocking was calculated with the student's t-test. P-values were considered significant when $p \leq 0.05$. T/NT ratios were reported as an average at each time point (without the blocking group).

MicroPET/CT imaging

The imaging study was performed in PC-3 tumor-bearing mice, of which 6 were used for the blocking experiment. Each PC-3 tumor-bearing mouse was injected via the penis vein with [^{18}F]TBN (10±2 MBq/mouse) in 0.1 mL saline under isoflurane anesthesia. Animals were placed prone in the μ-PET using a Focus 200 rodent scanner (CTI Siemens, Munich, Germany).

Dynamic data was acquired immediately after injection of the radiotracer for 60 minutes, 6 frames, 10 minutes per frame. Two hours after injection of the radiotracer, the mice were sacrificed, placed horizontal in the μ-PET and a 60min-static scan was performed at 2 h post injection after sacrificing the animals. For the blocking experiment, each of the mice was administered intravenously (penis vein) with an excess Aca-BN(7-14) (250 μg dissolved in 0.2 mL of saline) 30 min prior to administration of ^{18}FTBN (10±2 MBq/mouse. Images were acquired using the same procedure as described above. Images were reconstructed by using μ-PET. Inveon Research Workplace Software (Siemens Inveon Software, Erlangen, Germany).

Metabolic Stability

Male mice bearing PC-3 tumors were injected intravenously with [^{18}F]TBN tracer (10±2 MBq/mouse). Tracer uptake is expressed as SUV. The animals were sacrificed and dissected at 5 min and 20 min after injection. Blood, urine, liver, kidneys, and tumor were collected. Blood was immediately centrifuged for 5 min at 13,200 rpm. Organs were homogenized using an IKA Ultra-Turrax T8 (IKAWorks Inc.), suspended in 1 mL of PBS, and centrifuged for 5 min at 13,200 rpm. After removal of the supernatants, the pellets were washed with 500 mL of PBS. For each sample, supernatants of both centrifugation steps were combined and passed through Sep-Pak C18 cartridges. The urine sample was directly diluted with 1 mL of PBS and passed through Sep-Pak C18 cartridge. The cartridges were washed with 2 mL of H$_2$O and eluted with 2 mL of acetonitrile containing 0.1% TFA. The combined aqueous and organic solutions were concentrated to about 1 mL by rotary evaporation, passed through a 0.22-mm Millipore filter. Tumors and plasma were weighted and the amount of radioactivity was determined with the gamma counter. The soluble fraction of tumors and plasma samples was analyzed by Radio-TLC (R_f

[^{18}F]Fluoroazidobutane=0.89,   R$_f$ [^{18}F]TBN=0.57) eluent:MeCN/H$_2$O 3:7). After elution, radioactivity on TLC plates was analyzed by storage system (PerkinElmer) and the percentage of conversion of [^{18}F]TBN as a function of the tracer distribution time was calculated by ROI analysis using OptiQuant software.

Results and discussion
Synthesis and radiolabeling

[^{18}F]fluoro azido butane was prepared in yields ranging from 78 to 81%. Conjugation of [^{18}F]fluoro azido butane to 0.1 mg of propionyl-Lys3-Bombesin (1-14) using via Cu(I) mediated 1,3-dipolar cycloaddition yielded the desired [^{18}F]-labeled peptide in 15 min with a radiochemical yield of 93%. The total synthesis time was 60 min from the end of bombardment; the specific activity was around 90 GBq/µmol.

Increasing the amount of 3-propronyl-Lysine-Bombesine(1-14) from 0.05 to 0.1 mg resulted in increase of RCY of the triazole product   from 70 to 93%. With respect to 3-Fluorobutyl triazolyl –lysine-Bombesin (1-14) (^{18}FTBN), 1mol % of CuSO$_4$ showed a sufficient catalytic effect within a short time (Scheme (5.6) The measured lipophilicity, as expressed as Log P was 0.98.

Ch. 5
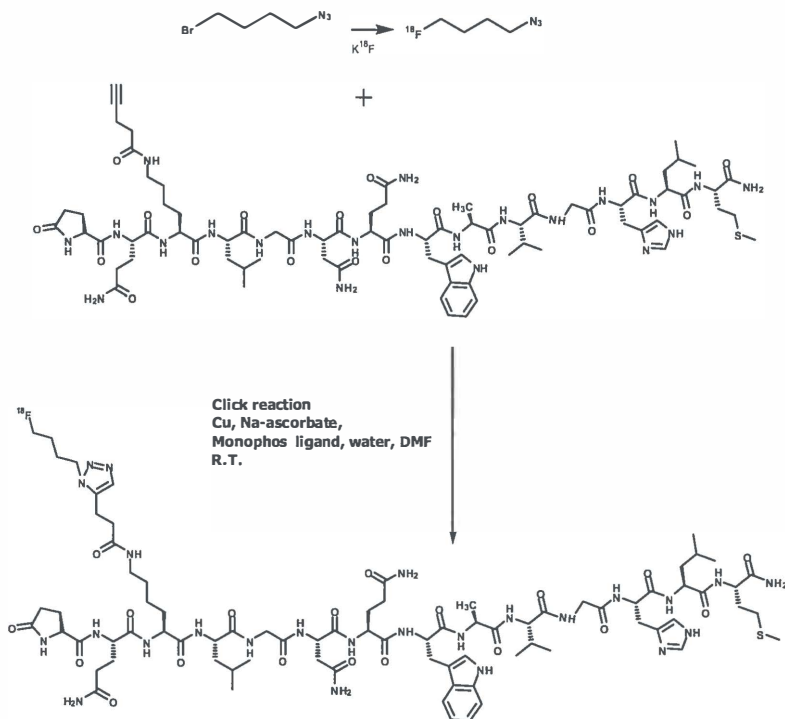
Scheme 5.6. Synthesis of [^{18}F]-TBN

In Vitro Competitive Receptor-Binding Assay

Using [^{125}I]-Tyr^4-BN(1-14) and [^{18}F]-TBN as the GRPR-specific radioligand, the binding affinities of were assessed via a competitive displacement assay using BN(1-14). Results were plotted in sigmoid curves for the displacement of [^{125}I]-Tyr^4-BN(1-14) and [^{18}F]-TBN as a function of increasing concentration of BN(1-14). The IC$_{50}$ values were determined at 16.3 nM, 20 nM for BN(1-14)with [^{125}I]-[Tyr4]-BN and [^{18}F]-TBN respectively (Figure 5.1).
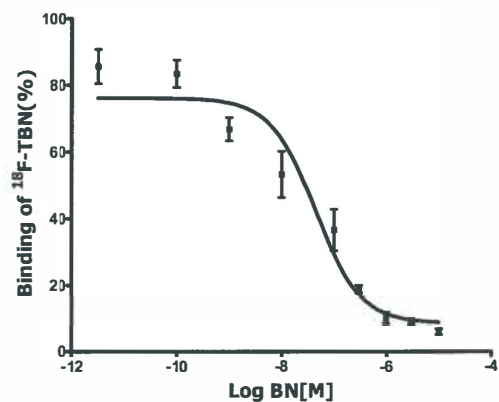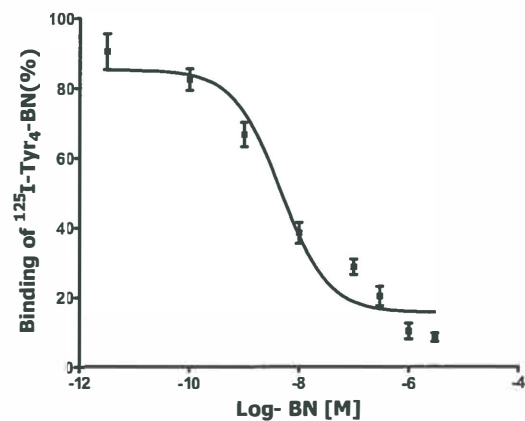
Figure 5.1. Competitive binding assay on PC-3 cells with [^{125}I]-[Tyr4]-BN and [^{18}F]-TBN
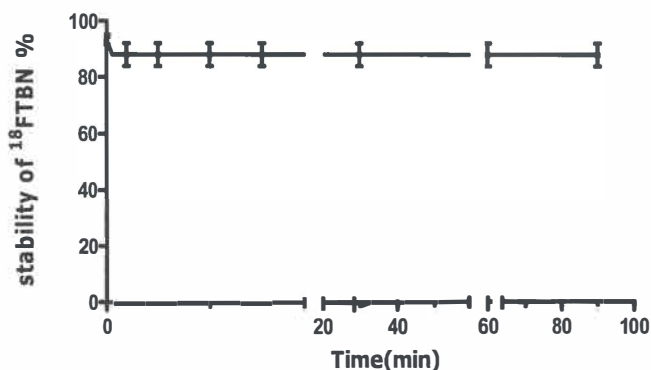
Stability of tracer

103

Figure 5.2. In vitro stability of ^{18}F-TBN in PBS

The stability of $[^{18}F]$-TBN in PBS was determined at 37 °C. After 90 min of incubation, HPLC analysis showed that 98% of the tracer was still intact. The stability of $[^{18}F]$-TBN in PBS and human plasma were also determined at 37 °C. After 90 min of incubation 98% (Radio-TLC) of radioactivity still corresponding to the intact tracer. This indicates that the tracer is highly stable in vitro (figure 5.2).

Internalization and efflux studies

The results of the internalization of $[^{18}F]$-TBN into PC-3 cells are shown in figure 5.3. Internalization occurred fast in the first 15 min and reached a plateau of 84% after 30 minutes remaining steady for 120 minutes during the experiment.
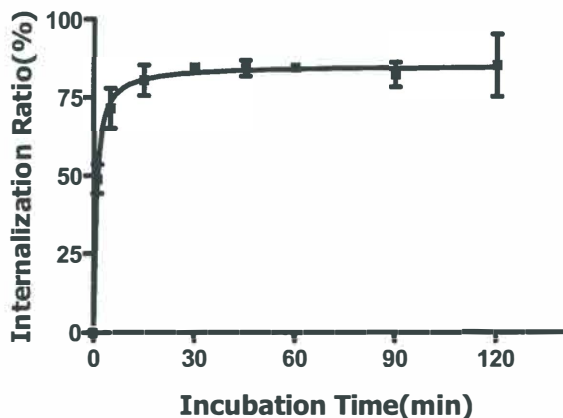
Figure 5.3. Internalization of $[^{18}F]$-TBN into PC-3 cells (n = 3, mean ± SD). Cell-associated data are expressed as % radioactivity/million cells

For a good PET tracer, not only tracer uptake, but also its retention is important. The results of the efflux study are depicted in figure 5.4. A moderate efflux rate in the first 60 min is shown with only 32% of radioactivity externalized by the PC-3 cells. After 90 min a relatively stable situation is created with just over 50% of added radioactivity remaining in the cells for the remainder of the experiment.
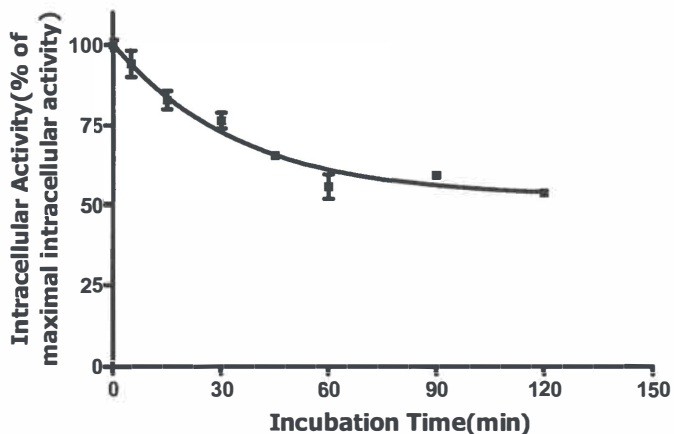
Figure 5.4. Efflux kinetics of ^{18}F-FTBN in PC-3 cell line (n = 3, mean ± SD). Cell-associated data are expressed as % radioactivity/million cells

Biodistribution experiments

Biodistribution of ^{18}F-FTBN was evaluated in PC-3 tumor xenografts bearing athymic nude mice. Biodistribution data are shown in table 5.1. Fast clearance of activity from the blood and high non-specific uptake in kidney was observed, suggesting that radioactivity is rapidly cleared mainly via the renal-urinary system. Low uptake of radioactivity in bone, muscle and the rapid clearance from blood resulted in favourable high T/NT ratios. Low uptake was detected in the GRPR-rich pancreas during the experiment, Uptake in tumor, stomach, small and large intestine was not significantly reduced in the study of GRPR blockade.

Organ	5 min %ID/g	T/NT	20 min %ID/g	T/NT	1h %ID/g	T/NT	2h %ID/g	T/NT	1h blocking +%ID/g
Bone	0.46±0.09	5.58	1.67±1.22	0.30	0.62±0.16	0.79	0.44±0.22	0.16	0.98±0.46
LargeInt.	0.90±0.56	2.51	0.83±0.56	0.96	0.52±0.07	1.01	0.60±0.27	0.18	0.41±0.26
Small Int.	1.41±1.21	1.66	2.32±0.91	0.23	1.63±0.76	0.30	1.53±1.27	0.18	1.33±0.69
Heart	0.67±0.71	7.02	0.32±0.27	2.19	0.47±0.17	1.03	0.28±0.30	1.32	0.31±0.24
Kidney	4.21±5.90	1.78	2.62±1.01	0.18	1.78±0.50	0.30	2.07±1.46	0.12	1.62±0.73
Liver	2.60±2.20	0.82	1.01±0.59	0.59	1.17±0.26	0.43	0.88±0.67	0.30	0.90±0.73
Lung	2.93±3.44	3.11	0.60±0.27	0.79	0.61±0.23	0.77	0.45±0.40	0.66	0.50±0.28
Muscle	0.50±0.44	19.27	0.25±0.22	2.81	0.39±0.10	1.28	0.26±0.22	1.24	0.30±0.26
Pancreas	1.01±1.02	4.12	0.63±0.28	0.83	0.60±0.17	0.82	1.38±1.49	0.42	0.53±0.35
Blood	1.16±0.58	3.29	0.46±0.33	1.51	0.54±0.18	0.88	0.37±0.41	1.48	0.38±0.34
Spleen	0.50±0.54	7.60	0.35±0.22	1.63	0.43±0.14	1.11	0.31±0.25	0.88	0.29±0.28
Stomach	0.57±0.52	4.45	0.59±0.16	0.76	0.50±0.26	0.99	0.55±0.24	0.41	0.41±0.03
Tumor	2.81±4.05	1.00	0.39±0.22	1.00	0.59±0.07	1.00	0.20±0.03	1.00	0.50±0.25

Table 5.1. Biodistribution and Tumor-to- Normal- Tissue Ratios of [18]FTBN after Intravenous Injection in PC3 prostate tumor in mouse tissues (expressed as Standard Uptake Values). Value are expressed as %ID/g, mean ± standard deviation (n=3 at each time point) or as T/NT ratios. Blocking was achieved by preinjection 250 μg of unlabeled Aca-BN(7-14).

Ch. 5

To investigate whether the radioactivity accumulation in the tumors was affected by metabolism of ^{18}F-FTBN, metabolite analysis of PC3 tumors was performed.

Plasma analysis of the mice injected with ^{18}F-FTBN revealed that 90% of the activity was present as compite at 60 min, indicating high *in vivo* stability. Figure 5.5 indicate that 80 % of ^{18}F-FTBN in PC3 tumors was metabolized to more polar metabolites.

Metabolite analysis of the tumors suggests that the enhanced radioactivity in PC3 tumors is due to conversion to ^{18}F-FTBN in intracellular domain. Plasma analysis revealed that ^{18}F-FTBN is highly stable *in vivo* during injection.
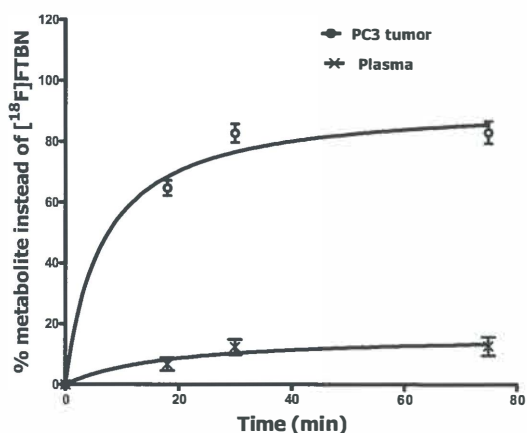

Figure 5.5. ^{18}F-FTBN metabolite analysis by Radio-TLC of soluble fraction of PC3 tumors.

PET Imaging

Small animal PET was performed in mice inoculated with PC3 tumor cells. Unfortunately using PET imaging with ^{18}F-FTBN tumor could not be visualized. Only high uptake was observed in biodistribution experiments.

Conclusion

In this study, it has been demonstrated that it is possible to use the CuAAC to label bombesin with [^{18}F] in a rapid and high yielding fashion using an alkyne modified bombesin and an azido prosthetic group. This approach fulfills many of the requirements that we set as ideal characteristics for a prosthetic group. The [^{18}F] is introduced in the last step of the synthesis, the labeling proceeds at room temperature in aqueous solution and can reach full conversion in 15 min. Most importantly, the system is modular so that a wide range of azides can be readily synthesized, altering the properties of the resulting peptide. We demonstrated that labeling with [^{18}F]-fluoroazidobutane results in the formation of a tracer [^{18}F]-TBN which retains its high affinity for GRP receptors *in vitro*. Tumor uptake and *in vivo* pharmacokinetics in PC-3 tumor-bearing mice were not in agreement with the *in vitro* results which possibly could be explained by low metabolic stability *in vivo*.

Ch. 5

References

- Ananias HJ, de Jong IJ, Dierckx RA, van de Wiele C, Helfrich W, Elsinga PH. Curr Pharm Des. 2008, 14(28), 3033-47.

- Baidoo K E, Lin K S, Zhan Y, Finley P, Scheffel U, Wagner H N, Bioconjug Chem., 1998, 9, 218-25.

- Chang Y S, Jeong J M, Lee Y S, Kim H W, Rai G B, Lee S J, Lee D S, Chung J K, Lee M C, Bioconj. Chem., 2005, 16, 1329-1333.

- Chen X, Park R, Hou Y, Tohme M, Shahinian A H, Bading J R, Conti P S, J. Nucl. Med., 2004, 45, 1390–1397.

- Ferro-Flores G, Arteaga de Murphy C, Rodriguez-Cortés J, Pedraza-López M, Ramírez-Iglesias M T, Nucl. Med. Commun., 2006, 27, 371-6.

- Kolb H C, Finn M G, Sharpless K B, Angew. Chem., Int. Ed. 2001, 40, 2004–2021.

- Mindt T L, Struthers H, Brans L, Anguelov T, Schweinsberg C, Maes V, Tourwe D, Schibli R, J. Am. Chem. Soc., 2006, 128, 15096-15097.

- Prasuhn D E. Jr, Yeh R M, Obenaus A, Manchester M, Finn M G, Chem Commun. 2007, 12, 1269-71.

- Reubi J C, Waser B, Eu. J. Nucl. Med. Mol. Imaging., 2003, 30, 781-93.

- Santos-Cuevas C L, Ferro-Flores G, Arteaga de Murphy C, Ramírez Fde M, Luna-Gutiérrez M A, Pedraza-López M, García-Becerra R, Ordaz-Rosado D, Int. J. Pharm. 2009, 22, 75-83.

- Tornoe C W, Christensen C, Meldal M, J. Org. Chem., 2002, 67, 3057–3064.

Chapter 6

Synthesis of ^{18}F-RGD-K5 by catalyzed [3 + 2] cycloaddition for imaging integrin $\alpha_v\beta_3$ expression in vivo

Leila Mirfeizi[a], Joe Walsh[b], Hathmuth Kolb[b,] Lachlan Campbell-Verduyn [c], Rudi A. Dierckx[a], Ben L. Feringa[c], Philip H. Elsinga[a*] Tjibbe de Groot [f], Ivan Sannen [d,] Guy Bormans [d,], Sofie Celen[d],

[a]Department of Nuclear Medicine and Molecular Imaging, University Medical Center Groningen, University of Groningen, Groningen, The Netherlands. [b]Siemens Molecular Imaging Biomarker Research, Culver City CA, USA. [c]Stratingh Institute for Chemistry, University of Groningen, Groningen, The Netherlands. [d]Laboratory for Radiopharmacy, Faculty of Pharmaceutical Sciences, KU Leuven, Leuven, Belgium [f]Department of Nuclear Medicine, U.Z. Gasthuisberg, KU Leuven, Leuven, Belgium

Abstract

In the last few years click chemistry reactions, and in particular copper-catalyzed cycloadditions have been used extensively for the preparation of new bioconjugated molecules such as ^{18}F-radiolabelled radiopharmaceuticals for positron emission tomography (PET). This study is focused on the synthesis of the Siemens imaging biomarker ^{18}F-RGD-K5. This cyclic peptide contains an amino acid sequence which is a well known binding motif for integrin $\alpha_v\beta_3$ involved in cellular adhesion to the extracellular matrix. We developed an improved "click" chemistry method using Cu(I)-Monophos as catalyst to conjugate [^{18}F]fluoropentyne to the RGD-azide precursor yielding ^{18}F-RGD-K5. A comparison is made with the registered Siemens method with respect to synthesis, purification and quality control. [^{18}F]RGD-K5 was obtained after 75 min overall synthesis time with an overall radiochemical yield of 35% (EOB). The radiochemical purity was > 98 % and the specific radioactivity was 100-200 GBq/μmol at the EOS.

Introduction

Integrins are heterodimeric ($\alpha-\beta$) transmembrane proteins expressed at the cell surface that are involved in cellular adhesion to the extracellular matrix [Plow 2000, Gottschalk 2002]. They stimulate vascular endothelial cell migration and invasion, regulate their growth, survival and differentiation and they serve as receptors for a variety of extracellular matrix proteins including vitronectin, fibronectin, fibrinogen and osteopontin. They are involved in many biological processes such as angiogenesis, thrombosis, inflammation, osteoporosis and cancer, playing a key role in many severe human diseases [Hynes 1992, 2002a, Brooks, 1994]. So far, 18 α and 8 β subunits of integrins have been identified: they form 24 heterodimers, each with distinct ligand binding properties. Among the integrin superfamily, $\alpha_v\beta_3$ and $\alpha_5\beta_1$ integrins, targeted by the RGD sequence, play a pivotal role in the formation of new blood vessels in tissues (angiogenesis) [Tamkun, 1986, Hynes 2002b, Hwang 2004, Ruoslahti 1987]. $\alpha_v\beta_3$ and $\alpha_5\beta_1$ integrins are overexpressed on activated endothelial cells during physiological and pathological angiogenesis [Ruegg 2003].

Since $\alpha_v\beta_3$ integrin is expressed on tumor cells of various types (melanoma, glioblastoma, ovarian and breast cancer) where it is involved in the processes that govern metastasis, it represents an attractive target for cancer therapy and has stimulated ongoing research to define high affinity ligands [Pierschbacher 1984, Meyer 2006].

RGD containing integrin ligands have a large number of medical applications ranging from noninvasive visualization of integrin expression in vivo to the synthesis of functionalized biomaterials. Over the past decade, a variety of radiolabeled cyclic peptide antagonists with structures based on the RGD sequence have been evaluated as integrin $\alpha_v\beta_3$-targeted radiotracers [Liu 2006 and 2009]. The PET tracers [^{18}F]Galacto-RGD, [^{18}F]-AH111585 and [^{18}F]RGD-K5 are currently under clinical investigation for visualization of integrin $\alpha_v\beta_3$ expression in cancer patients [Beer 2006, Cho 2009, Doss 2009, Haubner 2005, Kenny 2008, McParland 2008].

Due to its favourable β-energy and half-life, fluorine-18 is the most frequently used radionuclide in PET. However, rapid and direct non carrier-added ^{18}F-labeling of complex biomolecules such as peptides is not straight forward. The main approach to label peptides with ^{18}F is via fluorination of prosthetic groups which are then conjugated to the biomolecule [Okarvi 2001, Wester 2007]. [^{18}F]Galacto-RGD, a glycosylated cyclic pentapeptide, is labeled via ^{18}F-acylation with 4-nitrophenyl-2-[^{18}F]fluoropropionate

[Haubner 2004]. The acylation methodology is however complex and time consuming. Synthesis of [^{18}F]Galacto-RGD via this prosthetic group method, requires a total synthesis time of about 200 min of which the production of the ^{18}F-prosthetic group takes about 130 min [Haubner 2004]. Another strategy, which has been applied for the synthesis of [^{18}F]-AH111585, involves chemoselective oxime formation between the aminooxy functionality of the peptide and the carbonyl group of the ^{18}F-labeled aldehyde prosthetic group 4-[^{18}F]fluorobenzaldehyde [Glaser 2008, Poethko 2004]. Introduction of fluorine-18 can also be achieved by chelation of aluminium fluoride [McBride, 2010].

Recently, the copper(I)-catalysed Huisgen 1,3-dipolar cycloaddition reaction (CuAAC) between terminal alkynes and azides resulting in 1,4-disubstituted 1,2,3-triazoles [Rostovtsev 2002, Tornøe 2002] has found its way in radiopharmaceutical chemistry [Glaser, 2009]. The main advantages of this 'click chemistry' approach are selectivity, reliability and short reaction times while only mild reaction conditions are required [Bock, 2006, Kolb 2006]. The ^{18}F-labeling of peptides has been the area that has benefited the most from click chemistry [Glaser, 2007, Marik 2006]. The additional advantage of this chemistry is that there is no need of protective groups when labeling peptides. Both alkynes [Marik 2006] and azides [Glaser 2007] have been radiolabeled with fluorine-18 to produce ^{18}F-peptides.

As a result of a collaboration between the PET-centers in Leuven (Belgium), Groningen (The Netherlands) and Siemens (MIBR, Los Angeles, USA), we report an improved and simplified procedure to prepare [^{18}F]RGD-K5 using a Cu-catalyst based on phosphoramidite ligand [Campbell-Verduyn 2009] . This paper describes in detail the optimized radiosynthesis (Scheme 6.1) and QC procedure of [^{18}F]RGD-K5, and compares it with the registered method by Siemens. The efficient radiosynthesis procedure can generally be applied for other click reactions using [^{18}F]fluoroalkynes as prosthetic group.

Matherials and Methods

General

Reagents and solvents were obtained from commercial suppliers (Aldrich, Fluka, Sigma, and Merck) and used without further purification. RGD-K5 azide and ^{19}F-RGD-K5 were
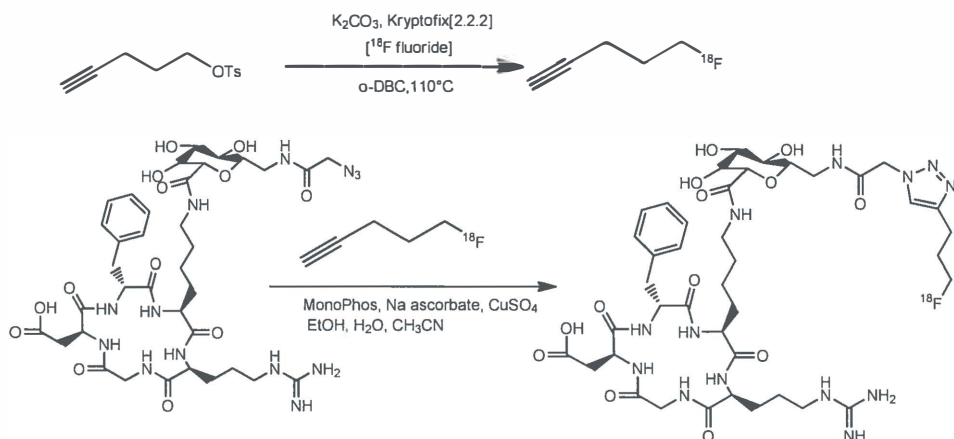
prepared by Siemens. For radiolabeled compounds, radioactivity detection on TLC was performed with Cyclone phosphor storage screens (multisensitive, PerkinElmer). These screens were exposed to the TLC strips and subsequently read out using a Cyclone phosphor storage imager (PerkinElmer) and analyzed with OptiQuant software. HPLC analysis was performed in Groningen with an Elite LaChrom VWR Hitachi L-2130 pump system (Darmstadt, Germany) connected to a UV-spectrometer (Elite LaChrom VWR Hitachi L-2400 UV detector) and a Bicron frisk-tech radiation detector. In Leuven, HPLC analysis was performed on a LaChrom Elite Hitachi HPLC system (Darmstadt, Germany) connected to a UV spectrometer (Waters 2487 Dual γ absorbance detector). For the analysis of radiolabeled compounds, the HPLC eluate after passage through the UV detector was led over a 3 in. NaI(Tl) scintillation detector (Wallac, Turku, Finland) connected to a multi channel analyzer (Gabi box, Raytest, Straubenhardt Germany). The output signal was recorded and analyzed using a GINA Star data acquisition system (Raytest, Straubenhardt, Germany).

Radiolabeling

Production of [^{18}F]fluoride

Aqueous [^{18}F]fluoride was produced via the ^{18}O(p,n)^{18}F nuclear reaction by irradiation of 97 % enriched [^{18}O]water (2-4 mL; Rotem HYOX18, Rotem Industries, Beer Sheva, Israel). The [^{18}F]fluoride solution was passed through a Sep-Pak Light Accell Plus QMA anion exchange cartridge (Waters) to trap the [^{18}F]fluoride and recover the ^{18}O-enriched water. The [^{18}F]fluoride was eluted from the cartridge with 1 mL of K$_2$CO$_3$ solution (4.5 mg/mL) into a conical glass reaction vial containing 20 mg Kryptofix 2.2.2. To this solution, 1 mL acetonitrile was added and the solvents were evaporated at 130 °C. The [^{18}F]KF/Kryptofix complex was dried 3 times by the addition of 0.5 mL acetonitrile, followed by evaporation of the solvent.

Scheme 6.1. A) Production of 5-[^{18}F]fluoro-1-pentyne: nucleophilic substitution between pentynyl tosylate and anhydrous [^{18}F]fluoride in ortho-dichlorobenzene (o-DCB). B) MonoPhos Cu(I)-catalysed Huisgen cycloaddition of [^{18}F]fluoropentyne with the RGD-K5 azide precursor resulting in the 1,4-disubstituted triazole [^{18}F]RGD-K5.

A solution of pent-4-ynyl-4-methylbenzenesulfonate (20-25 mg, 84-105 μmol) in 0.8-1 mL anhydrous 1,2- dichlorobenzene was added to the Kryptofix 2.2.2 K^{18}F residue and the mixture was heated for 10 min at 110 °C to provide [^{18}F]fluoropentyne which was simultaneously distilled with a gentle flow of helium to a second reactor containing the click reaction mixture. The click reaction mixture contained 0.1 mg RGD-K5 azide precursor(2-((2S,5R,8S,11S)-8-(4-((3S,4S,5R,6R)-6-((2-azidoacetamido)methyl)-3,4,5-trihydroxytetrahydro-2H-pyran-2-carboxamido)butyl)-5-benzyl-11-(3-guanidinopropyl)-3,6,9,12,15-pentaoxo-1,4,7,10,13-pentaazacyclopentadecan-2-yl)acetic acid; TFA salt) in the presence of 0.2 mg phosphoramidite Monophos, 1 mol% (0.05 mg) CuSO$_4$.5H$_2$O (reduced to Cu(I) with 5 mol% (0.25 mg) sodium ascorbate), in either 0.25 mL EtOH and 0.25 mL CH$_3$CN (Groningen) or 0.084 mL EtOH, 0.125 mL CH$_3$CN and 0.042 mL water (Leuven) (Table 2). The subsequent conversion to radiolabeled [^{18}F]RGD-K5 was followed

by radio-TLC (Rf [^{18}F]RGD-K5 = 0.4 (eluent: MeOH/H$_2$O 2:1)). After reacting at room temperature for 10 min, the crude [^{18}F]RGD-K5 was diluted with 1.5 mL of 0.025 M Na$_2$HPO$_4$ pH 7 and purified by semi-preparative RP-HPLC using an XBridge C18 column (5 µm, 4.6 mm x 150 mm column, Waters) eluted with 0.025M Na$_2$HPO$_4$ pH 7.0 and EtOH 88/12 at a flow rate of 1ml/min (Leuven) or by semi-preparative RP-HPLC using an XBridge C18 column (5 µm, 10 mm x 150 mm column, Waters) eluted with 0.025M Na$_2$HPO$_4$ pH 7.0 and EtOH 86/14 at a flow rate of 4 mL/min (Groningen). UV detection of the HPLC eluate was performed at 254 nm. [^{18}F]RGD-K5 was collected after 20-25 min (Figure 6.2). On average, about 11 GBq (n=24, ranging from 3.7 to 19.5 GBq) of purified [^{18}F]RGD-K5 was collected in a 1.3-2.6 mL volume (mobile phase). This HPLC-purified fraction was diluted with preparative HPLC mobile phase and passed through an apyrogenic 0.22 µm membrane filter (Millex®-GV, Millipore, Ireland). A final solution of 370 MBq/mL was obtained by further dilution with saline which was passed through the same membrane filter.

Ch. 6

Quality control procedures

Quality control procedures for [^{18}F]RGD-K5 are based upon the current requirements for radiopharmaceuticals laid out in the European Pharmacopoeia [Ph.Eur. 6.0-Radiopharmaceutical Preparations].

The radiochemical identity of [^{18}F]RGD-K5 is checked using an analytical HPLC system consisting of an XBridge C$_{18}$ column (3.5 µm, 3 mm × 100 mm; Waters) eluted with 0.025 M Na$_2$HPO$_4$ (pH 7) and CH$_3$CN (90:10 v/v) at a flow rate of 0.8 mL/min. UV detection of the HPLC eluate is performed at 210 nm (Figure 6.3).

In Groningen QC was performed on a Phenomenex Prodigy C$_{18}$ column (5 µm, 4.6 mm x 150 mm column, Waters with CH$_3$CN and water (40:60 v/v) in the presence of 0.1 % TFA as eluent at a flow rate of 3mL/min. The radiochemical identity of [^{18}F]RGD-K5 is confirmed using authentic RGD-K5 as an external reference material. After injection and analysis of a solution of the reference material RGD-K5, a blank injection of preparative HPLC mobile phase is performed. The retention time of [^{18}F]RGD-K5 should be the same (± 10 %) as the retention time observed for the RGD-K5 reference standard. The radiochemical purity and specific activity is analyzed using the same HPLC system. The total of radiolabeled side

products should be ≤ 5%. Rather than setting a lower limit for specific activity, the maximum mass of RGD-K5 which is administered to a patient is limited to < 96 µg and the mass of the RGD-K5 azide precursor should be < 5 µg per administered dose, these limits were defined in relation to toxicity tests findings performed by Siemens. Residual solvent analysis is performed using GC (direct injection). For the residual class 2 solvent acetonitrile a limit of 4.1 mg per patient dose is set as described in the European Pharmacopoeia. 1,2-Dichlorobenzene is not described in the European Pharmacopoeia but has a no observed adverse effect level (NAOEL) of 120 mg/kg/day [http://www.epa.gov/iris/subst/0408.htm] in rats which is considerably higher than for chlorobenzene (27 mg/kg/day) [http://www.epa.gov/iris/subst/0399.htm]. For chlorobenzene the European Pharmacopoeia sets a limit of 3.1 mg per day.

In order to have a safety margin we have therefore set a limit of 1 mg of o-DCB per injected dose. To be safely administered to the patient, the amount of residual ethanol should be < 10% v/v. The drug product pH should be in the range 5-8. Testing of the integrity of the filter that is used for sterile filtration is done by bubble point determination. The bubble point pressure for the particular filter used should be ≥ 3.45 bar. Determination of the radionuclide identity and endotoxin and sterility testing are performed post batch release. Since $CuSO_4$ is being used in the manufacturing process of the radioligand, the finished drug product should be tested for residual levels of the metal reagent.

Result and discussion

Using our optimized click reaction condition we improved and simplified the original registered Siemens production method. Scheme 1 shows the two-steps radiosynthetic route to yield [^{18}F]RGD-K5. In a first step the labeling synthon 5-[^{18}F]fluoro-1-pentyne was prepared via nucleophilic fluorination of pentynyltosylate with anhydrous [^{18}F]KF-cryptate at 110 °C in o-DCB. The ^{18}F-labelled pentyne (Bp= 76 °C) was isolated from the tosyl precursor and unreacted ^{18}F$^-$ via distillation and was, without further purification, trapped in a receiving vial containing the RGD-K5 azide precursor. Effluent gasses that escaped from the receiving vial were collected in a balloon. We choose a high boiling point solvent (o-DCB, 179 °C) instead of acetonitrile (82 °C) to prevent co-distillation of the solvent. Acetonitrile co-distilling to the click reaction mixture was found to decrease the yield of the

click reaction and the efficiency of the HPLC purification. The distilled [^{18}F]fluoropentyne was efficiently trapped at room temperature in the click reactor (90 %) avoiding the need to use a cold trap. Radiometric detection showed that the amount of [^{18}F]fluoropentyne in the receiving vial saturated after about 10 min.

The phosphoramidite ligand Monophos showed to be an excellent ligand for complexation of Cu(I) in order to catalyze the click reaction [Campbell-Verduyn, 2009]. Monophos was far superior to the previously reported ligand TBTA [Chan, 2004]. In absence of the ligand only minor conversion to the triazole product [^{18}F]F-RGD-K5 was observed. Further reaction optimization was performed by varying the amount of RGD-K5 azide from 0.1 mg to 2 mg. (Figure 6.1)
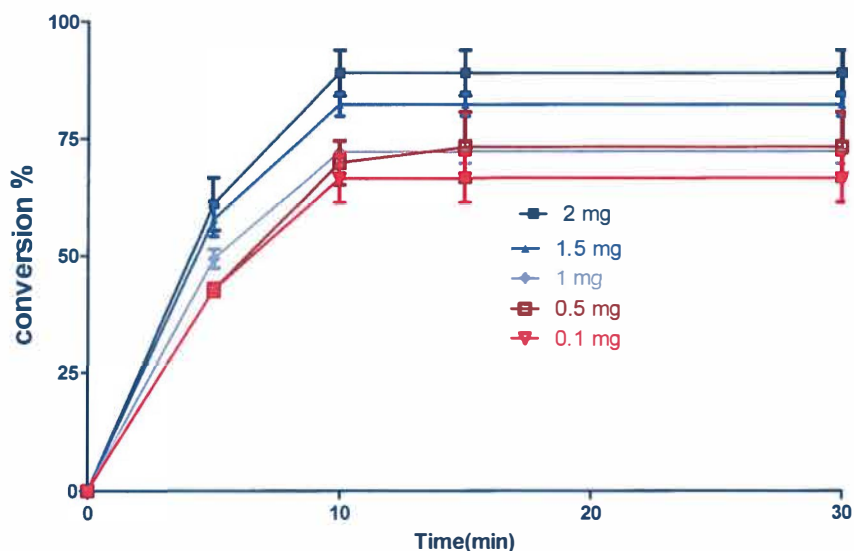
Figure 6.1. Radiochemical conversion of the click reaction as a function of time and amount of RGD-K5 azide precursor

Reactions with only 0.1 mg RGD-K5 azide yielded ^{18}F-RGD-K5 in excellent radiochemical yield. So far 1 mol % of CuSO$_4$ in the presence of 1.1 mol % Monophos showed sufficient catalytic effect within 15 min. These optimized conditions utilizing Cu(I) and Monophos as a potent catalyst provide an important tool to use reduced amounts of peptide precursor, that is expensive in many cases. Usually amounts of >1 mg peptide are used and no additional catalyst beside Cu(I) is employed. As a result of the dramatic acceleration of the click reaction by Monophos it was possible to substantially reduce the amounts of reactants such as sodium ascorbate, CuSO$_4$, catalytically active and amount of azide (Table 6.1).

Material and method	Optimized protocol	SIEMENS protocol
Synthesis of [^{18}F]fluoropentyne	24 mg pentynyl tosylate in 1 mL dichlorobenzene	24 mg pentynyl tosylate in 1 mL MeCN
RGD-K5 azide	0.1 mg	4 mg
Na-ascorbate	0.25 mg	40 mg
CuSO$_4$	0.05 mg in 0.25 mL H$_2$O	15 mg in 0.25 mL MeCN
Ligand	0.2 mg MonoPhos in 0.1 mL DMSO	15 mg TBTA
Purification by HPLC: Mobile phase	isocratic Phosphate buffer 0.025M pH 7 / EtOH 86/14 v/v (Groningen) or 88/12 v/v (Leuven)	gradient MeCN:H$_2$O 50/50 v/v+ 0.01% TFA
Formulation by C-18 seppak classic	None	Dilute HPLC fraction with 100 ml of water Elute with 1 ml ethanol

Table 6.1. Main differences between the optimized [^{18}F]RGD-K5 production procedure as described in this article and the original Siemens protocol

The crude click reaction mixture was purified using semi-preparative HPLC. Before injection, the mixture was diluted with phosphate buffer pH 7 to adjust the pH to that of the mobile phase resulting in sharper peaks. We evaluated different sizes and types of columns and found that the Waters XBridge C18 (5 µm, 4.6 x 150 mm) gave sharper peaks and provided the best separation between the azide precursor and [^{18}F]RGD-K5 (resolution 2.18). For the preparative HPLC purification we preferred an isocratic method with a mobile phase consisting of a phosphate buffer in combination with ethanol.

Using a mobile phase with ethanol as organic modifier eliminates post HPLC SepPak formulation resulting in a reduced synthesis time and a more simple and reliable tracer production [Serdons 2008]. Using the XBridge column in combination with a mobile phase consisting of 12 % ethanol in 0.025 M phosphate buffer pH 7, the unreacted azide precursor eluted at 20 min and [^{18}F]RGD-K5 at 25 min.

The RGD-K5 azide precursor and the reference compound RGD-K5 have their maximal UV absorption at 210 nm. The reference compound also absorbs at 254 nm, the azide precursor does not. Since for the preparative purification UV detection was performed at 254 nm, the trace of unreacted precursor is not visible in the UV channel of the preparative HPLC chromatogram of the crude radiolabeling mixture (Figure 6.2). Within the isocratic conditions unreacted [^{18}F]fluoropentyne is retained on the column and only elutes upon rinsing the HPLC column with EtOH/H$_2$O 70:30 v/v mixtures.
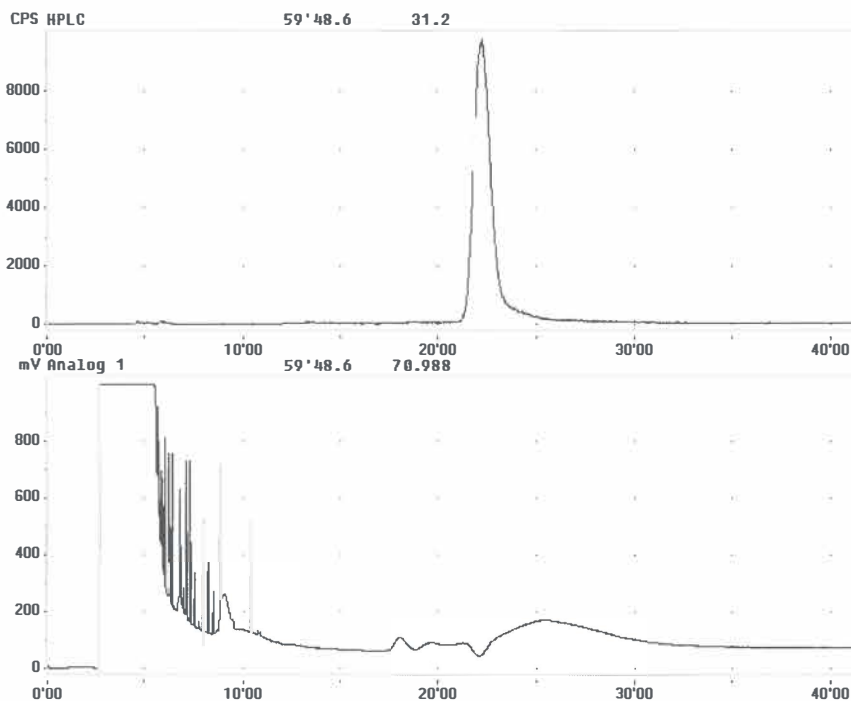
Ch. 6

Figure 6.2. Semi-preparative HPLC chromatogram of the purification of [^{18}F]RGD-K5. Upper channel: radiometric detection. Lower channel: UV detection at 254 nm. [^{18}F]RGD-K5 elutes at 22 min. Unreacted [^{18}F]fluoropentyne elutes during rinsing of the column.

The radiolabeled compound [^{18}F]RGD-K5 was obtained in 35% radiochemical yield based on [^{18}F]fluoride starting radioactivity (decay-corrected) in 75 min.

Analysis of the radiochemical identity, radiochemical and chemical purity and determination of specific radioactivity was performed on an analytical HPLC system consisting of a XBridge C18 column (3.5μm, 3 x 100 mm) eluted with a mobile phase consisting of 10 % acetonitrile in 0.025 M phosphate buffer pH 7. At 210 nm using a flow rate of 0.8 mL/min, [^{18}F]RGD-K5

elutes at 11 min. The radiochemical purity was higher than 98% and the specific radioactivity of [^{18}F]RGD-K5 was determined to be in the range of 100–200 GBq/μmol. For all productions, QC HPLC analysis (Figure 6.3) showed that the amount of RGD-K5 azide precursor (Rt= 6 min) in the final solution was lower than the detection limit (LOD 0.2 ng), confirming the efficient separation between the azide precursor and [^{18}F]RGD-K5 with the applied preparative HPLC system.
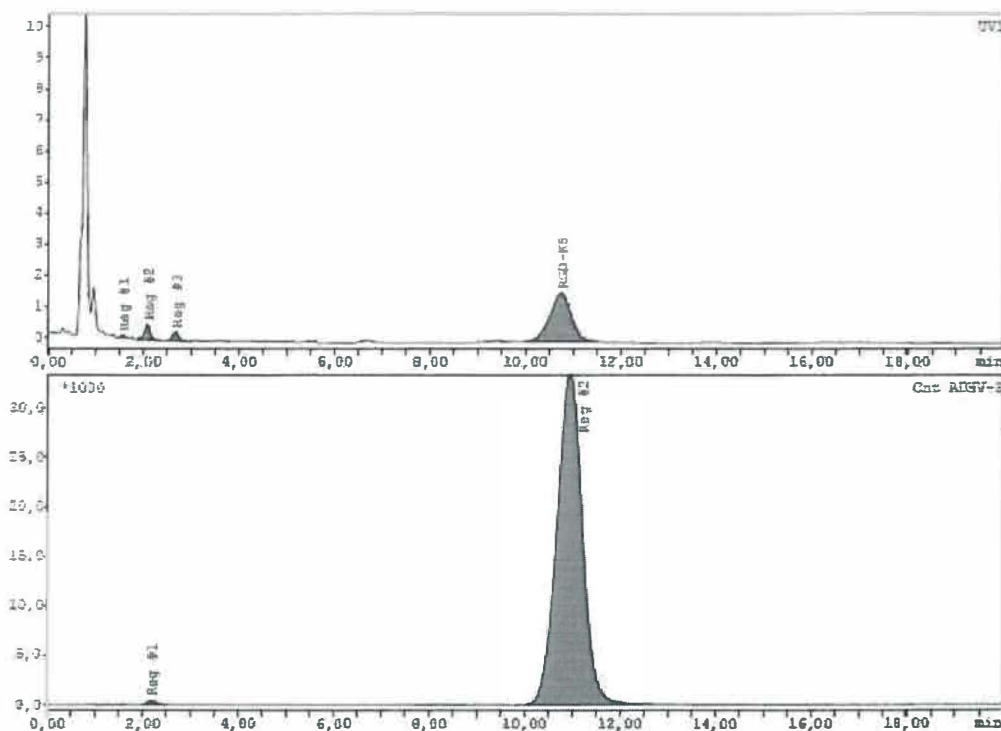

Figure 6.3. Quality control of [^{18}F]RGD-K5. Upper channel: UV detection at 210 nm. No trace of RGD-K5 azide precursor is observed at the expected retention time of 6-7 min. Lower channel: radiometric detection. (Performed by Leuven-Belgium)HPLC system consisting of an XBridge C$_{18}$ column (3.5 μm, 3 mm × 100 mm; Waters) eluted with 0.025 M Na$_2$HPO$_4$ (pH 7) and CH$_3$CN (90:10 v/v) at a flow rate of 0.8 mL/min.

For all productions, the amount of RGD-K5 in the final drug product was < 96 μg. The concentration of copper was determined for 5 batches of RGD-K5 using inductively coupled plasma mass spectrometry (ICP-MS) and was found to be 53±22 μg/L which corresponds to 1/10th of the concentration of naturally copper in plasma (50-150 μg/dL) (Merck Manual). If the total batch would be injected into a single subject this would result in the administration of < 0.5 μg which corresponds to less than 1/1000th of the daily recommended dose (1.2 mg/day), indicating that there is a large safety margin with regard to the copper content in the [^{18}F]RGD-K5 productions. Residual Kryptofix-[2.2.2] analysis was not performed as it was validated that Kryptofix does not co-distil with [^{18}F]fluoropentyne from the first reaction vial. The amount of acetonitrile and o-DCB in the final formulation were below the detection limit (LOD 0.0001 %). Ethanol was present (< 8 %) to increase radiochemical stability and to minimize the tracer being retained on the walls of the sterile filter, the vial and the syringes used to administer the drug product to the patient (Serdons 2008).

Radionuclide purity, sterility and endotoxin testing were performed post batch release. The radionuclide identity was determined using a two-time point radioactivity measurement in a dose-calibrator.

For all batches, the calculated half-life was in the range 105-115 min which is according to Ph.Eur. guidelines [Ph.Eur. 6.0-Radiopharmaceutical Preparations]. Bacterial endotoxin determination of the [^{18}F]RGD-K5 batches was done using the Limulus amebocyte lysate (LAL) test according to the Ph.Eur. guidelines [Ph.Eur. 6.0-Chapter 2.6.14: Bacterial Endotoxines]. For all batch productions the endotoxin content was < 1 IU/mL (limit set at 10 IU/mL). If the total batch volume (max 20 mL) would be injected to one volunteer the amount of injected IU would be well below the 175 IU per dose limit for radiopharmaceuticals specified in the Ph.Eur [Ph.Eur. 6.0-Chapter 2.6.14: Bacterial Endotoxines]. Sterility testing was done according to Ph.Eur. 6.0 and no growth of microorganisms was detected after 14 days incubation at 37 °C in any of the batches.

Conclusion

^{18}F-RGD-K5 was synthesized with high specific activity and high radiochemical yield using click chemistry. The beneficial effects of click chemistry for the synthesis of biomolecules containing the RGD system will ensure the growth of this area in the future. The monophos ligand accelerated Cu(I)-catalyzed 1,3-dipolar cycloaddition reaction was applied successfully. The QC system has been validated and allows the tracer to be used in clinical studies for visualization of neoangiogenesis in oncological patients in our hospitals.

Ch. 6

References

- Beer A J, Haubner R, Sarbia M, Goebel M, Luderschmidt S, Grosu A L, Schnell O, Niemeyer M, Kessler H, Wester H J, Weber W A, Schwaiger M, Clin. Cancer Res. 2006., 12, 3942-3949.
- Bock V D, Hiemstra H, Maarseveen JH, Eur. J. Org. Chem. 2006, 51-68.
- Brooks P C, Clark R A, Cheresh D A, Science, 1994, 264, 569–571.
- Campbell-Verduyn L S , Mirfeizi L , Dierckx R A, Elsinga P H, Feringa B L, Chem. Commun., 2009, 16, 2139–2141.
- Chan T R, Hilgraf R, Sharpless K B, Fokin V V, Org. Lett. 2004, 6, 2853-2855.
- Cho H J, Lee J D, Park J Y, Yun M, Kang W J, Walsh J C, Kolb H, Zhang J J, J. Nucl. Med. 2009, 50 (Suppl 2), 1910.
- Doss M, Alpaugh R K, Yu Y Q, J. Nucl. Med., 2009, 50 (Suppl 2), 447.
- European Pharmacopoeia 6.0 – Radiopharmaceutical Preparations (0125).
- European Pharmacopoeia 6.0 – Chapter 2.6.1: Sterility.
- European Pharmacopoeia 6.0 – Chapter 2.6.14: Bacterial Endotoxins.
- Glaser M, Arstad E, Bioconjugate Chem. 2007, 18, 989-993.
- Glaser M, Morrison M, Solbakken M, Arukwe J, Karlsen H, Wiggen U, Champion S, Kindberg G M, Cuthbertson A, Bioconjugate Chem., 2008. 19, 951-957.
- Glaser M, Robins E G, J. Label. Compd. Radiopharm., 2009, 52, 407-414.
- Gottschalk K E, Kessler H, Angew. Chem. Int. Ed., 2002, 41, 3767–3774.
- Haubner R, Kuhnast B, Mang C, Weber W A, Kessler H, Wester H J, Schwaiger M, Bioconjugate Chem. 2004, 15, 61-69.
- Haubner R, Weber W A, Beer A J, Vabuliene E, Reim D, Sarbia M, Becker K F, Goebel M, Hein R, Wester H J, Kessler, H, Schwaiger, M, PLoS Medicine. 2005. 2, 244-252.
- http://www.epa.gov/iris/subst/0408.htm
- http://www.epa.gov/iris/subst/0399.htm
- Hwang,R, Varner J V , Hematol. Oncol. Clin. North. Am., 2004, 18, 991-1006.
- Hynes R O, Cell 69, 1992, 11–25.
- Hynes R O Nat. Med., 2002a. 8, 918–921.
- Hynes RO, Cell 110, 2002b, 673–687.

- Kenny L M, Coombes R C , Oulie I, Contractor K B, Miller M, Spinks T J , McParland B, Cohen P S, Hui A M, Palmieri C , Osman S, Glaser M , Turton D, Al-Nahhas A, Aboagye E O , J. Nucl. Med., 2008. 49, 879-886.
- Kolb H C , Finn, M G , Sharpless K B , Angew. Chem. Int. Ed., 2001, 40, 2004-2021.
- Liu S, Mol. Pharm., 2006, 3, 472-487.
- Liu S, Bioconjugate Chem., 2009, 20, 2199-2213.
- Marik J, Sutcliffe J L, Tetrahedron Lett., 2006, 47, 6681-6684.
- McBride W J, D'Souza C A, Sharkey R M, Karacay H, Rossi E A, Chang C H, Goldenberg D M, Bioconjugate Chem., 2010, 21, 1331-1340.
- McParland B J, Miller M P, Spinks T J, Kenny L M, Osman S, Khela M K, Aboagye E, Coombes R C, Hui A M, Cohen P S, J. Nucl. Med., 2008. 49, 1664-1667.
- Meyer A, Auemheimer J, Modlinger A, Kessler H, Curr. Pharm. Des., 2006, 12, 2723–2747.
- Okarvi S M, Eur. J. Nucl. Med., 2001, 28, 929-938.
- Pierschbacher M, Ruoslahti D, Nature, 1984, 309, 30–33.
- Plow E F, Haas T A, Zhang L, Loftus J, Smith J S, J. Chem. Biol., 2000, 275, 21785–21788.
- Poethko T, Schottelius, M, Thumshirn G, Hersel U, Herz M, Henriksen G, Kessler H, Schwaiger M, Wester H J, J Nucl. Med., 2004, 45, 892-902.
- Rostovtsev V V, Green L G, Fokin V V, Sharpless K B, Angew. Chem. Int. Ed., 2002, 41, 2596-2599.
- Rüegg C, Mariotti A, Cell. Mol. Life Sci., 2003, 60, 1135–1137.
- Ruoslahti E, Pierschbacher M D, Science., 1987, 238, 491-497.
- Serdons K, Verbruggen A, Bormans G, J. Nucl. Med., 2008, 49, 2071.
- Tamkun J W, DeSimone D W, Fonda D, Patel R S, Buck C, Horwitz A F, Hynes R O, Cell, 1986, 46, 271–282.
- Tornøe C W , Christensen C, Meldal M, J. Org. Chem., 2002, 7, 3057-64.
- Wester H J, Schottelius M, Ernst Schering Research Foundation Workshop, 2007, 62, 79-111.

Ch. 6

Chapter 7

Feasibility of ^{18}F-RGD-K5 for ex vivo Imaging of Atherosclerosis in Detection of $\alpha_v\beta_3$ integrin expression

Reza Golestani[a†], Leila Mirfeizi[a†], Clark J. Zeebregts[b], Hendrikus H.Boersma[a,c], René A.Tio[d], Rudi A.J.O. Dierckx[a,e], Philip H. Elsinga[a], Riemer H.J.A. Slart[a]

[a]Departments of Nuclear Medicine and Molecular Imaging, [b]Surgery, Division of Vascular Surgery, [c]Clinical and Hospital Pharmacy, d-Cardiology, University Medical Center Groningen, University of Groningen, Groningen, the Netherlands, [e]Department of Nuclear Medicine, Ghent University Hospital, Ghent, Belgium

Abstract

Background: Given the fact that angiogenesis plays an important role in atherosclerotic plaque vulnerability, molecular imaging of angiogenesis can be used for determination of rupture-prone atherosclerotic plaques. $\alpha_v\beta_3$ integrin is a key player in the process of angiogenesis. Targetted imaging of $\alpha_v\beta_3$ integrin has been shown to be possible in previous studies on tumor models, using radiolabeled arginine-glycine-aspartate- (RGD-K5).

Our aim was to investigate feasibility of ex vivo detection of $\alpha_v\beta_3$ integrin in human carotid endarterectomy (CEA) specimens.

Methods CEA specimens, immediately after excision, were incubated in 5 Mbq ^{18}F-RGD-K5 for one hour followed by one hour emission microPET scan. The results were quantified in 4mm wide segments as percent incubation dose per gram (%Inc/g). A segmental-to-total ratio was calculated by dividing segmental %Inc/g by total specimen's %Inc/g. Presence of $\alpha_v\beta_3$ integrin and endothelial cells in each segment was confirmed by immunohistochemical staining for CD31 and $\alpha_v\beta_3$ integrin, respectively.

Results [^{18}F]-RGD-K5 uptake was heterogeneous in CEA specimens and was localized within the vessel wall. Significant correlations was observed between segmental-to-total ratio with $\alpha_v\beta_3$ integrin staining score (r = 0.58, p = 0.038) and CD31 staining score (ρ = 0.67, P < 0.002).

Conclusion This study, for the first time showed the feasibility of integrin imaging in determination of $\alpha_v\beta_3$ integrin expression and angiogenesis in atherosclerotic plaques.

Introduction

Intraplaque hemorrhage as a consequence of intraplaque pathology has been linked to vulnerability of atherosclerotic plaques to rupture and further cardiovascular complications (Virmani , 2005). Given the fact that most of cardiovascular events (including heart attacks and strokes) occur in non-stenotic atherosclerotic plaques (Naghavi , 2003), raise attention for development of non-invasive methods for detection of rupture-prone plaques to provide an individualized means for clinicians to risk stratify patients at higher risk for cardiovascular events.

Molecular imaging of angiogenesis targets variable players in the process of angiogenesis. Vascular endothelial growth factor (VEGF) (Nagengast , 2007), VEGF-receptor (Cai , 2006), and integrins (Schnell , 2009) have been targeted by molecular imaging probes. Imaging studies have shown promising results in detection of angiogenesis in oncology research. Among integrin proteins, specifically $\alpha_v\beta_3$ integrin, a cell surface receptor, plays a crucial role in process of angiogenesis by mediating adhesion of cells to extracellular matrix and migration of endothelial cells (Morrison, 2010). Because of its critical role, $\alpha_v\beta_3$ integrin imaging has been focus of many studies.

RGD containing integrin ligands have a large number of medical applications ranging from noninvasive visualization of integrin expression in vivo to the synthesis of functionalized biomaterials. Over the past decade, a variety of radiolabeled cyclic peptide antagonists with structures based on the RGD sequence have been evaluated as integrin $\alpha_v\beta_3$-targeted radiotracers [Liu, 2006, 2009]. The PET tracers [^{18}F]Galacto-RGD, [^{18}F]-AH111585 and [^{18}F]RGD-K5 are currently under clinical investigation for visualization of integrin $\alpha_v\beta_3$ expression in cancer patients [Beer, 2006; Cho, 2009; Doss, 2009; Haubner, 2005; Kenny, 2008; McParland, 2008].

High binding affinity of arginine-glycine-aspartate (RGD) peptide sequence for $\alpha_v\beta_3$ integrin has resulted development of multiple tracer for detection of $\alpha_v\beta_3$ integrin as a marker for angiogenesis (Liu, 2006). It has been shown that small animal positron emission tomography (PET) imaging of $\alpha_v\beta_3$ integrin is possible in highly $\alpha_v\beta_3$ integrin-expressing mouse tumors and mouse models of human tumor xenografts with a high tumor-to-background ratio and specificity (Haubner, 2001). The role of a single photon emission computed tomography (SPECT) RGD-based probe in detection of inflammation in mouse models of vascular remodeling has been demonstrated recently (Razavian, 2011).Moreover

131

the link between ^{18}F-galacto-RGD uptake and inflammation has been recently demonstrated in mouse models of atherosclerosis (Laitinen, 2009). In another study, feasibility of RGD-based imaging was showed in predicting scar formation in patients with myocardial infarction (Verjans, 2010).

In this study, for the first time we investigated whether it is feasible to detect $\alpha_v\beta_3$ integrin in human carotid endarterectomy (CEA) specimens using an ex vivo imaging method recently developed by our group (Masteling, 2011). This method allows using high resolution microPET system to illustrate heterogeneous tracer uptake within atherosclerotic plaque and correlating tracer uptake with pathologic finding of plaques in different regions. For this study we used a recently developed ^{18}F-labeled RGD compound which is produced using click chemistry method.

Methods and Methods

Study design and specimens

This study was designed according to previous work of our group on incubation of CEA specimens immediately after excision in a solution containing tracer followed by ex vivo high-resolution micro PET scan to visualize tracer uptake with great detail (Masteling, 2011). The study was approved by the institutional ethics review board of the University Medical Center Groningen, Groningen, the Netherlands. CEA specimens were included from 20 patients who underwent CEA because of significant symptomatic carotid artery stenosis in between January 2011 and June 2012. The samples contained the carotid bifurcation, the distal segment of common carotid artery, and proximal segments of both the internal and external carotid artery. In order to determine receptor-specific tracer uptake, in three CEA specimens co-incubation of samples with cold compounds (blocking) was performed and specimens were scanned.

Materials

Reagents and solvents were obtained from commercial suppliers (Aldrich, Fluka, Sigma, and Merck) and used without further purification. RGD-K5 azide and ^{19}F-RGD-K5 were

prepared by Siemens Molecular Imaging Biomarker Research (Culver City USA). For radiolabeled compounds, radioactivity detection on TLC was performed with Cyclone phosphor storage screens (multisensitive, Perkin Elmer). These screens were exposed to the TLC strips and subsequently read out using a Cyclone phosphor storage imager (PerkinElmer) and analyzed with OptiQuant software. HPLC analysis was performed with an Elite LaChrom VWR Hitachi L-2130 pump system (Darmstadt, Germany) connected to a UV-spectrometer (Elite LaChrom VWR Hitachi L-2400 UV detector) and a Bicron frisk-tech radiation detector. For the analysis of radiolabeled compounds, the HPLC eluate after passage through the UV detector was led over a 3 inch NaI(Tl) scintillation detector (Wallac, Turku, Finland) connected to a multi channel analyzer (Gabi box, Raytest, Straubenhardt Germany). The output signal was recorded and analyzed using a GINA Star data acquisition system (Raytest, Straubenhardt, Germany).

Synthesis of [^{18}F]RGD K5

Production of [^{18}F]fluoride Aqueous [^{18}F]fluoride was produced via the ^{18}O(p,n)^{18}F nuclear reaction by irradiation of 97 % enriched [^{18}O]water (2-4 mL; Rotem HYOX18, Rotem Industries, Beer Sheva, Israel). The [^{18}F]fluoride solution was passed through a Sep-Pak Light Accell Plus QMA anion exchange cartridge (Waters) to trap the [^{18}F]fluoride and recover the [^{18}O]-enriched water. The [^{18}F]fluoride was eluted from the cartridge with 1 mL of K_2CO_3 solution (4.5 mg/mL) into a conical glass reaction vial containing 20 mg Kryptofix 2.2.2. To this solution, 1 mL acetonitrile was added and the solvents were evaporated at 130°C. The [^{18}F]KF/Kryptofix complex was dried 3 times by the addition of 0.5 mL acetonitrile, followed by evaporation of the solvent.

Production of 5-[^{18}F]fluoro-1-pentyne and [^{18}F]RGD-K5 A solution of pent-4-ynyl-4-methylbenzenesulfonate (20-25 mg, 84-105 µmol) in 0.8-1 mL anhydrous 1,2-dichlorobenzene was added to the Kryptofix 2.2.2 K[^{18}F]F residue and the mixture was heated for 10 min at 110 °C to provide [^{18}F]fluoropentyne which was simultaneously distilled with a gentle flow of helium to a second reactor containing the click reaction mixture. The click reaction mixture contained 0.1 mg RGD-K5 azide precursor (2-((2S,5R,8S,11S)-8-(4-((3S,4S,5R,6R)-6-((2-azidoacetamido)methyl)-3,4,5-trihydroxytetrahydro-2H-pyran-2 carboxamido)butyl)-5-benzyl-11-(3-guanidinopropyl)-3,6,9,12,15-pentaoxo-1,4,7,10,13-

pentaazacyclopentadecan-2-yl)acetic acid; TFA salt) in the presence of 0.2 mg phosphoramidite Monophos, 1 mol% (0.05 mg) $CuSO_4.5H_2O$ (reduced to Cu(I) with 5 mol% (0.25 mg) sodium ascorbate), in either 0.25 mL EtOH and 0.25mL CH_3CN. The subsequent conversion to radiolabeled [^{18}F]RGD-K5 was followed by radio-TLC (Rf [^{18}F]RGD-K5 = 0.4 (eluent: $MeOH/H_2O$ 2:1)).

After reacting at room temperature for 10 min, the crude [^{18}F]RGD-K5 was diluted with 1.5 mL of 0.025 M Na_2HPO_4 pH 7 and purified by semi-preparative RP-HPLC using an XBridge C18 column (5 µm, 4.6 mm x 150 mm column, Waters) eluted with 0.025M Na_2HPO_4 pH 7.0 and by semi-preparative RP-HPLC using an XBridge C18 column (5 µm, 10 mm x 150 mm column ,Waters) eluted with 0.025M Na_2HPO_4 pH 7.0 and EtOH 86/14 at a flow rate of 4 mL/min. UV detection of the HPLC eluate was performed at 254 nm. [^{18}F]RGD-K5 was collected after 20-25 min (Figure 7.1). Purified [^{18}F]RGD-K5 was collected in a 1.3-2.6 mL volume (mobile phase). This HPLC-purified fraction was diluted with preparative HPLC mobile phase and passed through an apyrogenic 0.22 µm membrane filter (Millex®-GV, Millipore, Ireland). A final solution of 370 MBq/mL was obtained by further dilution with saline which was passed through the same membrane filter.

Quality control procedures

Quality control procedures for [^{18}F]RGD-K5 are based upon the current requirements for radiopharmaceuticals laid out in the European Pharmacopoeia [Ph.Eur. 6.0-Radiopharmaceutical Preparations].

QC system was performed on a Phenomenex Prodigy C_{18} column XBridge C18 column (5 µm, 4.6 mm x 150 mm column ,Waters with CH_3CN and water (40:60 v/v) in the presence of 0.1 % TFA as eluent at a flow rate of 3mL/min. The radiochemical identity of [^{18}F]RGD-K5 was confirmed using authentic RGD-K5 as an external reference material. After injection and analysis of a solution of the reference material RGD-K5, a blank injection of preparative HPLC mobile phase is performed. The retention time of [^{18}F]RGD-K5 should be the same (± 10 %) as the retention time observed for the RGD-K5 reference standard. The radiochemical purity and specific activity was analyzed using the same HPLC system. The total of radiolabeled side products were ≤ 5%. Residual solvent analysis is performed

using GC (direct injection). Quality control analyses were developed in collaboration with Leuven University, more detail is mentioned in chapter 6.

Micro PET procedure

For the preparation of incubation buffer, $[^{18}F]$-RGD-K5 (5.1 MBq ± 0.2, xx μg) was diluted in 15 ml phosphate-buffered saline (PBS). Immediately after surgery, the specimens were transported to the lab and incubated in the incubation buffer at room temperature. After one hour the plaques were flushed 3-5 times with PBS and fixed in a humid box to prevent dehydration, positioned and fixed on microPET bed. All specimens were scanned using a microPET focus 220 camera (Siemens Preclinical Solutions, Knoxville, TN, USA, Inc.) for 60 minutes. Thereafter, a microCT scan was performed using a microCAT II system (Siemens Preclinical Solutions, Knoxville, TN, USA) as the stereotactic position was maintained. MicroPET images were corrected for scatter and reconstructed applying an interactive reconstruction algorithm (OSEM 2D).

Ch. 7

Immunohistochemistry

Specimens were were serially cross-sectioned in 4 mm slices and numbered from proximal to distal. Formalin-fixed paraffin-embedded 5 μm-cut slides were made and were stained for $a_v\beta_3$ integrin and CD31 to show endothelial cells as a marker for new vessels. The level of staining was scored from 0-3, by assessment of the percentage of stained cells and the staining intensity.

Data Analysis and Statistics

Tracer uptake in microPET images was corrected for radioactive decay. MicroPET and microCT images were registered using AMIDE software (version 0.9.1, Stanford University) and a whole specimen 3-dimensional region of interest (ROI) was drawn manually in microCT images and was applied to microPET images. The mean percent incubation dose per gram tissue$_{total}$ (%Inc/g$_{total}$) in total specimen was calculated. Segmental ROIs were

drawn manually in accordance to the cut segments for immunohistochemical analysis to compare tracer accumulation with immunohistochemistry. In each segment a %Inc/g$_{segmental}$ was measured and ratio of %Inc/g$_{segmental}$ to %Inc/g$_{total}$ (segmental-to-total) was calculated for each segment.

Quantitative results were shown as mean ± SD. Segmental-to-total ratio of ^{18}F-RGDk5 uptake in each segment was compared with $\alpha_v\beta_3$ integrin and CD31 staining and correlation between variables were tested by use of Spearman correlation coefficients (ρ), we set the significance level (P) at 0.05.

Results

Feasibility and Specific Uptake

A total of 16 specimens were scanned (average weight 1.1 g). The mean length of the specimens was 2.1 ± 0.6 cm. The CEA specimens were transported from the operation room to the lab within 15 minutes after surgical excision. In all CEA specimens clear in specimens was seen (Figure 7.1). [^{18}F]-RGD uptake was heterogeneous in CEA specimens and was localized within the vessel wall (Figure 7.1A). A 3-dimensional 70% maximum uptake value isocontour region of interest was drawn to determine the hotspot inside the specimen. Mean %Inc/g in hotspot was 1.30% ± 0.34 (ranging from 0.65% to 1.93, and the mean %Inc/g in total specimen was 0.45% ± 0.19 (ranging from 0.14% to 0.77%). Average hotspot-to-total uptake ratio was 3.19 ± 0.91.

A blocking experiments were performed by incubation of CEA plaques in 550 times excess unlabeled compound (Cold RGD-K5) followed by incubation in ^{18}F-RGD. Using the same protocol, one hour after incubation an emission scan was performed and mean %Inc/g was calculated to show the effects of blocking on the tracer uptake. The results showed a significant decrease (6 times less accumulation) of the tracer in CEA specimens (0.45%Inc/g vs. 0.08%Inc/g).

Immunohistochemistry

In 13 slices $\alpha_v\beta_3$ integrin staining was performed. A very heterogeneous integrin expression was observed in samples. Immunohistochemical $\alpha_v\beta_3$ integrin staining was scored according to a semi-quantitative three-score scaling method based on staining intensity and amount of stained area. Comparing staining 5 scores and segmental-to-total ratio showed a moderate but significant correlation as indicated by the Spearman's correlation coefficient ($r = 0.58$, $p = 0.038$).

In 18 slices of the CEA specimens CD31 staining was performed (Figure 7.2). The level of CD31 staining was scored from 0-3, by assessment of the percentage of stained cells and the staining intensity. Semi-quantitative measures of segmental-to-total ratio and CD31 staining score is shown in table 7.1. The correlation between CD31 staining score and Segmental-to-total ratio was significant ($\rho = 0.67$, $P < 0.002$).

Discussion

Angiogenesis occurs in atherosclerotic plaques due to increase in size and hypoxia leads to formation of immature blood vessels which in turn exacerbate inflammation and intraplaque hemorrhage (Ribatti, 2008). These result in plaque instability and vulnerability to rupture. As such, clinical detection of angiogenesis in vessel walls can be used for the assessment of plaque vulnerability. Integrins play important role in the course of angiogenesis and among integrin proteins $\alpha_v\beta_3$ integrin, a cell surface receptor, plays a crucial role by mediating adhesion of cells to extracellular matrix and migration of endothelial cells (Morrison, 2010). Because of its critical role, $\alpha_v\beta_3$ integrin imaging has been focus of many studies. The RGD peptide sequence has shown high binding affinity for $\alpha_v\beta_3$ integrin and has been labeled with ^{18}F for molecular imaging of integrin in vivo.

In order to perform ex vivo study on CEA specimens with ^{18}F-RGD-K5, we performed quality control on ^{18}F-RGD to check whether the tracer is stable in vitro/ex vivo. For quality control, we resembled incubation condition with diluting ^{18}F-RGD-K5 in 15 ml PBS and tested stability of the tracer at one hour and two hours. For all productions, QC HPLC analysis

showed that the amount of RGD-K5 azide precursor (Rt= 6 min) in the final solution was lower than the detection limit (LOD 0.2 ng), confirming the efficient separation between the azide precursor and [^{18}F]RGD-K5 with the applied preparative HPLC system. In the next step we performed ex vivo imaging study on human CEA specimens. This research was designed according to a method developed by the department of Nuclear Medicine of UMCG for ex vivo depiction of carotid atherosclerotic plaques using a microPET camera system with a high spatial resolution (Masteling, 2011). The resolution of approximately 1 mm offers a unique opportunity to visualize atherosclerotic plaque in great detail to provide information on underlying processes within atherosclerotic plaque.

In a previous study, by our group, it was shown that ex vivo imaging of CEA specimens after incubation in a solution containing ^{18}FDG is feasible. The results of imaging significantly correlated with CD68 positive cells as surrogate markers of macrophages.

In this study we showed that [^{18}F]-RGD-K5 microPET imaging of CEA specimens is feasible. The uptake was heterogeneous along CEA specimens and differed plaque by plaque. The difference of uptake in different plaques raises the possibility that a proportion of surgically excised atherosclerotic plaques would have imposed lower risk of rupture according to [^{18}F]-RGD K5imaging. Future studies should be designed to investigate implications of high [^{18}F]-RGD K5uptake on the outcome of atherosclerotic plaques. Additionally, the correlation between [^{18}F]-RGD-K5 uptake with integrin levels and inflammation remain to be determined.

A satisfactory hotspot-to-average ratio was observed in [^{18}F]-RGD-K5 microPET images of CEA specimens. This makes [^{18}F]-RGD-K5 a promising tracer for visualization of $\alpha_v\beta_3$ integrin expression arterial tissue and enables us to recognize the target with a high target-to-background ratio. However, further studies need to be designed to determine optimal the time point for blood clearance and the possibility for detection of lesions in vivo.

A significant correlation was observed between [^{18}F]-RGD K5 in each segment and immunohistochemical analysis of $\alpha_v\beta_3$ integrin, confirming that [^{18}F]-RGD-K5 enables us to visualize integrin presence and quantify integrin levels in human atherosclerotic plaques. Addition of excess unlabeled compound resulted in six times less [^{18}F]-RGD-K5 accumulation in samples and indicated $\alpha_v\beta_3$ integrin-mediated tracer uptake. Good correlation of Segmental-to-total ratio with CD31 staining score ($\rho = 0.67$, $P = 0.002$) was demonstrated in our study.

CD31 immunostaining was used as an endothelium-specific immunohistochemical marker as indicator of new vessel formation. The correlation between segmental uptake in the lesion and intensity of CD31 staining confirms that ^{18}F-RGD-K5 imaging enables us to not only visualize underlying pathology of atherosclerotic disease but also quantitatively assessing angiogenesis formation.

In a previous study on [^{18}F]-RGD-K5 imaging of xenograft tumor models showed a rapid blood clearance of the tracer which demonstrated a two hours post-injection specific uptake value = 0.05 – 0.15 percent injected dose per gram (Haubner, 2001). In a patient study on nine individuals with malignant melanoma the same pattern of rapid decline in blood activity was demonstrated within 79 minutes after injection (Haubner, 2005). However, the specific uptake value of the tracer in blood in human study was higher than that of mouse model (1.17% injected dose per gram). In our study average %Inc/g of [^{18}F]-RGD-K5 in hotspot (after one hour incubation) was 1.30% ± 0.34 (ranging from 0.65% to 1.93). This result shows the potential for in vivo detection of $\alpha_v\beta_3$ integrin. However, the in vivo results of atherosclerotic plaque uptake and target-to-blood ratio in animal models and human subjects need to be experimentally determined.

Molecular imaging of vulnerable plaques requires not only a highly-avid, target-specific probe and a high spatial resolution imaging modality, but also a deep understanding on predictive value of various underlying pathobiological processes in the course of disease. Currently, many different molecular imaging probes are being tested to reveal macrophage content (Masteling, 2011- Chen, 2009), VEGF abundance (Golestani, In press), and (Razavian, 2011) levels of matrix metalloproteinases in experimental models of atherosclerosis. This study was the first to examine the feasibility of $\alpha_v\beta_3$ integrin ex vivo imaging in human atherosclerotic. A better understanding on the predictive role of underlying processes within atherosclerotic plaque is required to judge whether or not the each imaging probe is suitable for clinical application.

ch 7

Conclusion

This study demonstrated the potential of integrin imaging in determination of angiogenesis and vulnerability in atherosclerotic plaques. Noninvasive imaging and quantification of angiogenesis could provide clinicians with a new tool in stratifying risk for cardiovascular events. The QC system has been validated and allows the tracer to be used in clinical studies for visualization of neoangiogenesis in oncological patients in our hospitals.
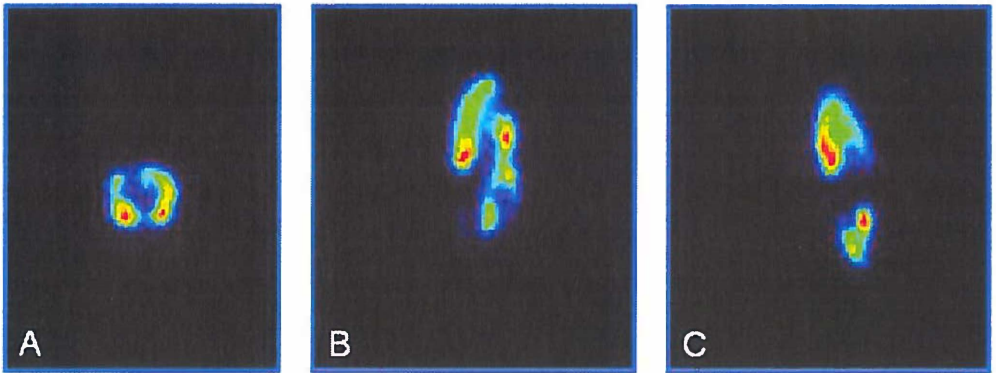

Figure7.1. Transversal (A), coronal (B), and saggital (C) sections of microPET image of a carotid endarterectomy specimen after 1 hour incubation in [^{18}F]-RGD-K5 shows heterogeneous uptake along specimen. Transversal image shows that area of higher uptake (red) is confined within vessel wall
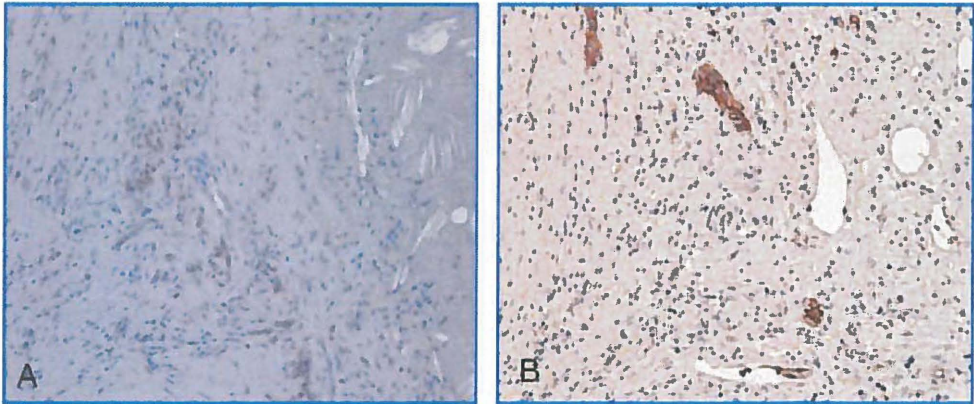
Figure7.2. Immunostaining for detection of $a_v\beta_3$ integrin (A) and CD31(B) in human carotid endarterectomy specimens showed endothelial cells (brown)

Sample	CD31 Score	Integrin Score	Segmental-to-total ratio
1	2	2	1.15
2	2	3	1.14
3	1	0	0.90
4	2	1	1.68
5	1	-	1.20
6	1	0	1.058
7	2	-	0.78
8	1	-	1.06
9	1	1	1.46
10	2	-	1.54
11	2	2	1.48
12	3	2	2.62
13	0	1	0.57
14	0	0	0.83
15	1	1	1.25
16	2	1	1.12
17	0	1	0.91
18	0	-	0.74

Table 7.1. Semi-quantified segment-to-total accumulation of ^{18}F-RGD-K5 PET results on and immunohistochemistry scores of the corresponding section in human carotid endarterectomy specimens

References

- Beer A J, Haubner R, Sarbia M, Goebel M, Luderschmidt S, Grosu A L, Schnell O, Niemeyer M, Kessler H, Wester H J, Weber W A, Schwaiger M, Clin. Cancer Res. 2006., 12, 3942-3949.
- Cai W, Chen K, Mohamedali K A, Cao Q, Gambhir S S, Rosenblum M G, J. Nucl. Med., 2006, 47, 2048-2056.
- Chen W, Bural G G, Torigian D A, Rader D J, Alavi A, Eur. J. Nucl. Med. Mol. Imaging., 2009, 36, 1619-7070.
- Cho H J, Lee J D, Park J Y, Yun M, Kang W J, Walsh J C, Kolb H, Zhang J J, J. Nucl. Med. 2009, 50 (Suppl 2), 1910.
- Doss M, Alpaugh R K, Yu Y Q, J. Nucl. Med., 2009, 50 (Suppl 2), 447.
- Golestani R, Zeebregts C, Terwisscha van Scheltinga A, Lub-de Hooge M, van Dam G, Glaudemans A, Molecular imaging, In Press.
- Haubner R, Wester H J, Weber W A, Mang C, Ziegler S I, Goodman S L, Cancer Res., 2001, 61, 1781-1785.
- Haubner R, Kuhnast B, Mang C, Weber W A, Kessler H, Wester H J, Schwaiger M, Bioconjugate Chem. 2004, 15, 61-69.
- Haubner R, Weber W A, Beer A J, Vabuliene E, Reim D, Sarbia M, PLoS. Med., 2005, 03, 1549-1676.
- Kenny L M, Coombes R C, Oulie I, Contractor K B, Miller M, Spinks T J, McParland B, Cohen P S, Hui A M, Palmieri C, Osman S, Glaser M, Turton D, Al-Nahhas A, Aboagye E O, J. Nucl. Med., 2008. 49, 879-886.
- Laitinen I, Saraste A, Weidl E, Poethko T, Weber A W, Nekolla S G, Circ. Cardiovasc. Imaging., 2009, 07, 331-338.
- Liu S., Mol. Pharm., 2006, 09,1543-8384.
- Masteling M G, Zeebregts C J, Tio R A, Breek J C, Tietge U J, de Boer J F, J. Nucl Cardiol., 2011, 18, 1066-1075.
- McParland B J, Miller M P, Spinks T J, Kenny L M, Osman S, Khela M K, Aboagye E, Coombes R C, Hui A M, Cohen P S, J. Nucl. Med., 2008. 49, 1664-1667.
- Morrison A R, Sinusas A J, J. Nucl. Cardiol. 2010, 17, 116-134.

- Nagengast W B, de Vries E G, Hospers G A, Mulder N H, de Jong J R, Hollema H, J Nucl. Med., 2007, 48, 1313-1319.
- Naghavi M, Libby P, Falk E, Casscells S W, Litovsky S, Rumberger J, Circulation., 2003, 108, 1664-1672.
- Razavian M, Marfatia R, Mongue-Din H, Tavakoli S, Sinusas A J, Zhang J, Arterioscler Thromb. Vasc. Biol., 2011, 22.
- Razavian M, Tavakoli S, Zhang J, Nie L, Dobrucki L W, Sinusas A J, J. Nucl. Med., 2011, 52, 1795-1802.
- Ribtti D, Levi-Schaffer F, Kovanen P T, Ann. Med., 2008, 40, 606-621.

- Okarvi S M, Eur. J. Nucl. Med., 2001, 28, 929-938.
- Schnell O, Krebs B, Carlsen J, Miederer I, Goetz C, Goldbrunner RH, Neuro. Oncol., 2009, 12, 861-870.
- Verjans J, Wolters S, Laufer W, Schellings M, Lax M, Lovhaug D, J. Nucl. Cardiol. 2010, 17, 1065-1072.
- Virmani R, Kolodgie F D, Burke A P, Finn A V, Gold H K, Tulenko T N, Arterioscler Thromb Vasc. Biol., 2005, 25, 2054-2061.

Chapter 8

Strain-Promoted 'Click' Chemistry for [18F]-Radiolabelling of Bombesin for Tumor Imaging

L. Mirfeizi[†, a], L. S. Campbell-Verduyn[†,b], A. K. Schoonen[b], R. A. Dierckx[a], P. H. Elsinga[a] and B. L. Feringa[b]

[a]University Medical Center Groningen, University of Groningen, Dept. of Nuclear Medicine and Molecular Imaging, Groningen,The Netherlands, [b]University of Groningen, Stratingh Institute for Chemistry, Groningen, The Netherlands

[†] The authors contributed equally to this work.

Abstract

Introduction

A new route to a strained aza-dibenzocyclooctyne has been developed. The strained cycloalkyne proved to react with [^{18}F]-containing azides to give the corresponding triazoles in minutes. [Lys3]-bombesin was modified with the cycloalkyne and subsequently labeled with three [^{18}F]-containing azides, via strain-promoted 'click' chemistry. The three resulting tracers proved to retain their high affinity for gastrin-releasing peptide receptors in vitro.

Copper-free 'click' chemistry could lend some advantages to the field of radiolabeling. Potential contamination of labeled compounds with traces of copper is a concern when the classic CuAAC is used to label biomolecules. Furthermore, methodology for labeling by CuAAC is not amenable to extension to in vivo pretargeting methodology. To date, there has been one reported instance of radiochemical labeling of a peptide with [^{111}In] for SPECT by a strained cyclooctyne. (Martin, 2010) Given the fast reaction parameters of the strain-promoted azide-alkyne cycloaddition, it could be a useful means by which to label peptides with the short lived [^{18}F].

Goal

We envisioned the use of [lys3]-bombesin, modified with a strained alkyne, to allow for rapid and facile labeling with [^{18}F] in the absence of possible copper contamination. A further advantage of this methodology would be the possibility to fine tune the properties of the resulting labeled peptide. The azide group can be designed to provide more or less hydrophilicity, bulk or charge to the peptide in question. The stability and in vitro binding affinity of the resulting tracers were to be investigated.

Results and Discussion

Our starting point was to find a suitable strained alkyne with the optimal balance of reactivity and stability. Although, as aforementioned, many options are available, some initial synthetic endeavors demonstrated that the synthesis of cyclooctynes is not necessarily trivial, nor are all of the reported cyclooctynes of appropriate stability. Van Hest and van Delft reported an aza-dibenzocyclooctyne, which proved to be simultaneously reactive and stable. (Debets, 2009) For our purposes, which involve rapid 'clicking' of a short lived

radioisotope as well as eventual in vitro and in vivo studies requiring a certain degree of stability, it appeared an ideal choice.

Introduction

Bombesin is a 14 amino acid (Pyr-Gln-Arg-Leu-Gly-Asn-Gln-Trp-Ala-Val-Gly-His-Leu-Met-NH_2) neuropeptide which binds with high affinity to the gastrin-releasing peptide receptor (GRPR). It has received much attention in the field of nuclear imaging as the GRPR is massively overexpressed on a variety of tumor cells, including breast and prostate tumor cells, lending it high potential as a radioligand for the diagnosis and imaging of cancer. (n Ananias, 2008) Much effort has been invested in the development of labeled analogues of bombesin. (Schroeder, 2010)   Bombesin is often modified in the form of [lys3]-bombesin (Figure 8.1) which allows for site selective introduction of the radionuclide at the terminal amino group of lysine. Amino acids 7-14 are known to be essential for receptor binding, thus modification in the third amino acid reduces potential for interference. (Schroeder, 2010) A variety of bombesin analogues for nuclear imaging have been synthesized, predominantly labeled with large metal-based radionuclides (^{64}Cu, ^{111}In, ^{68}Ga) through the commonly introduced chelating groups 1,4,7,10-tetraazacyclododecane-1,4,7,10-tetraacetic acid (DOTA) and 1,4,7-triazacyclononane-1,4,7-triacetic acid (NOTA). (Hoffman, 2009)
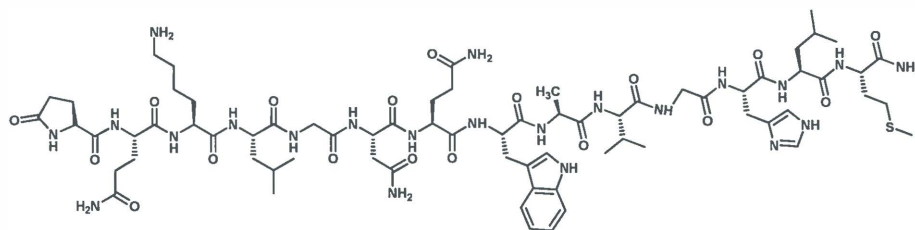
Figure 8.1. [Lys3]-Bombesin

Positron emission tomography is a nuclear imaging technique used extensively in diagnostic medicine and drug development. In the last decade, [^{18}F] ($t_{1/2}$~110 min) has been popularized as a non-metallic positron emission tomography (PET) radioisotope. With a longer half-life than other non-metallic radioisotopes for PET such as [^{11}C] ($t_{1/2}$~20 min) and

[13N] (t$_{1/2}$~10 min), it has the distinct advantage of allowing for off-site production and transportation of the radionuclide as well as allowing for scans to be performed over several hours. Furthermore, due to its low positron energy, it yields images with higher resolution than other radionuclides. (Schirrmacher, 2007) Very few instances of [18F] labeled bombesin can be found in the literature, due predominantly to the synthetic challenges associated with the introduction of [18F] when compared with simple chelation techniques used for metallic radionuclides. (Zhang, 2006) Notably, the synthetic time frame is also much reduced as compared to metallic radionuclides such as [64Cu] (t$_{1/2}$~12 h). A major disadvantage is the need for the multi-step synthetic procedures required to synthesize current prosthetic groups such as [18F]succinimidyl 4-fluorobenzoate ([18F]SFB) or [18F]4-fluorobenzaldehyde which are commonly used to introduce [18F] in the presence of a free amine. (Chang, 2005) Ideally, a prosthetic group should be easily synthesized, introduce the radionuclide in the last step of the synthesis, and should require only the mildest of conditions to attach it to the biomolecule of interest. Given these requirements, it was only natural that 'click' chemistry was utilized for the development of new prosthetic groups.

The azide-alkyne cycloaddition has been popularized under the banner of 'click' chemistry since the discovery that it proceeds regioselectively at room temperature in the presence of catalytic Cu(I). (Tornoe, 2002) The bioorthogonality of the azide and the alkyne has proven unparalleled. The robustness and versatility of this reaction along with its mild conditions makes it an attractive reaction for labeling target molecules with radionuclide containing prosthetic groups. Many groups have exploited the bioorthogonality of this reaction to allow for fast and straightforward labeling of sugar and peptide targets with [18F] and other radionuclides. (Hausner, 2008) The obvious limitation of this methodology for biological systems is the cytotoxicity of copper. Potential contamination of labeled compounds with traces of copper is a major drawback and it is not suitable for development of in vivo pre-targeting methodologies. In recent years, great strides have been made in developing copper-free chemistry through, amongst others, the use of strained cyclooctynes (Sletten, 2010) and in one instance has been used for the introduction of [111In] to a target peptide for SPECT imaging. (Martin, 2010) We envisioned the use of lys-[3]bombesin, modified with a strained alkyne, to allow for rapid and facile labeling with

Ch. 8

[^{18}F] in the absence of possible copper contamination. A further advantage of this methodology would be the possibility to fine tune the properties of the resulting labeled peptide. The azide group can be designed to provide more or less hydrophilicity, bulk or charge to the peptide in question. Furthermore, though we focus in this work on the use of bombesin, we would hope that the technique would be amenable to the use of other biomolecules as well. We present here the first instance of [^{18}F]-radiolabelling using copper-free 'click' chemistry, and its application to the synthesis of a [^{18}F]-labeled analogue of bombesin, a potent ligand for tumor imaging. We further demonstrate that the 'click' radiolabelling does not compromise the GRP receptor in vitro binding affinity in human prostate cancer cells.

Material and method

General

All reactions were carried out in oven dried glassware unless otherwise specified. Lys[3]-bombesin was purchased from Sigma-Aldrich and used as received as were all other chemicals unless specified otherwise. ^{1}H- and ^{13}C-NMR spectra were recorded on a Varian AMX400 (400 and 100.59 MHz) using CDCl$_3$ as solvent unless otherwise indicated. Chemical shift values are reported in ppm with the solvent resonance as the internal standard (CHCl$_3$: δ 7.26 for ^{1}H and δ 77.0 for ^{13}C). Data are reported as follows: chemical shifts, multiplicity (s=singlet, d=doublet, t=triplet, q=quartet, dd=doublet of doublets, dt=doublet of triplets, td=triplet of doublets, m=multiplet, br=broad), coupling constants (Hz), and integration. Flash chromatography was performed on silica gel. All thin layer chromatography was performed on Merck F-254 silica gel plates. Visualization of the TLC plates was performed with KMnO$_4$ staining reagent and UV light (254 nm). Mass spectra were recorded on an AEI-MS-902 mass spectrometer by EI (70 eV) measurements. Melting points are uncorrected. ^{1}H and ^{13}C NMR data are provided for all synthesized compounds. Spectra were in accordance with published experimental data and references are provided for known compounds. HRMS

mass data is provided for all new compounds. Reversed phase-HPLC analyses were performed on a Shimadzu LC-20AD VP, Waters Xterra MS C18 column (3.0 x 150 mm, partciel size 3.5 μm) using a gradient of MeCN/H_2O (0.1 % formic acid) at a flow of 0.5 mL/min.

Safety

Working with azides should always be done carefully. Organic azides, particularly those of low molecular weight, or with high nitrogen content, are potentially explosive. Heat, light and pressure can cause decomposition of the azides. Furthermore, the azide ion is toxic, and sodium azide should always be handled while protected with gloves. Heavy metal azides are particularly unstable, and may explode if heated or shaken.

Characterization of substrates and reference compounds

5H-dibenzo[7]annulen-5-one oxime (2)

A solution of hydroxylamine was prepared by dissolving 15.6 g (0.22 mol, 3.1 eq) of $NH_2OH \cdot HCl$ in a hot mixture of absolute alcohol (100.0 mL) and pyridine (75.0 mL). To this solution was added 15.0 g (0.073 mmol, 1.0 eq) of dibenzosuberenone and 20.0 mL of pyridine. The reaction mixture was heated at reflux for three hours, and the disappearance of starting material was monitored by thin layer chromatography. After completion of the reaction, the solvent was evaporated under reduced pressure, and the product was precipitated with water. The solid was filtered, washed with water (3 x 50 mL), dissolved in chloroform, and the organic layer was washed one further time with water. The organic layer was dried over $MgSO_4$ and the solvent evaporated to yield a pale yellow solid (15.3 g). Yield=95 %. mp 187 °C. ^{1}H NMR (400 MHz, $CDCl_3$): δ 10.10 (s, 1H), 7.67 (m, 1H), 7.57 (m, 1H), 7.28-7.37 (m, 6H), 6.86 (dd, J=28.0, 4.0 Hz, 2H); ^{13}C NMR (100.59 MHz, $CDCl_3$): 156.3, 135.4, 134.5, 133.8, 130.8, 130.6, 130.5, 129.4, 129.2, 129.1, 128.9 (2C), 128.8, 127.8, 127.6. HRMS (ESI+) (m/z) calculated for $C_{15}H_{12}NO$ [M + H]$^+$ 222.0913, measured 222.0903.

151

Dibenzo[b,f]azocin-6(5H)-one (3)

Trichlorotriazine (834.0 mg, 4.52 mmol) was added to 1.0 mL DMF in a sample vial. The solution was stirred, and white precipitate formed. The formation of the catalyst was monitored by thin layer chromatography until all of the TCT had been consumed. To this solution was added oxime **2** along with 10.0 mL DMF. The reaction mixture was stirred at room temperature for 24-72 h (depending on the amount of oxime in a given reaction). DMF was added if needed in cases where no solvent remained (depending on the scale of the reaction). The reaction was quenched with water and DCM was added to the solution. The organic phase was washed with saturated aqueous Na_2CO_3 (2 x 10 mL), 1 N aqueous HCl (2 x 10 mL) and brine (2 x 10 mL). The organic layer was dried over $MgSO_4$ and the solvent was removed under reduced pressure. The crude reaction mixture was purified by column chromatography (3:1 pentane:ethyl acetate, R_f: 0.65) to give a pale yellow solid (650.0 mg). Yield=65 %. mp 141-142 °C. ^1H NMR (400 MHz, $CDCl_3$): δ 8.76 (s, 1 H), 7.70-7.72 (m, 1H), 7.57-7.60 (m, 1H), 7.42-7.51 (m, 6H), 6.96 (s, 2H); ^{13}C NMR (100.59 MHz, $CDCl_3$):163.5, 134.3, 133.0, 130.4, 130.2, 129.7, 129.5, 129.2, 129.0, 128.7, 128.5, 128.0, 127.7. HRMS (ESI+) (m/z) calculated for $C_{15}H_{12}NO$ $[M + H]^+$ 222.0913, measured 222.0901.

5,6-dihydrodibenzo[b,f]azocine (4)

Amide 3 (2.00 g, 9.0 mmol) was dissolved in 25.0 mL dry CH_2Cl_2 and 45.0 mL of a 1.0 M solution of Dibal-H in CH_2Cl_2 was added dropwise to the solution at room temperature with stirring. The reaction mixture was stirred under N_2 at room temperature and the conversion followed by thin layer chromatography until all of the starting material was consumed. The reaction was then carefully quenched with an aqueous solution of ammonium chloride. An aqueous solution of Rochelle salts was subsequently added and the mixture was stirred vigorously for 45 min. A further 50 mL of DCM was added and the organic layer collected and washed with brine. After drying over $MgSO_4$ the solvent was removed under reduced pressure to yield a yellow oil which was purified by column chromatography (2:1 pentane:ethyl acetate, R_f: 0.8). The resulting compound was a yellow solid (1.40 g). Yield=75 %. ^1H NMR (400 MHz, $CDCl_3$): δ 7.24-7.62 (m, 1 H), 7.16-7.24 (m, 3H), 6.97 (d, J=8.0 Hz, 1H), 6.88 (t, J=8.0 Hz, 1H), 6.60 (t, J=7.2 Hz, 1H), 6.54 (d, J=12.8

Hz, 1H), 6.47 (d, J=8.4 Hz, 1H), 6.36 (d, J=13.2 Hz, 1H), 4.59 (s, 2H), 4.29 (br s, 2H); ^{13}C NMR (100.59 MHz, CDCl$_3$): 147.1, 138.1, 136.2, 134.7, 132.7, 130.1, 128.8, 127.9, 127.6, 127.4, 127.3, 121.7, 117.9, 117.7, 49.6.

Methyl 4-(dibenzo[b,f]azocin-5(6H)-yl)-4-oxobutanoate (5)

Amide 4 (2.00 g, 9.65 mmol) was dissolved in 25.0 mL dry DCM under a N$_2$ atmosphere. To the stirred solution was added triethylamine (2.67 mL, 19.3 mmol) and the mixture cooled to 0 °C whereupon methyl succinyl chloride (1.78 mL, 14.4 mmol) was added dropwise. The reaction was allowed to warm to room temperature, and stirred overnight. The reaction mixture was quenched with water and the mixture diluted with a further 20.0 mL of DCM. The organic layer was washed with 2 M aqueous NaOH (2 x 15 mL), 2 M aqueous HCl (2 x 15 mL), water (2 x 15 mL) and brine (1 x 10 mL). The organic layer was dried over MgSO$_4$ and the solvent was removed under reduced pressure. The resulting crude product was purified by column chromatography (4:1 pentane:ethyl acetate, R$_f$: 0.4) to yield a yellow-white solid (2.70 g). Yield=87%. mp 108 °C. ^{1}H NMR (400 MHz, CDCl$_3$): δ 7.24-7.26 (m, 5H), 7.12-7.16 (m, 3H), 6.79 (d, J=17.2 Hz, 1H), 6.61 (d, J=17.2 Hz, 1H), 5.51 (d, J=20.0 Hz, 1H), 4.25 (d, J=20.8, 1H), 3.61 (s, 3H), 2.55-2.60 (m, 1H), 2.39-2.48 (m, 2H), 1.99-2.10 (m, 1H); ^{13}C NMR (100.59 MHz, CDCl$_3$): 177.4, 170.8, 140.5, 136.4, 135.8, 134.5, 132.6, 131.8, 130.8, 130.1, 128.5, 128.2, 128.0, 127.2, 126.9, 54.4, 51.6, 29.5, 29.0. HRMS (ESI+) (m/z) calculated for C$_{20}$H$_{19}$NO$_3$ [M + Na]$^+$ 344.1257, measured 344.1250.

Methyl4-(11,12-dibromo-11,12-dihydrodibenzo[b,f]azocin-5(6H)-yl)-4-oxobutanoate (6)

Compound 5 (1.87 g, 5.82 mmol) was dissolved in dry CH$_2$Cl$_2$ (100.0 mL) under a N$_2$ atmosphere and the reaction vessel was cooled to 0 °C.Br$_2$ (0.93 g, 5.82 mmol) dissolved in 5.0 mL of dry CH$_2$Cl$_2$ was added dropwise to the cooled solution and the reaction mixture was allowed to stir for 1 h while at 0 °C. After 1 h, the reaction was quenched with aqueous

saturated Na_2SO_3 (10 mL) and the mixture diluted with a further 50.0 mL of CH_2Cl_2. The organic layer was washed with saturated aqueous Na_2SO_3 (3 x 15 mL), water (2 x 15 mL) and brine (1 x 15 mL). The organic layer was dried over $MgSO_4$ and the solvent was removed under reduced pressure. The compound was purified by column chromatography (3:1 pentane:ethyl acetate, R_f: 0.3) to yield a dark solid (2.46 g). Yield=88%. mp 108 °C. ^1H NMR (400 MHz, $CDCl_3$): δ 7.70 (d, J=7.6 Hz, 1H), 7.00-7.25 (m, 6H), 6.86 (d, J=7.6 Hz, 1H), 5.90 (d, J=9.6 Hz, 1H), 5.80 (d, J=14.8 Hz, 1H), 5.15 (d, J=10.0 Hz, 1H), 4.17 (d, J=14.8 Hz, 1H), 3.66 (s, 3H), 2.80-2.86 (m, 1H), 2.57-2.64 (m, 2H), 2.43-2.55 (m, 1H). ^{13}C NMR (100.59 MHz, $CDCl_3$): 173.5, 172.0, 138.3, 137.0, 136.9, 132.8, 130.8, 130.7, 130.6, 129.6, 129.5, 128.9, 128.8, 128.6, 60.0, 55.5, 52.5, 51.7, 30.6, 29.2. HRMS (ESI+) (m/z) calculated for $C_{20}H_{19}Br_2NO_3$ $[M + Na]^+$ 503.9603, measured 503.9606.

Methyl 4-(11,12-didehydrodibenzo[b,f]azocin-5(6H)-yl)-4-oxobutanoate (7)

To a cold solution (-40 °C) of compound 6 (245.0 mg, 0.512 mmol) dissolved in 17.0 mL freshly distilled THF under Ar atmosphere was added dropwise 1.02 mL of a commercial solution of tBuOK (1.0 M in THF). The progress of the reaction was monitored by GC-MS. After 3 h, a further 0.4 mL of tBuOK solution was added and the mixture left to react for a further hour. The mixture was poured onto water (15 mL) and extracted with CH_2Cl_2 (3 x 30 mL). The combined organic layers were washed with brine (2 x 25 mL) and water (1 x 10 mL). A mixture of methyl ester, and tert-butyl ester products were detected in the crude ^1H NMR. The desired methyl ester product was isolated by column chromatography (3:1 pentane:ethyl acetate, R_f: 0.2) to give a clear yellow oil (109.5 mg). Yield=67 %. ^1H NMR (400 MHz, $CDCl_3$): δ 7.68 (d, J=7.2 Hz, 1H), 7.48-7.50 (m, 1H), 7.27-7.49 (m, 6H), 5.16 (d, J=14.0 Hz, 1H), 3.67 (d, J=13.6 Hz, 1H), 3.56 (s, 3H), 2.68-2.74 (m, 1H), 2.58-2.63 (m, 1H), 2.35-2.38 (m, 1H), 1.93-1.97 (m, 1H). ^{13}C NMR (100.59 MHz, $CDCl_3$): δ 173.3, 171.7, 151.4, 148.0, 132.3, 129.3, 128.8, 128.5, 128.1, 127.7, 127.1, 125.5, 123.1, 122.6, 114.9, 107.7, 55.4, 51.6, 29.6, 29.0. HRMS (ESI+) (m/z) calculated for $C_{20}H_{17}NO_3$ $[M + Na]^+$ 342.1101, measured 342.1102.

4-(11,12-Didehydrodibenzo[b,f]azocin-5(6H)-yl)-4-oxobutanoic acid (8)

Compound 7 (42.5 mg, 0.13 mmol) was dissolved in 1.7 mL dry THF. A solution of LiOH (6.4 mg, 0.26 mmol) in 0.6 mL H_2O was added dropwise to the stirred reaction mixture. The progress of the reaction was monitored by thin layer chromatography and upon full conversion, a further 6.0 mL of H_2O was added. The reaction mixture was then made basic to a pH of 14 using 2 M aqueous NaOH. The water layer was washed with CH_2Cl_2 (3 x 10 mL) and then acidified to a pH of 2 using 2 M aqueous HCl. The aqueous layer was then extracted with CH_2Cl_2 (3 x 15 mL) and the resulting organic layers of this extraction procedure were combined, dried over $MgSO_4$ and the solvent was removed under reduced pressure. Pure product was obtained as a white solid (30.6 mg). Yield= 77 %. mp 163-164 °C. ^1H NMR (400 MHz, $CDCl_3$): δ 7.67 (d, J=7.2 Hz, 1H), 7.25-7.43 (m, 7H), 5.16 (d, J=13.6 Hz, 1H), 3.67 (d, J=13.6 Hz, 1H), 2.68-2.74 (m, 1H), 2.56-2.63 (m, 1H), 2.32-2.40 (m, 1H), 1.94-2.00 (m, 1H). ^{13}C NMR (100.59 MHz, $CDCl_3$): δ 177.8, 172.6, 151.2, 147.9, 132.5, 129.3, 128.7, 128.5, 128.1, 127.6, 127.4, 125.8, 123.2, 122.9, 115.3, 107.7, 55.9, 29.7, 29.6. HRMS (ESI+) (m/z) calculated for $C_{19}H_{15}NO_3$ [M + Na]$^+$ 328.0944, measured 328.0949.

2,5-dioxopyrrolidin-1-yl 4-(didehydrodibenzo[b,f]azocin-5(6H)-yl)-4 oxobutanoate (9)

Carboxylic acid 8 (26.0 mg, 0.085 mmol) was dissolved in 5.0 mL dry CH_2Cl_2. To this solution was added 1-ethyl-3-(3-dimethylaminopropyl)carbodiimide (EDC) (0.02 mL, 0.094 mmol) and N-hydroxysuccinimide (10.8 mg, 0.094 mmol). The reaction mixture was allowed to stir overnight at room temperature after which time it was diluted with a further 10 mL of CH_2Cl_2. The reaction mixture was washed with citric acid (5 %, 2 x 5 mL) and with saturated aqueous $NaHCO_3$ (2 x 5 mL) and brine (1 x 10 mL). The compound was then purified by column chromatography (1:1 pentane:ethyl acetate, R_f: 0.5) to yield the pure compound as a yellow oil (28.0 mg). Yield=82 %. ^1H NMR (400 MHz, $CDCl_3$): δ 7.68 (d, J=7.6 Hz, 1H), 7.24-7.41 (m, 7H), 5.17 (d, J=14.0 Hz, 1H), 3.69 (d, J=14.0 Hz, 1H), 2.92-2.99 (m, 1H),

2.72-2.77 (m, 1H), 2.78 (s, 4H), 2.61-2.68 (m, 1H), 2.05-2.10 (m, 1H). ^{13}C NMR (100.59 MHz, CDCl$_3$): δ 172.6, 170.2, 168.9, 168.3, 151.0, 147.8, 132.3, 129.1, 128.6, 128.3, 127.8, 127.2, 125.5, 123.0, 122.7, 115.0, 107.5, 55.6, 29.2, 26.4, 25.5. HRMS (ESI+) (m/z) calculated for C$_{23}$H$_{18}$N$_2$O$_5$ [M + Na]$^+$ 425.1108, measured 425.1121.

1-(Azidomethyl)-4-fluorobenzene.

To a stirred solution of 1-(bromomethyl)-4-fluorobenzene (472.6 mg, 2.5 mmol) in a water/acetone mixture (1:4) was added NaN$_3$ (1.5 eq). The resulting suspension was stirred at room temperature for 24 h. DCM was added to the mixture and the organic layer was separated. The aqueous layer was extracted with DCM (3 x 10 mL) and the combined organic layers were dried over MgSO$_4$. Solvent was removed under reduced pressure to give the product as a pale yellow oil, sufficiently pure to use without further purification (374.0 mg). Yield= 99%. Spectroscopic data is in accordance with literature values. ^{1}H NMR (400 MHz, CDCl$_3$): δ 7.27-7.39 (m, 2H), 7.00-7.11 (m, 2H), 4.30 (s, 2H); ^{13}C (100.59 MHz, CDCl$_3$): δ 162.5 (d, J=130.7 Hz), 131.4, 129.9 (d, J= 45.2 Hz), 115.7 (d, J=110.0 Hz), 54.0; ^{19}F NMR (200 MHz, CDCl$_3$): δ -112.3.

Methyl 4-(1-(4-fluorobenzyl)-1H-dibenzo[b,f][1,2,3]triazolo[4,5-d]azocin-8(9H-yl)-4-oxobutanoate (10)

To a solution of aza-dibenzocyclooctyne 9 (80 mg, 0.25 mmol) dissolved in 5.0 mL CH$_2$Cl$_2$ was added 1-(azidomethyl)-4-fluorobenzene (57 mg, 0.38 mmol). The reaction mixture was allowed to stir for 1 h at room temperature, after which the solvent was evaporated and the crude product was purified by column chromatography (1:1 pentane:ethyl acetate) to yield the product as a white solid (94.1 mg). Yield=80 %. Two isomers are formed as determined by ^{1}H NMR (1:1). ^{1}H NMR (400 MHz, CDCl$_3$): δ 7.67-7.73 (m, 1H), 7.44-7.49 (m, 2H), 7.38-7.42 (m, 1H), 7.24-7.31 (m, 1H), 7.17-7.24 (m, 2H), 6.93-7.10 (m, 5H), 5.99 (d, J=16.9 Hz, 1H), 5.58 (s, 2H), 4.33 (d, J=16.9 Hz, 1H), 3.60 (s, 3H), 2.44 (m, 1H), 2.23 (m, 1H), 2.09 (m, 1H), 1.80 (m, 1H). ^{13}C NMR (100.59 MHz, CDCl$_3$):

δ173.2, 171.3, 163.7, 161.3, 143.1, 140.0, 135.9, 134.9, 131.8, 131.2, 130.7, 128.9, 129.6, 129.3, 129.1, 129.0, 127.9, 127.1, 124.3, 116.0, 115.8, 52.0, 51.6, 51.4, 29.2, 28.9. HRMS (ESI+) (m/z) calculated for $C_{27}H_{23}N_4O_3F$ [M + H]$^+$ 471.1827, measured 471.1789; (ESI+) (m/z) calculated for $C_{27}H_{23}N_4O_3F$ [M + Na]$^+$ 493.1646, measured 493.1606.

Peptide Chemistry
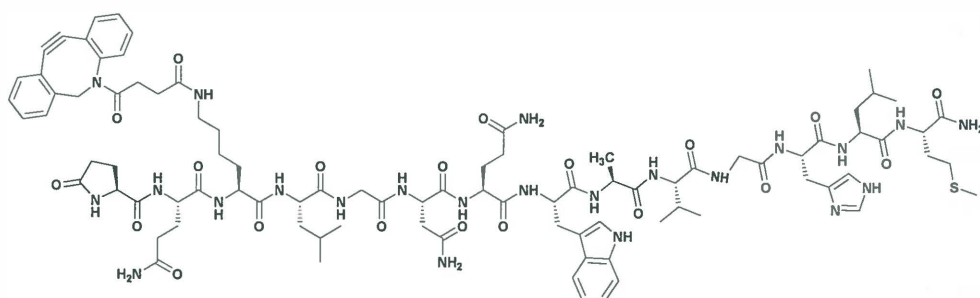
Aza-DBCO-BN

[Lys3]-bombesin (0.18 mg, 1.0 eq) was weighed into a 2.0 mL Eppendorf tube along with 9 (0.5 mg, 5.0 eq). 200 µL of dry DMF and 10.0 eq of diisopropylethyl amine were added and the resulting solution was stirred at room temperature for 24 h. The solvent was removed by lyophilization. Full conversion of lys[3]-bombesin could be observed by RP-HPLC. The product was purified by preparative RP-HPLC yielding Aza-DBCO-BN in 25 % yield. Retention time=32.0 min. HRMS (ESI+) (m/z) calculated for $C_{90}H_{123}N_{23}O_{20}S$ [M + H]$^+$ 1878.9108, measured 1878.9078.

Radiochemistry General

[^{18}F] fluoride was obtained by proton bombardment of an [^{18}O] enriched water target via the $^{18}O(p,n)^{18}F$ reaction. The radioactivity was trapped by passing the target water through a preactivated Sep-Pak light QMA cartridge (Waters). A 1 mL H$_2$O solution of K$_2$CO$_3$

(4.5 mg) and Kryptofix 222 (20 mg) was used to elute the [^{18}F]-fluoride from the cartridge into a conical glass vial. This eluate was evaporated to dryness by three consecutive azeotropic distillations after with acetonitrile (3 × 500 µL) under a gentle stream of nitrogen gas (130 °C). Analytical as well as semipreparative RP-HPLC was performed for monitoring and purification. Isolation of radiolabeled peptides was performed using a reversed-phase RP-C18 column (4.6 mm × 250 mm, 10 µm). The flow was set at 2.5 mL/min using a gradient system starting from 90% solvent A (0.01 M phosphate buffer, pH=6.0) and 10% solvent B (acetonitrile) (0-2 min) and ramped to 45% solvent A and 55% solvent B at 35 min. The analytic HPLC was performed using the same gradient system but with a reversed-phase Grace Smart RP-C18 column (4.6 mm × 250 mm, 5 µm) and a flow of 1 mL/min.

Results and Discussion

Synthesis and radiolabelling

The reaction with cyclooctyne modified bombesin was performed in DMF at room temperature and proceeded to completion in 15 min. The resulting tracer was also purified by RP-HPLC yielding the desired triazole tracers: [^{18}F]-BnTOxBN (retention time=16 min), [^{18}F]-BuTOxBN (retention time=19 min) and [^{18}F]-PEGTOxBN (retention time=22 min) with radiochemical yields of 31%, 37% and 19%, respectively. The specific activities were 62 GBq/µmol, 57 GBq/µmol , 60 GBq/µmol.

Cell culture.

The GRPR-positive PC-3 human prostate cancer cell line (ATCC, Manassas, Virginia, USA) was cultured at 37 °C in a humidified 5 % CO_2 atmosphere. The cells were cultured in RPMI 1640 (Lonza, Verviers, France) supplemented with 10 % fetal calf serum (Thermo Fisher Scientific Inc., Logan, Utah, USA) and subcultured twice a week after detaching with trypsin-EDTA.

In Vitro Competitive Receptor-Binding Assay.

In vitro GRPR binding affinities and specificities of BN(1-14) were assessed via a competitive displacement assay. Experiments were performed with PC-3 human prostate cancer cells according to a method previously described. (Schroeder, 2008) The 50% inhibitory concentration (IC$_{50}$) values were calculated by fitting the data with nonlinear regression using GraphPad Prism 5.0 (GraphPad Software, San Diego, California, USA). Experiments were performed with triplicate samples. Results were plotted in sigmoidal curves for the displacement of [^{18}F]-BnTOxBN, [^{18}F]-BuTOxBN and [^{18}F]-PEGTOxBN as a function of increasing concentration of BN(1-14). The tracers displayed high affinity for binding to GRPRs within PC-3 cell with IC$_{50}$ values of 29 nM , 30 nM and 40 nM for [^{18}F]-BnTOxBN, (Figure 8.1) [^{18}F]-BuTOxBN, (Figure 8.2) and [^{18}F]-PEGTOxBN, (Figure 8.3), respectively.
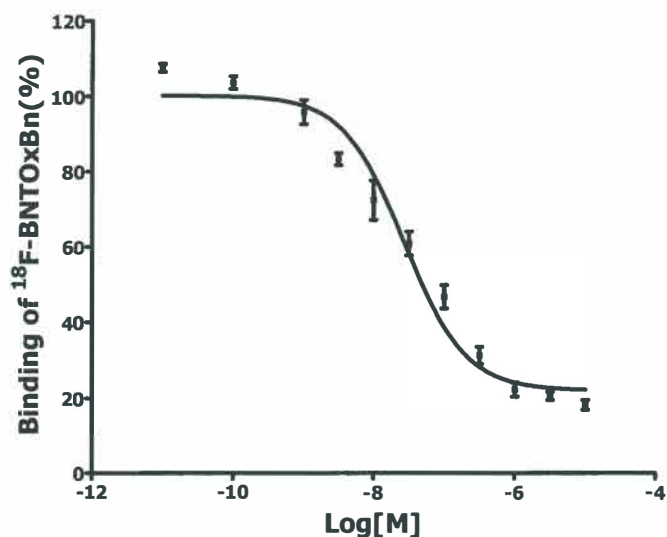
Figure 8.1. Competitive Binding Assay on PC-3 cells with **[^{18}F]-BnTOxBN**
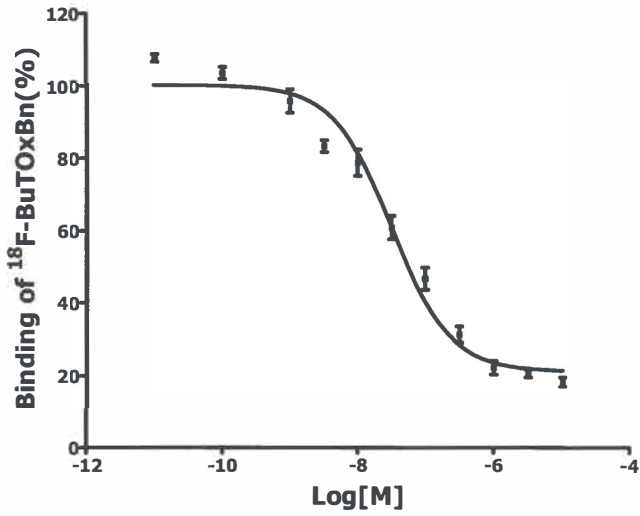
Figure 8.2. Competitive Binding Assay on PC-3 cells with [^{18}**F**]-**BuTOxBN**
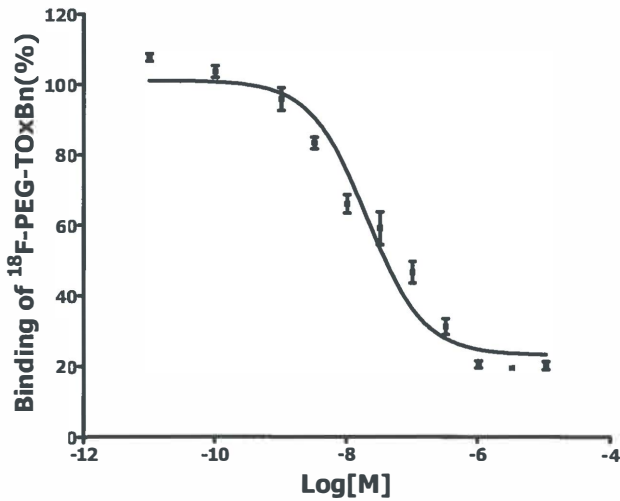
Figure 8.3. Competitive Binding Assay on PC-3 cells with [^{18}**F**]-**PEGTOxB**

Octanol/Water Partition Coefficient Study.

Water partition coefficients were determined at pH =7.4. 5 µL containing 500 kBq of the radiolabeled compound in PBS was added to a vial containing 1.2 mL 1-octanol and PBS (1:1). After vortexing for 1 min, the vial was centrifuged for 5 min at 10 000 rpm to ensure complete separation of layers. Then, 40 µL of each layer was taken in a pre-weighed vial and measured in the γ-counter. Counts per unit weight of sample were calculated. The lop P values were found to be 1.27, 0.26 and -0.43 for [18F]-BnTOxBN, [18F]-BuTOxBN and [18F]-PEGTOxBN, respectively.

Our starting point was to find a suitable strained alkyne with the optimal balance of reactivity and stability. Van Hest and van Delft reported an aza-dibenzocyclooctyn 7, which proved to be simultaneously reactive and stable (Debets, 2009). For our purposes, which involve rapid 'clicking' of a short lived radioisotope and eventual in vitro and in vivo studies, it appeared an ideal choice. We opted for an alternate and shorter synthetic route to our target molecule 9 (Scheme 8.1). Starting from commercially available dibenzosuberenone 1, oxime 2 can be formed in 95% yield by refluxing in the presence of hydroxylamine hydrochloride. The crucial step of this synthesis is the subsequent Beckmann rearrangement giving amide 3 in 67% yield. (Luca, 2002) The amide was reduced with Dibal-H to amine 4. Amine 4 is thus reached in three steps, rather than five, starting with the very inexpensive precursor 1 (1g~1 €) rather than 2-ethynylaniline (1g~55 €) as published. A short linker can be introduced by reaction of 4 with methyl succinyl chloride in the presence of triethylamine. Bromination proceeds smoothly in 88% yield, followed by subsequent debromination with a solution of potassium tert-butoxide in THF. Basic hydrolysis affords carboxylic acid 8. To allow us to couple the strained alkyne to our peptide, we form the N-hydroxysuccinimide ester 9.

Ch. 8
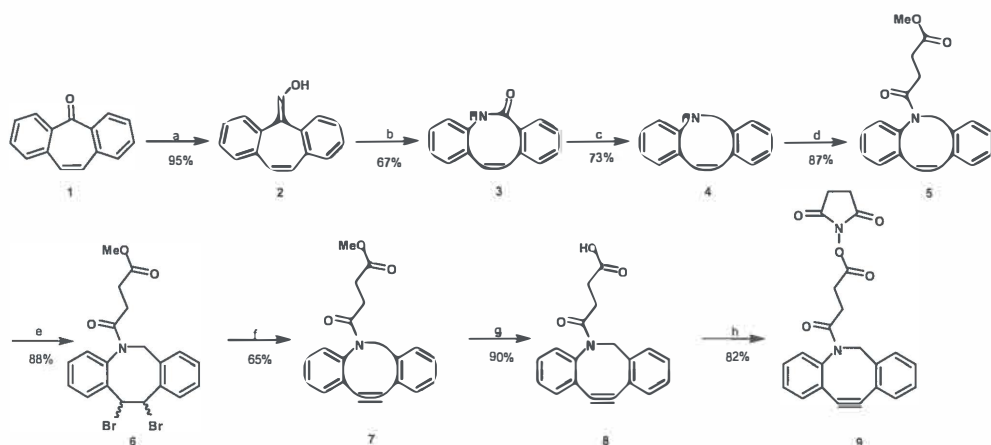
Scheme 8.1. Reagents and conditions: a) NH₂OH·HCl (3.0 eq), pyridine/ethanol (1:1), reflux; b) TCT (1.0 eq), DMF, r.t.; c) Dibal-H (5.0 eq), CH₂Cl₂, r.t.; d) Et₃N (2.0 eq), methyl succinyl chloride (1.5 eq), CH₂Cl₂, r.t.; e) Br₂ (1.0 eq), CH₂Cl₂, 0 °C; f) 1.0 M tBuOK in THF, THF, -40 °C, Ar atm.; g) LiOH (2.0 eq), H₂O, r.t.; h) EDC (1.1 eq), NHS (1.1 eq), CH₂Cl₂, r.t.; TCT= trichlorotriazine, DMF= dimethylformamide, Dibal-H= diisobutyl aluminum hydride, THF= tetrahydrofuran, EDC= N-(3-Dimethylaminopropyl)-N'-ethylcarbodiimide, NHS= N-hydroxysuccinimide.

Of key importance to the field of radiochemistry is high reactivity, allowing for the rapid introduction of the short-lived radiolabel under biocompatible conditions. Before proceeding with the modification of bombesin, we tested the reactivity of the aza-benzocylooctyne with several fluorine containing azides in pseudo in vivo conditions (Scheme 8.2). Strained alkyne **7** could be reacted with a [¹⁸F]-labeled azide by simply stirring the two reactants together in a mixture of human plasma and DMSO. We found that alkyne **7** could be fully converted to the corresponding triazoles within 15 min. With the hydrophilic [¹⁸F]-PEGylated azide **10**, triazole **11** was isolated with a radiochemical yield (RCY) of 42 %. With the more lipophilic [¹⁸F]-fluorobenzyl azide **12**, product was isolated with an RCY of 31 %. Furthermore, it is key to note that the reaction is performed in human plasma. Considering the eventual application of radiolabelling in vivo, it was important to confirm that the selected strained alkyne was not too fragile to withstand any exposure to a biological environment. Given that

with alkyne **7** full conversion to triazoles in less than 15 min could be achieve, we concluded that the reaction was fast enough for the desired time scale for labeling with [^{18}F].
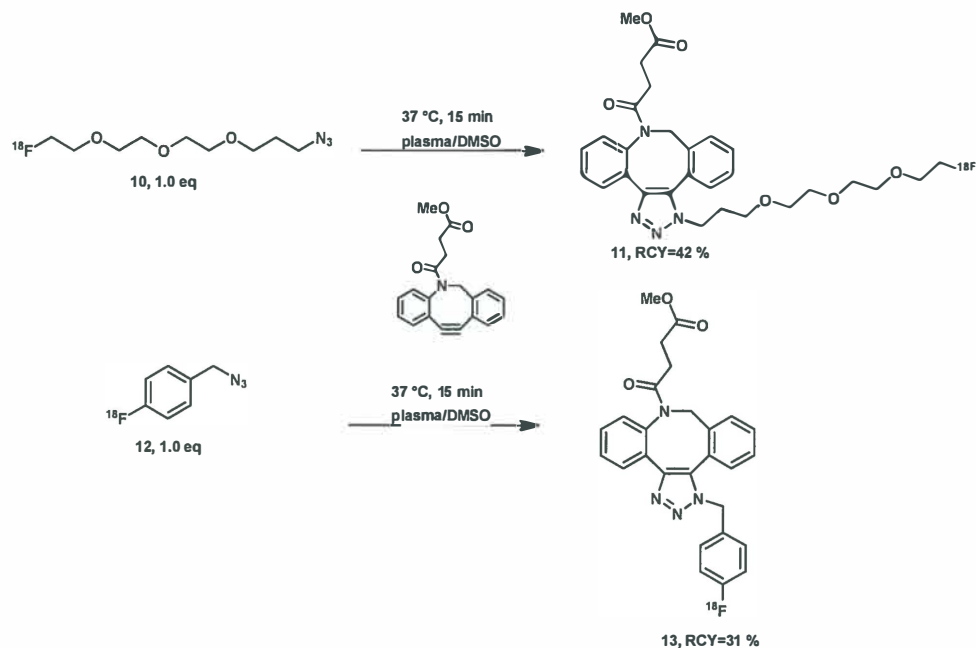
Scheme 8.2. Strain-promoted 'click' chemistry for labelling with [^{18}F].

Thus, succinimidyl ester **9** was conjugated to lys[3]-bombesin under basic conditions (Scheme 8.3). Full conversion to the product **Aza-DBCO-BN** was achieved after 24 h as determined by RP-HPLC, and subsequently **Aza-DBCO-BN** was purified by RP-HPLC and characterized by mass (ESI-MS). With the target bombesin analogue modified with a strained alkyne, we tested the efficiency of the copper-free [3+2] cycloaddition with various [^{18}F]-containing azides.

163
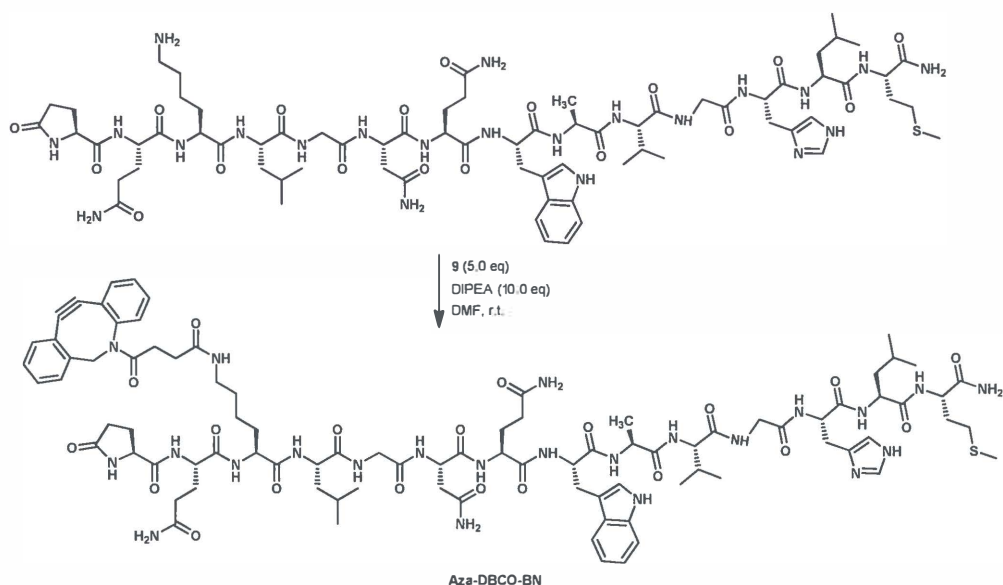
Scheme 8.3. Modification of bombesin with **9**.

Three [18F]-containing azides were selected to react with **Aza-DBCO-BN** (Scheme 4). As indicated, one advantage of this methodology is the ease with which the properties of the resulting peptidic tracer can be modified by simply changing the azides. [18F]-PEGylated azide **10**, [18F]-fluorobenzyl azide **12** and [18F]-fluoroazidobutane **14** were reacted with **Aza-DBCO-BN** at room temperature in DMF for 15 min, during which time complete conversion of the starting material could be detected by radio-TLC to give triazoles **[18F]-PEGTOxBN** (**15**), **[18F]-BnTOxBN** (**16**) and **[18F]-BuTOxBN** (**17**), respectively. The logarithmic partition coefficients were determined for all three tracers and were found to be -0.43, 1.27 and 0.26, respectively. This provides us with tracers ranging from the quite hydrophilic **[18F]-PEGTOxBN** to the more hydrophobic **[18F]-BnTOxBN**.

The binding affinity of all three tracers for gastrin-releasing peptide receptors was tested using PC3 human prostate cancer cells. The in vitro binding was determined by performing a competitive receptor binding assay with the receptor specific radioligand **[125I]-tyr[4]-BN** (a displacement assay). The 50 % inhibitory concentrations (IC$_{50}$) were determined to be 40 nM, 29 nM and 30 nM for **15**, **16**, and **17**, respectively (Figure. 8.3). All three tracers maintain high affinity for the GRPRs even after modification.
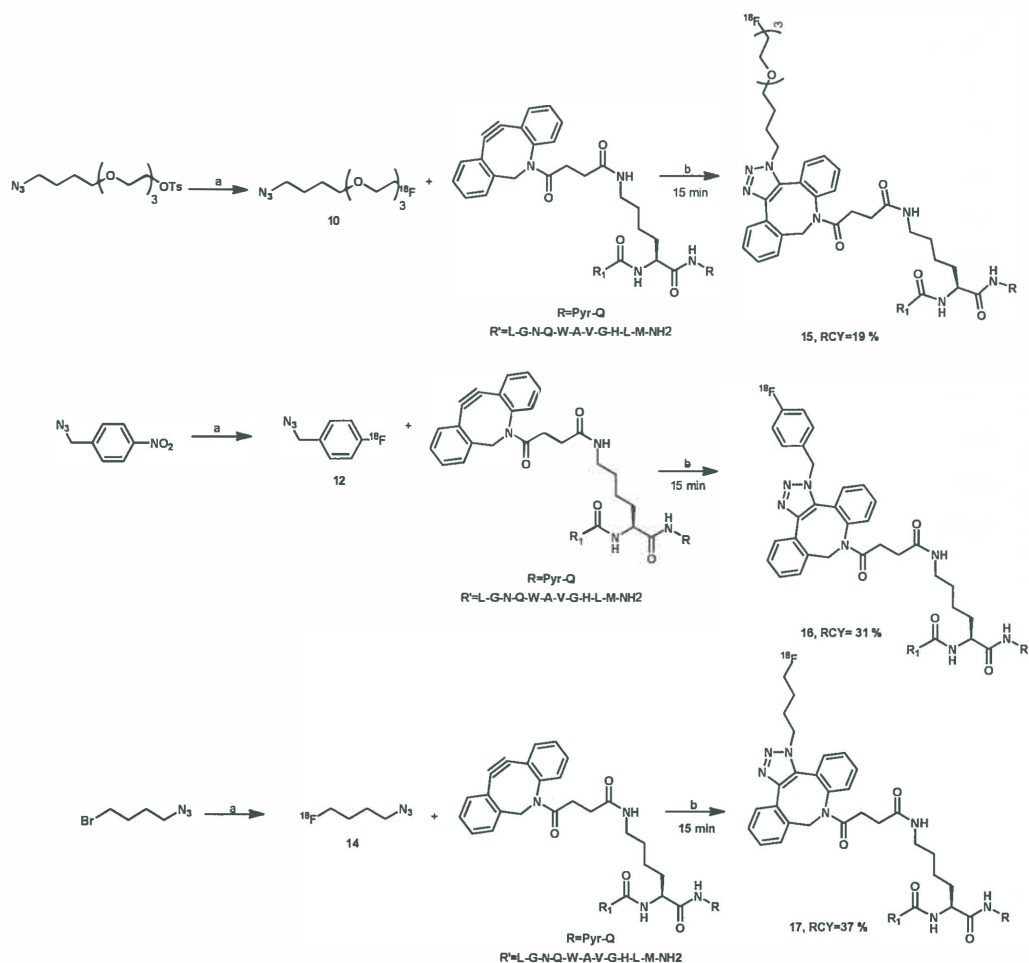
Scheme 8.4. Aza-dibenzycyclooctyne modified bombesin labeled with various [18F]-bearing. Azides. Reagents and conditions: a) K[18F], MeCN, 110 °C; b) DMF, r.t.

Thus we were able to achieve rapid radiolabelling of bombesin with [^{18}F] using a very straightforward protocol. Simple stirring of the radionuclide-containing azide with the modified bombesin analogue for 10-15 min at room temperature suffices to reach the target peptides in modest to good yields. Furthermore, the azide can be readily varied, as we have shown from a more lipophilic aromatic azide to a hydrophilic PEGylated azide. As a result, peptides with different properties are readily accessible from the same modified peptide allowing for rapid modification and fine tuning. In this way, the optimal lipophilicity for cellular uptake and metabolic clearance can be achieved. To the best of our knowledge, this is the first example of [^{18}F]-radiolabelling using copper-free click chemistry. We have also developed a simplified and relatively inexpensive route to the target aza-dibenzocyclooctyne hopefully rendering it more accessible for future use in a clinical setting. Although we describe herein the modification and labelling of bombesin and demonstrate that it maintains high affinity for the targeted receptors, ideally, this methodology would be applied to imaging via pre-targeting. For molecules with longer pharmacokinetics such as antibodies, and thus not amenable to the use of the short-lived [^{18}F], it would be highly advantageous to be able to administer the [^{18}F] radionuclide to the target in vivo. In this way, the use of radionuclides for imaging such targets will not be limited to the longer-lived metallic radioisotopes, and higher resolution images can be achieved using [^{18}F]. Studies along these lines will be reported in due course.

References

- Ananias H J K , de Jong I J, Dierckx R A J O, van de Wiele C, Helfrich W, Elsinga P H, Curr. Pharm. Des. 2008, 14, 3033-3047.
- Chang Y S, Jeong J M, Lee Y S, Kim H W, Rai G B, Lee S J, Lee D S, Chung J K, Lee M C, Bioconjate Chem., 2005, 16, 1329-1333.
- Debets M J, van Berkel S S, Schoffelen S, Rutjes F P J T, van Hest J C M, van Delft F L, Chem. Commun., 2009, 97-99.
- Hausner S H, Marik J, Gagnon M K J, Sutcliffe J L, J. Med. Chem., 2008, 51, 5901-5904.
- Hoffman T J, Smith C J, Nucl. Med. Bio., 2009, 36, 579-585.
- De Luca L, Giacomelli G, Porcheddu A, J. Org. Chem., 2002, 67, 6272-6274.
- Martin M E, Parameswarappa S G, O'Dorisio M S, Pigge F C, Schultz M K, Bioorg. Med. Chem. Lett., 2010, 20, 4805-4807.
- Schirrmacher R, Wängler C, Schirrmacher S, Mini-Reviews in Org. Chem., 2007, 4, 317-329.
- Schroeder R P J, Müller C, Reneman S, Melis M L, Breeman W A P, de Blois E, Bangma C H, Krenning E P, van Weerden W M , de Jong M, Eur. J. Nucl. Med. Mol. Imaging., 2010, 37, 1386-1396.
- Sletten E M, C.R. Bertozzi, Angew. Chem. Int. Ed., 2009, 48, 6974-6998.
- Tornøe C W, Meldal M, Peptides, 2001, 263-264.
- Varvarigou A, Bouziotis P, Zikos C, Scopinaro F, de Vincentis G, Cancer Biother. Radio., 2004, 19, 219-229.
- Zhang X, Cai W, Cao F, Schreibmann E, Wu Y, Wu J C, Xing L, Chen X, J. Nucl. Med., 2006, 47, 492-501.

Ch. 8

Chapter 9

Summary

Summary

There is a huge need for specific PET-radiopharmaceuticals. The discipline of radiochemistry involves a set of unique challenges that the chemist must consider: short synthetic time frames (as the radionuclide is constantly decaying), very small amounts of radioactive reagents, and limited available methods of characterization. Superimposed on these challenges is the stringent requirement that the products be consistently pure and that the results be reproducible as ultimately the protocols may be used to prepare compounds for injection in patients. Therefore new radiochemistry needs to be developed. In this thesis, the preparation of several receptor binding ligands is described via the 1,3-dipolar cycloaddition of azides and alkynes, also called a click reaction for [^{18}F]-radiolabelling of Positron Emission Tomography (PET). The work described in this thesis meets the challenges in radiochemistry that are focused on:

-   Short synthesis time
-   Very small amount of reagents
-   Easy and reliable synthesis
-   Versatility of the labeling method.

Therefore the copper-catalyzed 1,3-dipolar cycloaddition of alkynes and azides (CuAAC) and the copper-free cycloaddition promoted by ring strain have proven to be both reliable and orthogonal ligation methods. The CuAAC reaction meets the challenges mentioned above such as being fast; it can be applied under a wide range of conditions, and is selective. In a field where simple and fast reactions are crucial, it is only normal that "click" chemistry emerged as an excellent radiolabeling technique.

Throughout this thesis, two main goals were pursued: The first is to develop click chemistry methodology for the synthesis of PET tracers with focus on ^{18}F as radionuclide and the second part was to apply click chemistry for the synthesis and evaluation of biologically active molecules.

In chapter 3, we performed 1,3-dipolar cycloadditions in the presence of copper(I) and we optimized our radiolabeling procedure to reach high radiochemical yields (RCY). In addition we accelerated the CuAAC reaction by the addition of MonoPhos ligand. MonoPhos, a simple phosphoramidite ligand, which had the effect of significantly reducing reaction times in combination of very low amounts of reagents. Conjugation of [^{18}F]fluoroalkynes to various amounts (> 0.01 mg) of acetylenes or azide via CuI mediated 1,3-dipolar

cycloaddition yielded the desired ^{18}F-labeled triazole products in 10 min with yields of 54–99% and excellent purity radiochemical purity (97–99%). The total synthesis time was 30 min from the end of bombardment. In conclusion, a highly versatile fast ligand-accelerated copper catalyzed click reaction for the introduction of ^{18}F was developed.

In chapter 4, we described a new PET tracer for cerebral beta-adrenergic receptors based on the ^{18}F-click methodology described in chapter 3. (Scheme 9.1) This work focused on exploiting the selectivity of the CuAAC by combination with an enzymatic transformation. A racemic epoxide can be stereoselectively ring opened with an azide to produce azidoalcohols. 'Click chemistry' was successfully applied to the synthesis of ^{18}F-fluorination of (R)-1-((9H-carbazol-4-yl)oxy)-3-4(4-((2-(2-(fluoromethoxy)-ethoxy)methyl)-1H-1,2,3-triazol-1-yl)propan-2-ol (^{18}F-FPTC) resulting in excellent radiochemical yields purity (97-99%). A tracer based on the new motif β-hydroxytriazole design was synthesized reteining its affinity for cerebral β-adrenergic receptors (AR). FPTC demonstrated high in vitro binding affinity for the β-AR. The high affinity (IC 50 = 50-60 nM) and moderate lipophilicity (logP +2.48) as important criteria predict the suitability of a the compound for in vivo imaging. However the ex vivo biodistribution and microPET images showed that these criteria proved insufficient to ensure visualization of β-ARs in the brain.

Ch. 9
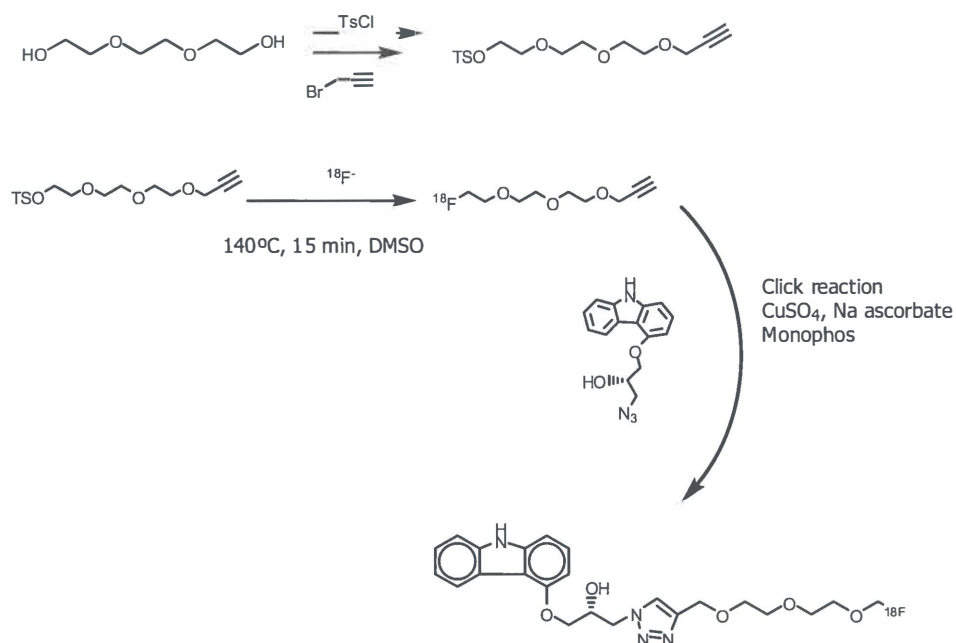
Scheme 9.1. Synthesis of ^{18}F-FPTC

In the study described in chapter 5, we developed a modified bombesin, a peptide which has a high affinity for the gastrin releasing peptide receptor (GRPR) which is particularly overexpressed on several kind of tumor cells, such as prostate cancer. Bombesin is a 14 amino acid peptide sequence peptide. Amino acids 7-14 are considered to be the sequence responsible for binding to the GRP-receptor. We used the 1,3-dipolar cycloaddition to label the peptide modified at the [lys3]-position. A terminal alkyne was attached to the [Lys3] residue of the 14 amino acid peptide sequence, where [^{18}F] was readily introduced using a complementary azide. (Scheme 9.2) The tracer proved to have good in vitro properties. But preclinical data demonstrated that no tumor uptake could be measured.
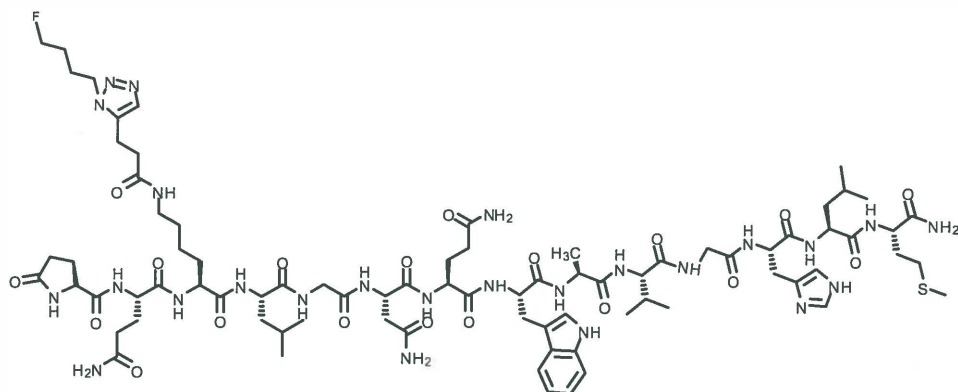
Schem 9.2. Fluoro Triazolyl Lysine 3 Bombesin   (FTBN3)

In chapter 6, we focused on the synthesis of the Siemens imaging biomarker ^{18}F-RGD-K5. This cyclic peptide contains an amino acid sequence which is a well known binding motif for integrin $\alpha_v\beta_3$ involved in cellular adhesion to the extracellular matrix. We developed an improved "click" chemistry method using Cu(I)-Monophos as catalyst to conjugate [18F]fluoropentyne to the RGD-azide precursor yielding ^{18}F-RGD-K5. (Scheme 9.3) A comparison is made with the registered Siemens method with respect to synthesis, purification and quality control. [18F]RGD-K5 was obtained after 75 min overall synthesis time with an overall radiochemical yield of 35% (EOB). The radiochemical purity was > 98 % and the specific radioactivity was 100-200 GBq/µmol at the EOS.

Ch. 9
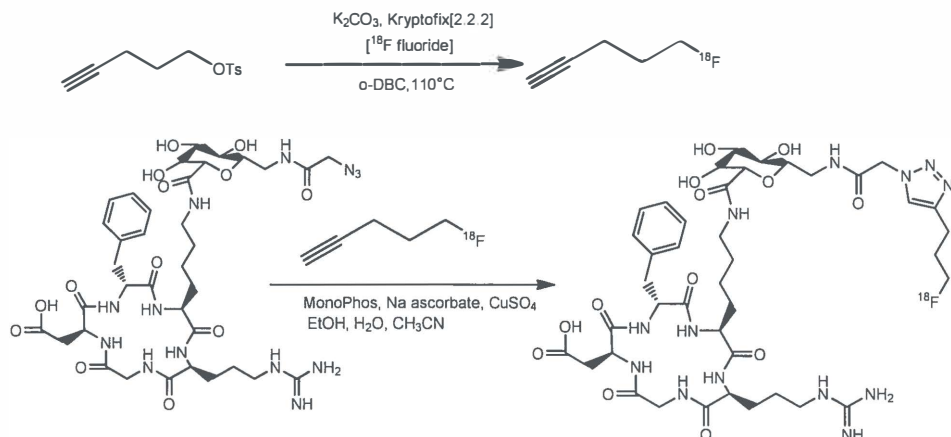
Scheme 9.3. A) Production of 5-[^{18}F]fluoro-1-pentyne: nucleophilic substitution between pentynyl tosylate and anhydrous [^{18}F]fluoride in ortho-dichlorobenzene (o-DCB). B) MonoPhos Cu(I)-catalysed Huisgen cycloaddition of [^{18}F]fluoropentyne with the RGD-K5 azide precursor resulting in the 1,4-disubstituted triazole [^{18}F]RGD-K5.

In chapter 7, for the first time demonstrated the potential of integrin imaging in determination of angiogenesis and vulnerability in atherosclerotic plaques. Noninvasive imaging and quantification of angiogenesis could provide clinicians with a new tool in stratifying risk for cardiovascular events. The QC system has been validated and allows the tracer to be used in clinical studies for visualization of neoangiogenesis in oncological patients in our hospitals.

In chapter 8, we were able to achieve rapid radiolabelling of bombesin with [^{18}F] using a very straightforward protocol using copper-free click conditions. Simple stirring of the radionuclide-containing azide with the modified bombesin analogue for 10-15 min at room temperature sufficed to reach the [18F]-target peptides in modest to good yields. Furthermore, the azide can be readily varied, as we have shown, from a more lipophilic aromatic azide to a hydrophilic PEGylated azide. (Scheme 9.4) As a result, tracers with different properties are readily accessible from the same substrate allowing for rapid modification and fine tuning. In this way, the optimal lipophilicity for cellular uptake and

metabolic clearance can be achieved. Although we describe herein the modification and labelling of [lys3]-bombesin and demonstrate that it maintains high affinity for the targeted receptors, this methodology would be extended to imaging making use of the technique of pretargeting.
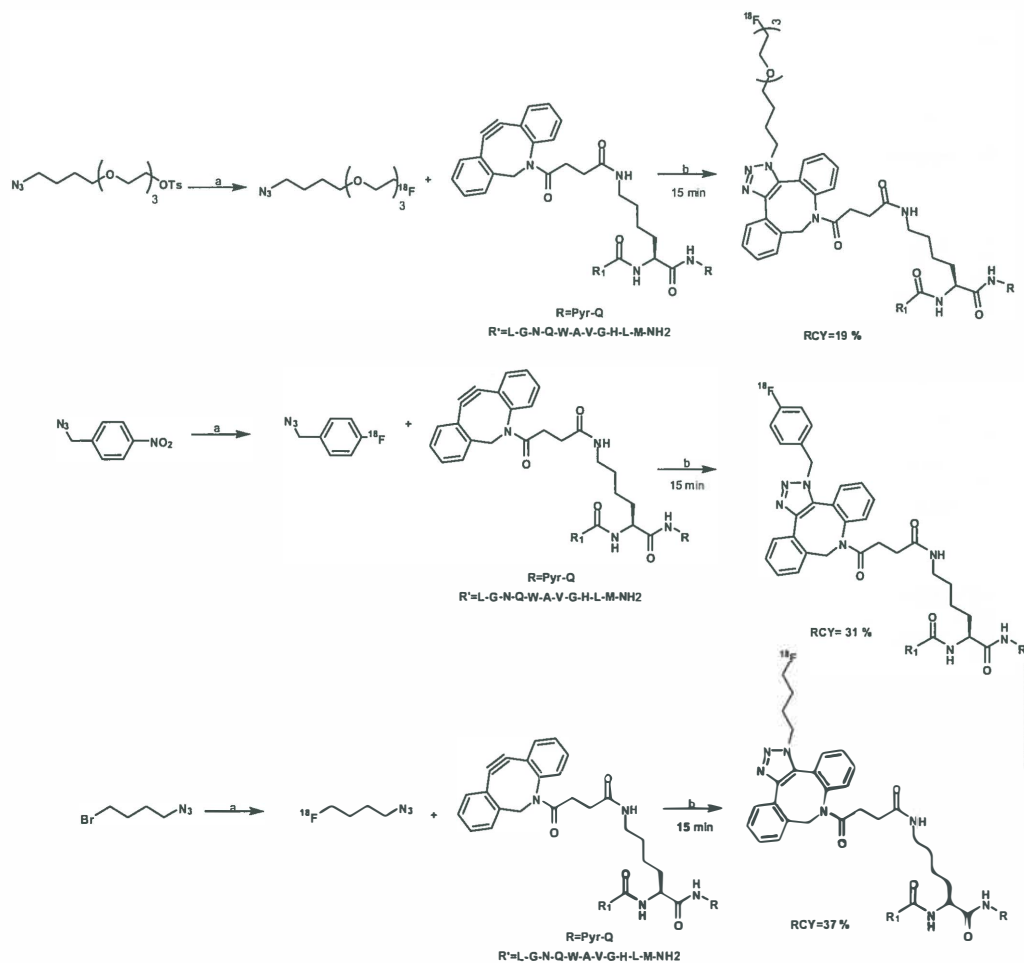
Scheme 9.4. Aza-dibenzycyclooctyne modified bombesin labeled with various [18F]-bearing

Azides. Reagents and conditions: a) K[^{18}F], MeCN, 110 °C; b) DMF, r.t.

In conclusion Click chemistry is a highly valuable approach for biomedical application. One of the unique and important properties of click chemistry is its bio-orthogonal character. Covalent and rapid linkage of two components under environmentally friendly, nontoxic conditions are properties that are completely complementary to the development of novel agents for the development of both imaging and therapeutic products.

Ideally, methodologies which are adaptable to a wide range of target molecules and prosthetic groups can be developed. The advantages gained from the intrinsic simplicity of such protocols would be achieved economically, practically and would benefit the fields of nuclear imaging and medicine.

Click chemistry may offer the perfect platform for such advances in labelling due to its exquisite selectivity and tolerance to a wide range of conditions.

In addition applications of Cu-free click chemistry include mammalian disease models where the bioavailability and pharmacokinetic properties of the reagents become important. The cyclooctynes that are currently employed for Cu-free click chemistry are not very soluble in aqueous solutions. The hydrophobicity of these cyclooctyne scaffolds could also promote binding to membranes or nonspecific binding to serum proteins, thereby reducing their bioavailable concentrations and increasing the noise in PET-images.

Finally the suitability of azide labeling and Cu-free click chemistry should enable applications in many areas of glycobiology. For example, direct imaging of glycan trafficking under conditions of cell stimulation or pharmacological intervention has been demonstrated already in cells, tissues, or even whole organisms.

Chapter 10

Future perspectives

Click chemistry is applied in diverse areas such as bioconjugation, drug discovery, materials science, and radiochemistry. Click chemistry has increasingly found applications in many aspects of drug discovery, by generating lead compounds through combinatorial methods. Bioconjugation via click chemistry is also employed in proteomics and nucleic research. In radiochemistry, selective radiolabeling strategies of biomolecules for imaging and therapy have been realized.

The work presented in this PhD-thesis has resulted in versatile methodology based on click chemistry to prepare PET-tracers. The evaluation of these PET-tracers is already underway and forthcoming in vivo study results will provide grounds for further radiopharmaceutical development in this field. This chapter describes applications where click chemistry can play an important role in the near future.

Application for multimodality imaging tracers

In the near future, click chemistry can be further developed as a versatile synthetic method to produce dual modality probes for PET-MRI and PET-optical imaging. Using the versatile Cu catalyzed azide alkyne cycloaddition, the radionuclide ^{18}F can be rapidly introduced to a molecule already bearing the necessary functionalities for MRI or optical imaging.

Concepts for PET scanners integrated into an MRI tomograph have emerged and the first commercially available cameras have entered the market. The excellent soft-tissue contrast of MRI and the multifunctional imaging options it offers, such as spectroscopy, functional MRI, and arterial spin labeling, complement the molecular information of PET. PET can verify the localization of probes where concentration is too low to detect by MRI, making it a powerful tool for probe development. The combination of MRI and PET is particularly synergistic because MRI can not only provide anatomical context for the PET images but also allow high-resolution imaging of probe distribution.

Dual PET-MRI biomarkers i.e. tracers that are visible with PET as well as with MRI can add an extra dimension. The superior sensitivity of PET over MRI, with a factor of >1000, imposes constraints on the design of these dual PET-MRI biomarkers. Magnetic nanoparticles that are coupled to radionuclides are feasible and can be imaged with PET in combination with MRI. Here, the radiolabelled part of the nanoparticle is used to spot a

region of interest inside the body and to quantify biomarker uptake. Then, with MRI, the correct localization of the dual modality probe inside the target region is performed, based on the MRI contrast produced by the biomarker. Furthermore, biomarkers that allow PET and MRI labeling might be of interest for cross-validation studies.

In addition to PET-MRI, PET and optical imaging are a promising combination for dual imaging technology as well. They both have high sensitivity resulting in a PET-optical probe that can be present in low quantities while still allowing good images from both techniques. The deep tissue imaging of PET and the longer lasting optical imaging allows for the possibility for the localization of a disease with PET and then the visual guidance of fluorescence during surgery all with one probe. A particular advantage is offered when using short lived isotopes such as ^{11}C and ^{18}F resulting in low radiation dose for the patient and possibility for repeated measurements. The fluorescent label gives information about the distribution and metabolic breakdown of the labeled drug or tracer during a longer period even after decay of the radioactivity. Thus far the synthesis of dual modality probes has mainly focused on the use of long lived isotopes. While these are useful isotopes, they have the intrinsic disadvantage of exposing the subject to radioactivity for longer periods of time. Short lived isotopes present an extra challenge to the synthesis since the introduction and subsequent purification of the isotope has to occur within a small time frame, preferably less than an hour.

Dual PET-MRI-tracers could be prepared by coupling the ^{18}F-alkyne or azide to inorganic nanoparticles. It has already been shown that "click" nanoparticles were able to stably circulate for hours in vivo after intravenous injection (>5 h circulation time), extravasate into tumors, and penetrate the tumor interstitium.

Cross-linked, fluorescent, superparamagnetic iron oxide nanoparticles have been derivatized with an azido-PEG group. So conjugation with ^{18}F-alkynes to these azido-PEG nanoparticles via cycloaddition would be feasible. This strategy opens the way to attach different tags, resulting in nanoparticles suitable for multimodality imaging, including MRI, PET and optical imaging. The synthetic difficulties that arise with the use of short lived radioisotopes are hopefully overcome by introducing the radioactive label as a last step via 'click' chemistry.

Ch. 10

In vivo copper-free click application for pretargeting

The bioorthogonality of the Cu(I)-catalyzed click chemistry reaction and the fact that it proceeds readily in water at various pHs makes it suitable for biological applications. The main disadvantage is that copper is cytotoxic so this type of reaction cannot be performed *in vivo* and requires purification to eliminate traces of copper before labelled molecules can be monitored in biological systems. This is why considerable effort has been put into developing click reactions that proceed rapidly without copper, the so-called Cu-free click chemistry. For instance, an alkyne that is sufficiently reactive in the absence of copper catalysis can be obtained by introducing ring strain and/ or electron withdrawing groups. The group of Bertozzi in particular has done significant work in this area, and have synthesized a library of cyclooctynes with varying properties and reactivities. A great challenge will be to utilize the copper free click reaction *in vivo* for pretargeting purposes in antibody imaging. Pretargeting is a multistep process so far used in radioimmunotherapy and imaging oncology that separates antibody targeting as first step from the radionuclide targeting in the second step.

Bispecific antibodies with radiolabeled peptides and streptavidin conjugates/fusion proteins with radiolabeled biotin have been examined clinically with promising initial results. The benefit of using ^{18}F in pretargeting is that it is a radionuclide with very favourable properties regarding half life, availability, and spatial resolution. The idea is to first administer an azide or alkyne derivatized antibody. At the optimal time point where specific over non-specific binding is maximal (usually a few days) the ^{18}F-radiolabelled counterpart is injected and should click on to the derivatized antibody.

Since the alkyne-azide cycloaddition will likely be too slow under in vivo copper-free conditions, more efficient click chemistry methods should be investigated for such as the inverse electron demand Diels-Alder cycloaddition connecting tetrazine and norbornene. Applying such a click chemistry approach, modification of an antibody can be performed with norbornene. The complementary tetrazine can be modified with the appropriate leaving group for [^{18}F]-fluorination or a chelator for radiometallations. In addition to [^{18}F]-strategies, introduction of chelators could help in making comparisons between bioconjugates labeled with different radiometals, because the chelator modified antibodies are synthesized using identical ligation conditions.

Pretargeting strategies could also be applied to nanoparticles and multimodality biomarkers. New chemistry is required to optimize nanoparticles design and manufacturing and to optimize the formation of a site-specific stable bioconjugate linkages between the nanoparticles and the targeting molecules, and between the nanoparticles and the PET radionuclide. Therefore several click chemistry methods are already being developed. Novel nanoparticle materials are being developed that have the intrinsic ability to bind to PET radionuclides either *in vitro* or *in vivo* allowing pretargeting approaches. Non-nanoparticle approaches are also being developed in which single targeting molecules can be labelled with both paramagnetic contrast and radionuclides. Once general production methods have been developed, specific targeted dual modality probes will be synthesized.

In conclusion, possible applications using click chemistry holds many challenges in the field of (radio)chemistry and biotechnology.

Ch. 10

Chapter 11

Samenvattingen

Samenvatting

Er is een grote behoefte aan specifieke PET-radiofarmaca. Binnen het vakgebied van de radiochemie zijn er een aantal uitdagingen voor de chemicus, te weten korte synthesetijden (omdat het radionuclide snel vervalt), kleine hoeveelheden radioactief gemerkt reagentia en beperkte karakterisatiemogelijkheden. Bovenop deze uitdagingen bestaat er nog de vereiste dat de producten zeer zuiver moeten zijn en de resultaten reproduceerbaar, omdat de radiofarmaca worden gebruikt voor humane studies. Nieuwe radiochemische methoden moeten daarom worden ontwikkeld. In dit proefschrift wordt de synthese van een aantal receptor liganden beschreven met behulp van de 1,3-dipolaire cycloadditie van azides en alkynen, ofwel een klikreactie voor [^{18}F] voor gebruik voor Positron Emissie Tomografie (PET). Het werk dat is beschreven in dit proefschrift richt zich op de volgende uitdagingen in radiochemie:

- Korte synthesetijd
- Zeer kleine hoeveelheden reagentia
- Eenvoudige en betrouwbare synthese
- Brede toepasbaarheid van de methode

De koper-gekatalyseerde 1,3-dipolaire cycloadditie van alkynen en azides (CuAAC) en de koper-vrije cycloadditie geactiveerd door ringspanning bleken betrouwbare labellingsmethoden te zijn. De CuAAC reactie voldoet aan de uitdagingen zoals eerder genoemd. De reactie is snel, selectief en kan worden toegepast in aanwezigheid van verschillende reactieomstandigheden. Daarom is klikchemie uiterst geschikt als labellingsmethode voor PET-radiofarmaca.

In dit proefschrift worden twee doelen nagestreefd: het eerste doel was de ontwikkeling van een 18F-klikchemie methode om PET-radiofarmaca te maken, het tweede doel was om de klikchemie toe te passen op biologisch actieve moleculen.

In hoofdstuk 3 voerden we 1,3-dipolaire cycloaddities uit in aanwezigheid van koper(I). We optimaliseerden de labellingsprocedure om hoge radiochemische opbrengsten te halen. Daarnaast versnelden we de CuAAC reactie door toevoeging van het ligand MonoPhos. MonoPhos, een eenvoudige phosphoramidiet ligand, verkortte de reactietijden in combinatie met zeer lage hoeveelheden reagentia. De conjugatie van [^{18}F]fluoroalkynen aan verschillende hoeveelheden (> 0.01 mg) azides gaven de gewenste ^{18}F-triazoolproducten in

10 min met opbrengsten van 54–99% en goede zuiverheid (97–99%). De totale synthesetijd was 30 min vanaf het einde van bestraling. Geconcludeerd kan worden dat een goed toepasbare klikreactie gekatalyseerd door koper(I) en MonoPhos is ontwikkeld om 18F-radiofarmaca te maken.

In hoofdstuk 4 beschreven we een nieuwe PET tracer voor beta-adrenerge receptoren in de hersenen, gemaakt met behulp van de ^{18}F-click methode beschreven in hoofdstuk 3 (Schema 9.1). Het werk richtte zich op de combinatie van klikchemie en een enzymatische omzetting. Racemisch epoxide kan stereoselectief geopend worden met een azide om zodoende azidoalcoholen te produceren. Klikchemie werd succesvol toegepast op de synthese van (R)-1-((9H-carbazol-4-yl)oxy)-3-4(4-((2-(2-(fluoromethoxy)-ethoxy)methyl)-1H-1,2,3-triazol-1-yl)propan-2-ol (^{18}F-FPTC) met hoge radiochemische opbrengst en zuiverheid. FPTC bezit de nieuwe structuur β-hydroxytriazole waarbij bleek dat de affiniteit voor de beta-adrenerge receptoren behouden bleef. De redelijk hoge affiniteit (IC 50 = 50-60 nM) en geschikte lipofiliciteit (logP +2.48) zijn twee belangrijke criteria om te voorspellen of de tracer geschikt is voor in vivo beeldvorming. Helaas lieten de ex vivo biodistributie en microPET beelden zien dat deze criteria onvoldoende waren om beta-adrenerge receptoren in de hersenen af te beelden.

Ch. 11

185
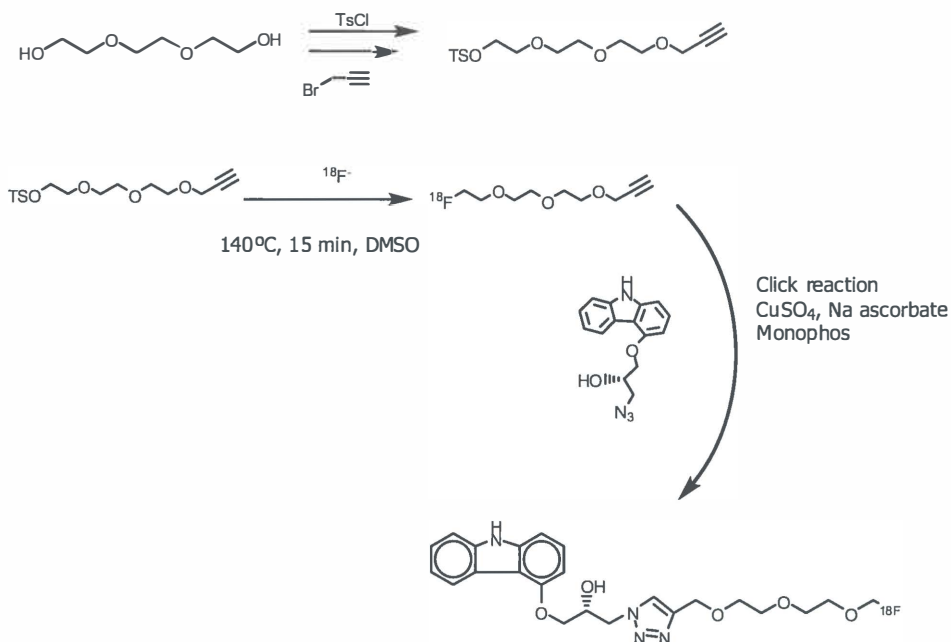
Scheme 9.1. Synthese van ^{18}F-FPTC

In een studie beschreven in hoofdstuk 5 ontwikkelden we gemodificeerd bombesine, een peptide dat een hoge affiniteit heeft voor de gastrine afscheidende peptide receptor (GRPR) die in verhoogde concentraties voorkomt op verschillende soorten tumor cellen, zoals in prostaat kanker. Bombesine is een peptide van 14 aminozuren. De aminozuren 7-14 zijn verantwoordelijk voor binding aan de GRP-receptor. Wij gebruikten de 1,3-dipolaire cycloadditie om het peptide te labellen op de [lys3]-positie. Een terminale alkyn werd verbonden aan het [Lys3] residu van de 14 aminozuur peptide, waar [^{18}F] werd geïntroduceerd als complementaire azide (Scheme 9.2). De tracer bezat goede vitro bindingseigenschappen. Echter uit preklinische data bleek dat geen tumor opname gemeten kon worden.

Schema 9.2. Fluoro Triazolyl Lysine 3 Bombesine   (FTBN3)

In hoofdstuk 6 hebben we ons gericht op de synthese van de Siemens imaging biomarker ^{18}F-RGD-K5. Dit cyclische peptide bevat een aminozuurvolgorde waarvan bekend is dat het bindt aan $\alpha_v\beta_3$ integrines, die een rol spelen in celadhesie aan de extracellulaire matrix. We hebben een verbeterde "klik" chemie method ontwikkeld met gebruik van Cu(I)-Monophos als katalysator om [^{18}F]fluoropentyn aan de RGD-azide precursor te koppelen, met als resultaat het product ^{18}F-RGD-K5 (Schema 9.3). Deze methode is vergeleken met de geregistreerde Siemens methode wat betreft de synthese, zuivering en kwaliteitscontrole. [^{18}F]RGD-K5 werd verkregen na 75 min synthesetijd en een radiochemische opbrengst van 35% (EOB). De radiochemische zuiverheid was > 98 % en de specifieke activiteit was 100-200 GBq/µmol.

Scheme 9.3. A) Productie van 5-[^{18}F]fluor-1-pentyn: nucleofiele substitutie tussen pentynyl tosylaat en gedroogd [^{18}F]fluoride in ortho-dichloorbenzeen (o-DCB). B) MonoPhos Cu(I)-gekatalyseerde Huisgen cycloadditie van [^{18}F]fluoropentyn met de RGD-K5 azide precursor resulterend in 1,4-disubstitueerd triazool [^{18}F]RGD-K5.

In hoofdstuk 7 is voor de eerste keer de mogelijkheid van integrine beeldvorming voor het bepalen van angiogenese en kwetsbaarheid van atherosclerotische plaques beschreven. Niet-invasieve beeldvorming en kwantificatie van angiogenese kunnen artsen een manier geven om risico's bij cardiovasculaire ziekten in te schatten. Het kwaliteitscontrole systeem voor RGD-K5 is gevalideerd en biedt nu de mogelijkheid om de tracer toe te passen in klinische studies naar neoangiogenese bij kankerpatiënten.

In hoofdstuk 8 hebben we een snelle [^{18}F]-labellingsmethode beschreven voor bombesine met [^{18}F] waarbij gebruik werd gemaakt van reactiecondities zonder koperkatalyse. Het [^{18}F]-azide en het alkyn-gemodificeerde bombesine werden 10-15 min bij kamertemperatuur geroerd. Hierdoor werd het [18F]bombesine in redelijk tot goede opbrengsten gemaakt. Als bijkomend voordeel kon het azide worden gevarieerd wat betreft lipofiliciteit (Schema 9.4). Het resultaat was dat tracers met verschillende eigenschappen eenvoudig beschikbaar zijn gekomen vanuit hetzelfde substraat. Op deze manier kan een optimale lipofiliciteit voor celopname en metabole klaring worden verkregen. We beschrijven hier de verandering en labeling van [Lys3]-bombesine en laten zijn dat de hoge affiniteit

188

voor de receptoren behouden blijft. De methode zou in de toekomst kunnen worden uitgebreid om pretargeting concepten te kunnen onderzoeken.
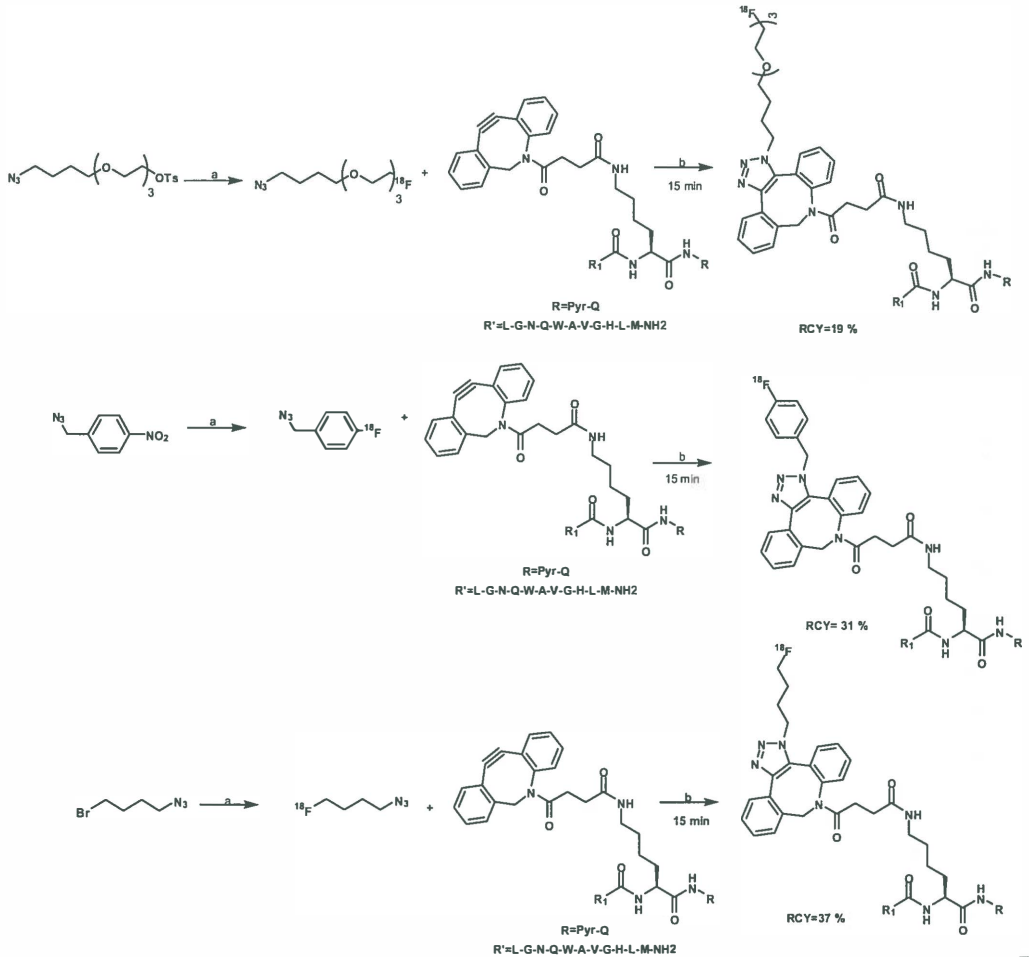
Scheme 9.4. Aza-dibenzycyclooctyn gemodificeerde bombesine gelabeled met verschillende [^{18}F]-azides. Reagentia en condities: a) K[^{18}F], MeCN, 110 ºC; b) DMF, r.t.

Geconcludeerd mag worden dat klikchemie een waardevolle manier is voor biomedische toepassingen. Een van de unieke eigenschappen van klikchemie is het bioorthogonale karakter. Een snelle covalente koppeling van twee componenten onder milieuvriendelijke en

189

niet-toxische condities die volledig complementair zijn en kan worden gebruikt voor de ontwikkeling van nieuwe stoffen voor diagnostiek of therapie.

Acknowledgments

I would like to thank Paul, Remko, Elco, Johan, Leonie, Clara, Hedy, Aafke, Yvonne 1, Yvonne 2 and the rest of the colleagues in the NGMB department, for having a nice time in coffee break.

To my dear roommates and good friends: Ines, Valentina, Mehrsima, Ania, Daneille, Andrea and Alexandre. I am very happy and lucky to have met you and having such a nice and funny company in these years with you. YOU DON'T KNOW!!! but I WILL TELL YOU that, I cannot imagine my time without you in my second home.

I want to thank Giuseppe bello ;), Federica bella ;), David, Erika, Anneik, Reza, Hans, Zilin, Nisha, Katica and Nathalie for all the amazing time that we spent together during and after the working hours.

To the rest of PhD student, Heli, Shiva, Khayum, Siddesh, Soumen Paul, Gaurav, Willem Jan and Vladimir, thank you for all the nice moments we shared.

Thanks to all my friends outside the world of nuclear medicine: Solmaz, Christian, Ghazaleh, Emad, Gabi and Martijn.

To my dear paranymphs Silvana and Janine thank you very much for all your support and help. Thank you for being my good friends since 2007, when I started my PhD project.

I want to thank my lovely sisters, Lida, Zhila and Gilda to be always with me.

Thanks to my dear sister-in-laws Mahta and Elham for having nice conversations.

I want to thank my parents-in-law, to thinking of me during these years. Merci!

And I would like to extend my gratitude to my dear Parents: Sima & Ahmad for their unparalleled love and support from the beginning of my life till now. Merci Maman va Baba jun.

I cannot find words to express my gratitude to you, my lovely husband, my dearest Vahid. I cannot thank you enough for everything you have done for me. Without your love and support I would not be where I am today. You have been persistently inculcating self-confidence in me, repeating continuously that I should believe more in myself.

Thank you for your understanding and your endless love. Thank you for understanding a workaholic wife during all the long evenings that I have been working. And you made a delicious dinner with nicely decorated dining table for me. It couldn't be better…

List of abbreviations

AChE	acetylcholinesterase
Aza-DBCO	aza-dibenzocyclooctyne
BBB	blood-brain barrier
[^{18}F]SFB	N-succinimidyl 4-[^{18}F]fluorobenzoate
β-ARs	beta adrenergic receptors
BN	Bombesin
Bq	Becquerel (MBq: megabecquerel)
CEA	Carotid endarterectomy
DMF	Dimethylformamide
DMSO	Dimethyl sulfoxide
CUAA	Copper-Catalyzed Azide-Alkyne Cycloaddition
DIPEA	N,N'-diisopropylethylamine
DIFO	difluorinated cyclooctyne
EGFR	Epidermal rowth factor receptor
EC50	Half maximal effective concentration
EOS	end of synthesis
FDG	2-[^{18}F]Fluoro-2-Deoxy-D-Glucose
^{18}F-FPTC	^{18}F-fluorination of (R)-1-((9H-carbazol-4-yl)oxy)-3-4(4-((2-(2-(fluoromethoxy)-ethoxy)methyl)-1H-1,2,3-triazol-1-yl)propan-2-ol
FTBN3	Fluoro Triazolyl Lysine 3 Bombesin
HPLC	high-performance liquid chromatography
IC50	Half maximal inhibit concentration
ICYP	iodocyanopindolol
K_1/k_2	partition coefficient

196

k_3/k_4	binding potential
NOD mouse	Non-obese diabetic mice
o-DCB	ortho-dichlorobenzene
p.i	post injection
PBS	phosphate-buffered saline
PC	Prostate canter
PET	positron emission tomography
QC	Quality control
RGD	radiolabeled arginine-glycine-aspartate
RCY	Radio chemical yeild
ROI	region of interest
SD	standard deviation
SPE	solid-phase extraction
SPECT	single-photon emission computed tomography
SUV	standardized uptake value
TBTA	tris-(Benzyltriazolylmethyl)amine
TAC	time activity curve
TFA	Trifluoroacetic acid
THF	etrahydrofuran
TLC	thin-layer chromatography
V_T	volume of tracer
V_{max}	Maximum rate

12013359